

**Synthesis of Bridged and Unbridged Group (IV) Metallocene  
Complexes as Catalyst Precursors for  
Ethylene Polymerization**

**Dissertation**

zur Erlangung des akademischen Grades eines  
Doktors der Naturwissenschaften (Dr. rer. nat.) der Fakultät für  
Biologie, Chemie und Geowissenschaften der  
Universität Bayreuth

Vorgelegt von

**Mohamed Elnaiem Mohamed Abdelbagi**

aus Khartoum, Sudan

Bayreuth, Germany

2011

This thesis fulfils the requirements of the doctoral degree of the Faculty of Biology, Chemistry and Geological Sciences at the University of Bayreuth.

Thesis submitted: 11.10.2011

Date of Scientific Colloquium: November 22, 2011

Examination Committee:

Prof. Dr. Helmut G. Alt	(1. Referee)
Prof. Dr. Jürgen Senker	(2. Referee)
Prof. Dr. Rainer Schobert	(Vorsitzender)
Prof. Dr. Peter Strohriegl	

The following work was performed during the period from April 2008 to March 2011 under the supervision of Prof. Dr. Helmut G. Alt at the Lehrstuhl für Anorganische Chemie II and at the Lehrstuhl für Makromolekulare Chemie I der Universität Bayreuth.

My sincere acknowledgement to my supervisor

**Herrn Professor Dr. Helmut G. Alt**

for his guidance, encouragement and enthusiastic support during the course of this research work.

I am grateful to the DAAD for the financial support

## **Acknowledgement**

I am very grateful to Dr. Christian Görl for his guidance and help in research work and thesis writing. Thanks are also due to his valuable suggestions and the wonderful leisure time activities we shared.

My thanks are also due to Dr. Matthias Dötterl for translating the summary.

I am grateful to Dr. Khalil Ahmed for his assistance in GC/MS and NMR measurements during the first stages of my research.

I would like to express my deep thanks and gratitude to my labmates in the "Alt group": Dr. Christine Denner, Dr. Haif Alshammari, Dr. Hamdi Elagab, Dr. Julian Lang, Dr. Andrea Rimkus, Dr. Tanja Englmann and Frank Lüdel for their help, support and valuable suggestions.

I would like to express my gratitude to all members in AC II and MC I at the University of Bayreuth for providing a friendly and cooperative atmosphere.

To all my friends in Bayreuth, I wish to express my sincere thanks for genuine relations and wonderful time I spent with them.

Finally I would like to extend my deepest thanks and gratitude to my family members in Sudan for their constant encouragement and moral support throughout the period of my study.

To

My Parents

&

My Children *Ahmed & Rahaf*

With my Love

## Abbreviations

[1,2-3]	Reference number
$\alpha$ -	alpha-
Å	Angstrom
$\beta$ -	beta-
n-Bu	n-Butyl
°C	Degree Celsius
cat.	catalyst
CDCl <sub>3</sub>	deuterated chloroform
CD <sub>2</sub> Cl <sub>2</sub>	deuterated methylene chloride
C <sub>6</sub> D <sub>6</sub>	deuterated benzene
Cen	Centroid
Cp	Cyclopentadienyl
C <sub>q</sub>	quaternary carbon
$\delta$	chemical shift in ppm
d	doublet in NMR spectroscopy
dd	doublet of doublet in NMR spectroscopy
Et	ethyl
Flu	Fluorenyl
g	gram
GC	gas chromatography
h	hour
Hz	Hertz
Ind	Indenyl
i-Pr	isopropyl
kg	kilogram
M	metal
M <sup>+</sup>	Molecular ion
MAO	methylaluminoxane
Me	methyl

## Abbreviations

---

mg	milligram
min	minute
ml	milliliter
mol	mol
mmol	millimol
m/e	mass/elemental electric charge
$M_n$	number average molar mass
$M_w$	weight average molar mass
MS	mass spectrometry
NMR	Nuclear Magnetic Resonance
n.d.	not determined
PE	polyethylene
Ph	phenyl
PP	polypropylene
ppm	parts per million
q	quartet in NMR spectroscopy
r.t.	room temperature
s	singlet in NMR spectroscopy
THF	tetrahydrofuran
TMA	trimethylaluminum
t	triplet in NMR spectroscopy
X	halide

## Contents

<b>1</b>	<b>Introduction</b>	<b>1</b>
1.1	General	1
1.2	Research goal	7
<b>2</b>	<b>General Part</b>	<b>8</b>
2.1	Unbridged 1- and 2-substituted bis(silylindenyl) zirconium (IV) and hafnium (IV) complexes	8
2.1.1	General remarks	8
2.1.2	Preparation of the 1-substituted silylindenyl compounds <b>5-8</b>	9
2.1.3	Preparation of the 2-substituted silylindenyl compounds <b>9-12</b>	11
2.1.4	Characterization of compounds <b>1-12</b>	12
2.1.5	Synthesis of the transition metal complexes	20
2.1.6	Characterization of the complexes	22
2.1.7	Ethylene polymerization experiments	32
2.1.7.1	General aspects and mechanism	32
2.1.7.2	Ethylene polymerization activities of complexes <b>13-18</b>	34
2.1.7.3	Ethylene polymerization activities of complexes <b>19-24</b>	35
2.1.7.4	Comparison between the polymerization activities of 1- and 2-substituted zirconocenes	37
2.1.7.5	Polymer analysis	38
2.2	1,2-Bis(dimethylsilyl)phenylidene-bridged zirconocene and hafnocene dichloride complexes	40
2.2.1	General remarks	40
2.2.2	Synthesis of the ligand precursor	41
2.2.3	Characterization of compound <b>27</b>	42
2.2.4	Synthesis and characterization of compounds <b>29</b> and <b>30</b>	44
2.2.5	Synthesis and characterization of the 1,3-bis(dimethylsilyl)phenylidene bridged bis(indenyl) compound <b>33</b>	46
2.2.6	Synthesis of 1,2-phenylidene-bis(inden-1-yl)dimethylsilyl complexes of zirconium ( <b>34</b> ) and hafnium ( <b>35</b> )	49

## Contents

---

2.2.7	Characterization of the complexes <b>34</b> and <b>35</b>	49
2.2.8	Crystal structures of complexes <b>34</b> and <b>35</b>	54
2.2.9	Reactions of compounds <b>29</b> , <b>30</b> and <b>33</b> with zirconium tetrachloride	59
2.2.10	Ethylene polymerization experiments with complexes <b>34</b> and <b>35</b>	60
2.3	2,2'-Bis(methylene)biphenylidene-bridged 1-indenyl complexes of group (IV) metals	63
2.3.1	General remarks	63
2.3.2	Preparation of the ligand precursors <b>38</b> and <b>39</b>	63
2.3.3	Characterization of compounds <b>38</b> and <b>39</b>	65
2.3.4	Synthesis of the titanium, zirconium and hafnium complexes <b>40-42</b>	68
2.3.5	Characterization of the complexes <b>40-44</b>	69
2.3.6	Crystal structure of complex <b>41</b>	73
2.3.7	Ethylene polymerization studies of complexes <b>40-44</b>	76
2.4	9-Substituted silylfluorenyl complexes of zirconium and hafnium	80
2.4.1	General remarks	80
2.4.2	Synthesis of the potential ligand <b>45</b>	80
2.4.3	Characterization of compound <b>45</b>	80
2.4.4	Synthesis of complexes <b>46</b> and <b>47</b>	83
2.4.5	Characterization of complexes <b>46</b> and <b>47</b>	84
2.4.6	Ethylene polymerization experiments with complexes <b>45</b> and <b>46</b>	86
<b>3.</b>	<b>Experimental Part</b>	<b>87</b>
3.1	General	87
3.2	NMR spectroscopy	87
3.3	GC/MS	87
3.4	Mass spectrometry	88

## Contents

---

3.5	Elemental analysis	88
3.6	DSC analysis	88
3.7	Viscosimetry analysis	89
3.8	Single crystal X-rays diffraction	89
3.9	Polymerization of ethylene	90
3.10	Synthesis procedures	90
3.10.1	General synthesis of the arylchlorodimethylsilane compounds <b>1-4</b>	90
3.10.2	General synthesis of the 1-(aryldimethylsilyl)indenyl compounds <b>5-8</b>	91
3.10.3	Synthesis of 2-bromoindene	91
3.10.4	General synthesis of the 2-(aryldimethylsilyl)indenyl compounds <b>9-12</b>	91
3.10.5	General synthesis of the transition metal complexes <b>13-24</b>	92
3.10.6	Preparation of 1,2-bis(chlorodimethylsilyl)benzene ( <b>26</b> )	93
3.10.7	Preparation of 2-methylindene ( <b>28</b> )	93
3.10.8	General synthesis of the ligand precursors <b>27, 29, and 30</b>	93
3.10.9	Preparation of 1,3-bis(chlorodimethylsilyl)benzene ( <b>32</b> )	94
3.10.10	Preparation of 1,3-bis(inden-1-yl)dimethylsilylbenzene ( <b>33</b> )	94
3.10.11	General synthesis of the transition metal complexes <b>34 and 35</b>	95
3.10.12	Preparation of 2,2'-bis(bromomethyl) biphenyl ( <b>37</b> )	95
3.10.13	Preparation of 2,2'-bis(inden-1-yl)methyl biphenyl ( <b>38</b> )	96
3.10.14	General synthesis of the transition metal complexes <b>40-42</b>	96
3.10.15	General synthesis of the transition metal complexes <b>43 and 44</b>	97
3.10.16	Preparation of 9-tolyldimethylsilylfluorene ( <b>45</b> )	97
3.10.17	General synthesis of the transition metal complexes <b>46 and 47</b>	98
<b>4</b>	<b>Summary</b>	99
<b>5</b>	<b>Zusammenfassung</b>	103
<b>6</b>	<b>References</b>	108

## 1. Introduction and research goals

### 1.1 General

Catalytic olefin polymerization represents one of the most important processes which attracted a tremendous interest in industry and research during the last 30 years. Polyolefin materials include polyethylenes (PEs), polypropylenes (PPs), ethylene/ $\alpha$ -olefin copolymers, and ethylene/propylene/diene elastomers (EPDMs) etc. Among the various types of polyolefins, polyethylene is considered to be the most common polyolefin. Polyolefins attract great attention because they are produced from inexpensive and readily available raw materials and characterized by unique properties including chemical inertness, high mechanical strength, low density, flexibility, processibility, and recyclability.

Polyolefin products have an impact on almost all human activities with a wide range of applications including food packages, plastic bags, squeeze bottles, containers, storage boxes, toys, disposable diapers, bullet-proof vests, gasoline tanks and components of automotive and engineering industry. Due to this, the total annual worldwide production of polyethylene and polypropylene exceeded 105 million tons in 2005<sup>[1]</sup> (including 64 million tons for polyethylene and 41 million tons for polypropylene) which increases annually by 7%. This counts for higher than 50% of the total production of plastic materials.

Polyethylene was accidentally synthesized by the German chemist Pechmann<sup>[2]</sup> and characterized by his colleagues Bamberger and Tschirner<sup>[3]</sup>. However, its commercial scale production started 40 years later at the British company Imperial Chemical Industrial (ICI) using a radical polymerization process under high pressure<sup>[4]</sup>.

The first catalytic synthesis of polyethylene was discovered by Banks and Hogan at Phillips Petroleum company in the year 1951<sup>[5]</sup>. They used chromium trioxide supported on silica gel (commonly known as “Phillips catalyst”) to polymerize ethylene at moderate conditions. In 1953, Ziegler<sup>[6,7]</sup> used titanium halides along with organoaluminum compounds (trimethylaluminum, diethylaluminum chloride) to polymerize ethylene even at milder conditions compared with the Phillips catalyst. Later on, Natta<sup>[8]</sup> used the Ziegler catalyst system to polymerize propylene. Ziegler and Natta were awarded the

Nobel Prize in chemistry in 1963 for their work<sup>[9,10]</sup>. Advantageously, both the Phillips and the Ziegler catalyst are cheap and can also be heterogenized on an inorganic support like aluminum oxide or silica gel thus avoiding the problematic fouling (accumulation of the produced polymer on the reactor walls disturbing the reaction control). Accordingly, still the major amount of the polyethylene is produced with the heterogeneous Phillips and Ziegler catalyst systems.<sup>[11]</sup>

On the other hand, the disadvantage of these catalyst systems is their “multi-site” nature, as each site produces a polymer of different molecular weight resulting in complex polymer mixtures with varying molecular weights and microstructures.<sup>[12]</sup>

The next breakthrough in the field of catalytic olefin polymerization was the application of metallocene catalysts. Metallocene complexes are characterized by the presence of one or two cyclopentadienyl, indenyl, or fluorenyl rings which form  $\pi$  bonds with the central transition metal (mainly from group IV). In 1957, the first catalytically active metallocene catalyst system  $\text{Cp}_2\text{TiCl}_2\text{-AlEt}_2\text{Cl}$  ( $\text{Cp} = \eta^5\text{-C}_5\text{H}_5$ ) was discovered by Breslow and Natta.<sup>[13,14]</sup>

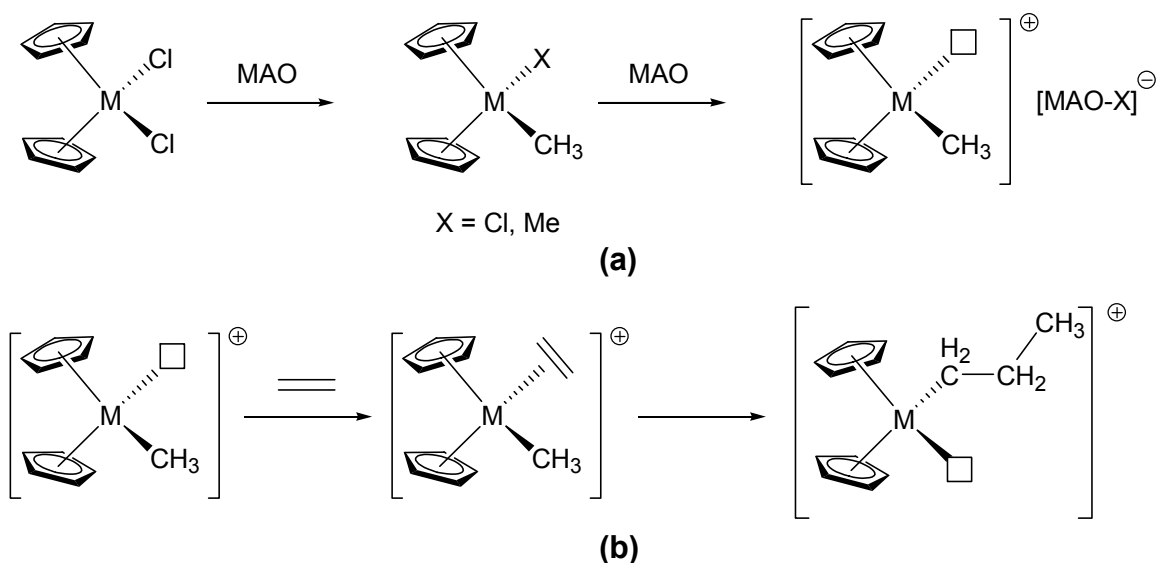
The activities of these catalysts were poor, so the metallocene complexes were only used for mechanistic studies of olefin polymerization reactions, in which hydrocarbon-soluble (homogeneous) systems were preferred rather than a heterogeneous Ziegler system. However, this situation changed dramatically in 1980 when Sinn and Kaminsky<sup>[15,16]</sup> reported the use of methylaluminoxane (MAO) as a cocatalyst in the polymerization of olefins. MAO was obtained by partial hydrolysis of trimethylaluminum and has a dynamic structure (including chains, rings, and cages) in which the aluminum and oxygen atoms are alternately positioned and free valences are saturated with methyl groups.<sup>[17]</sup>

When a metallocene (especially zirconocene) complex is activated with MAO, the activity of the resulting catalyst is enhanced by factors of 10-100 greater than the most active Ziegler-Natta systems.<sup>[18]</sup>

The activation of a metallocene catalyst results in the formation of the catalyst active site which is probably an ion pair formed by a cationic metallocene complex and an anionic methylaluminoxane counter ion. This proceeds by methylation of the metallocene dichloride complex and thus replacement of one or two chloro ligands with

methyl groups from free trimethylaluminum (TMA) which is present in MAO (up to 10% of the overall Al content). In a subsequent step, the abstraction of one methyl group or the remaining chloro ligand generates the catalytically active metallocene cation  $[\text{Cp}_2\text{ZrMe}]^+$ .<sup>[19,20]</sup>

The polymerization of ethylene can be explained by the Cossee-Arlman<sup>[21-23]</sup> mechanism (Scheme 1).



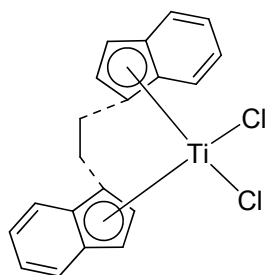
**Scheme 1:** (a) The activation of a metallocene complex with MAO.

(b) Cossee-Arlman mechanism for the insertion of ethylene.

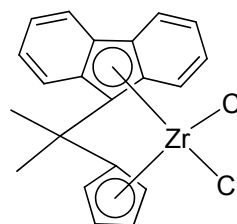
In contrast to the previously mentioned heterogeneous catalysts, metallocene complexes are single site catalysts and therefore have the potential to produce polymers with narrow molecular weight distributions ( $\text{PD} \approx 2$ ) and relatively uniform microstructures.<sup>[24]</sup> Moreover, due to their homogeneous nature, it is quite easy to predict structure-property relationships of the metallocene catalysts.<sup>[25]</sup> Thus, these catalysts can be tailored by tuning the chemical environment around the metal center to enhance the productivity or to produce poly( $\alpha$ -olefin)s with special stereoregularities and high degrees of tacticity.

The next milestone was reached in 1982 when Brintzinger<sup>[26]</sup> synthesized the C<sub>2</sub>-symmetric ethylidene bridged metallocene complex, *rac*-(C<sub>2</sub>H<sub>4</sub>)(Ind)<sub>2</sub>TiCl<sub>2</sub>, which was used as the first metallocene catalyst to produce isotactic polypropylene.<sup>[27]</sup>

In 1988, Razavi<sup>[28]</sup> synthesized the mixed ansa-metallocene complex [Zr(CpCMe<sub>2</sub>Flu)Cl<sub>2</sub>] which was an efficient catalyst for syndiotactic polypropylene production.



Brintzinger catalyst

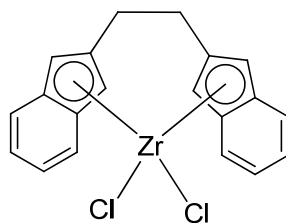


Razavi catalyst

### Scheme 2: Metallocene catalysts for stereoselective propylene polymerization.

The efficiency of ansa-metallocene catalysts in the stereoselective polymerization of  $\alpha$ -olefins, established by Brintzinger and Razavi, has led to the development of versatile ansa-metallocene complexes used as catalyst precursors in the copolymerization of  $\alpha$ -olefins. For instance, the dimethylsilylene bridged metallocene complex<sup>[29]</sup> *rac*-Me<sub>2</sub>Si(Ind)<sub>2</sub>ZrCl<sub>2</sub> is also a notable catalyst precursor that polymerizes propylene with higher activity and isospecificity than the ethylidene bridged analogues.

Ansa-metallocene complexes with two indenyl ligands linked at the 2, 2'-positions have also received an increasing interest due to their high efficiency in the homopolymerization and copolymerization of  $\alpha$ -olefins. A family of complexes derived from ethylidene-bridged bis(2-indenyl) zirconium dichloride were developed by Shaverien et al.<sup>[30,31]</sup> After activation with MAO, they exhibited high productivities and 1-hexene incorporation rates.

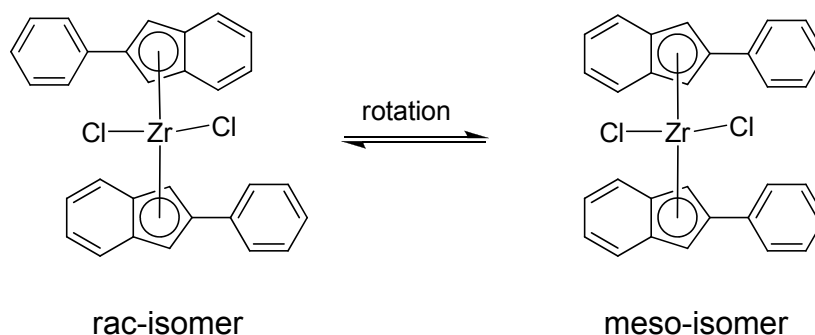


**Scheme 3:** Ethylidene-bridged bis(2-indenyl)zirconium complex.

The main drawbacks of this type of catalysts are the low overall reaction yields, since multiple steps are involved in their synthesis due to the inactivity of the indenyl C2-position (especially against carbon nucleophiles).<sup>[32]</sup>

The ethylidene bridged bis(fluorenyl) complexes of zirconium and hafnium have proved to be excellent catalysts for the MAO-facilitated polymerization of ethylene.<sup>[33]</sup>

Compared to the bridged bis(indenyl) metallocene complexes, unbridged bis(indenyl) analogs have received little attention. This is because the untethered indenyl ligands are free to rotate resulting in poly( $\alpha$ -olefin)s with non-stereospecific structures.<sup>[34]</sup> However, Waymouth and co-workers<sup>[35-38]</sup> revealed that metallocene catalysts derived from bis(2-phenylindenyl)zirconium dichloride yield elastomeric stereoblock polypropylene. The proposed mechanism involves interconversion between an aspecific (meso form) and an isospecific (rac form) state of the catalyst. The meso isomer forms atactic blocks and the rac isomer forms isotactic blocks in the same polymer chain.<sup>[39]</sup>



**Scheme 4:** The different conformations of Waymouth's catalyst.<sup>[35-38]</sup>

The publication of Waymouth's complex has opened up a path for extensive ongoing studies directed to explore the relationships between catalyst activity, polymer properties and substituent effects at the 1- and 2-positions of the indenyl rings of unbridged metallocene complexes.<sup>[40-44]</sup>

2-Substituted bis(indenyl) metallocene catalysts have met particular interest in the production of linear low density polyethylene (LLDPE) due to their high comonomer incorporation rate in the copolymerization of ethylene with  $\alpha$ -olefins (particularly 1-hexene).<sup>[45-48]</sup> On the other hand, the activities of 1-substituted metallocene catalysts in the polymerization of olefins are significantly higher than the 2-substituted analogues bearing the same ligands.

Electron donating groups, when connected directly to indenyl or cyclopentadienyl ligands, are known to have a favourable effect on the catalyst activity in ethylene polymerization reactions by stabilizing the metal coordination site, while the presence of electron withdrawing groups leads to the opposite effect providing less active catalysts.

## 1.2 Research goals

As indicated in chapter 1.1, the ligand structure plays a key role in terms of the activity and selectivity of a catalyst. Minor changes in the ligand structure or the bridging moiety can lead to dramatic effects on the productivity and selectivity of a catalyst.

Keeping this in focus, our primary interest is to synthesize new bridged metallocene complexes and unbridged metallocene complexes with functionalized silyl substituents at the 1- and 2- positions of the indenyl ring. The proposed potential ligands include:

- 1,2-bis(dimethylsilyl)phenylidene bridged bis(indenyl) compounds.
- 2,2'-dimethyl-1-1'-biphenylidene bridged bis (indenyl) compounds.
- 2-silyl substituted indenyl compounds.
- 1-silyl substituted indenyl compounds.
- 9-silyl substituted fluorenyl compounds.

Group (IV) metal complexes derived from the above mentioned potential ligands should be synthesized and their catalytic activity in ethylene polymerization, in combination with methylaluminoxane (MAO) as a cocatalyst, should be tested. We were also interested in the extent to which the steric and electronic properties of these substituents affect the subsequent catalyst performance and the control over polymer properties through "structure-property relationships".

## 2. General Part

### 2.1 Unbridged 1- and 2-substituted bis(silylindenyl) zirconium (IV) and hafnium (IV) complexes

#### 2.1.1 General remarks

Metallocene complexes received substantial attention in industry and research due to their capability of being highly active catalyst precursors for ethylene homopolymerization, copolymerization and stereospecific polymerization of higher  $\alpha$ -olefins. Unlike traditional Ziegler and Natta<sup>[8-10]</sup> catalysts, the facile ligand modification with various substituents has led to the preparation of a large number of metallocene complexes to improve the activity of the catalysts and the properties of the produced polyolefins. The size, nature and position of the substituents attached to the cyclopentadienyl, indenyl, or fluorenyl moieties play a key role on the catalytic activity as well as on the molecular weight and molecular weight distribution of the produced polymer.<sup>[49-56]</sup>

Since Waymouth et al.<sup>[35,57]</sup> have reported the successful application of unbridged bis( $\eta^5$ -2-phenylindenyl) zirconium dichloride, activated with MAO, in the production of elastomeric polypropylene (ePP), a wide range of unbridged bis(2-indenyl) metallocene complexes bearing siloxy, amino, aryl, alkyl and alkenyl substituents at the 2-position of the indenyl moiety have been synthesized and investigated as catalyst precursors for the polymerization of olefins.<sup>[58-67]</sup> The symmetric metallocene complexes derived from substituted indenenes exist in two conformations: *rac*- and *meso*-diastereomers. The ratio *rac*/*meso* depends on the bulkiness of the substituent.<sup>[68]</sup>

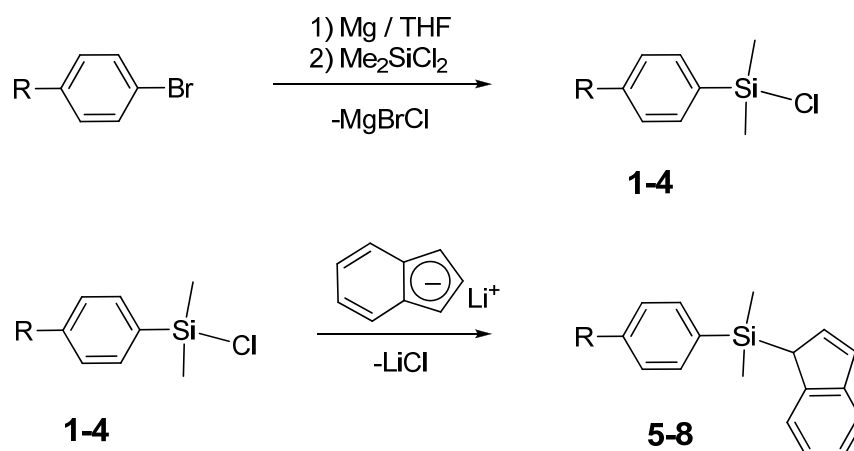
Silyl groups have been extensively used as bridging groups in ansa-metallocene complexes.<sup>[25]</sup> However, little has been reported on the catalytic behavior of unbridged indenyl complexes containing silyl substituents attached directly to the ligand. The synthesis of *rac*- and *meso*-bis(1-dimethylsilylindenyl)-zirconium dichloride was briefly described in a review<sup>[69]</sup>, while the syntheses of 1- and 2-substituted bis[(trialkylsilyl)indenyl]-zirconium dichlorides were only recently reported in the literature.<sup>[70-73]</sup>

In this study, novel complexes of the type  $[1-(4\text{-XC}_6\text{H}_4\text{SiMe}_2)\text{-}\eta^5\text{-Ind}]_2\text{MCl}_2$  and  $[2-(4\text{-XC}_6\text{H}_4\text{SiMe}_2)\text{-}\eta^5\text{-Ind}]_2\text{MCl}_2$  (where X = Me, MeO, F; M = Zr and Hf) are reported. The characteristic features of these ligands are the bulky silyl groups functionalized with an electron donating group (Me), a hetero atom with a lone pair of electrons (MeO) or an electron withdrawing group (F). The substituents were chosen to cover a wide range of electronic properties and located at the 4-position of the aryl moiety. The behavior of these complexes towards ethylene polymerization, after activation with MAO, is investigated.

### 2.1.2 Preparation of the 1-substituted silylindenyl compounds 5-8

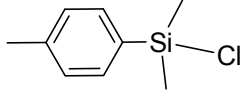
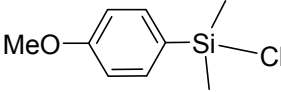
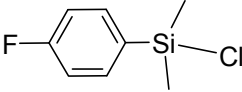
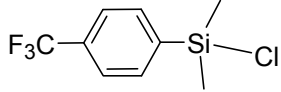
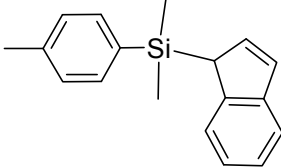
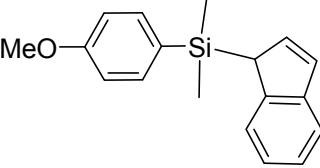
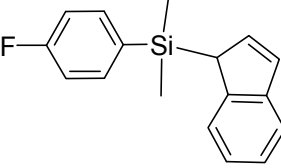
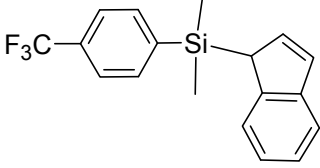
The reactions of the arylchlorodimethylsilanes **1-4** with stoichiometric amounts of indenyllithium, freshly prepared via deprotonation of indene with *n*-butyllithium (*n*-BuLi), afforded the 1-silyl substituted indenyl compounds **5-8** (Scheme 5). The arylchlorodimethylsilanes **1-4** as intermediates were prepared according to published methods<sup>[74,75]</sup> through reactions of 4-substituted bromobenzene derivatives with magnesium and a two fold excess of dichlorodimethylsilane in THF (Scheme 5).

In these reactions, a large excess of dichlorodimethylsilane was used to avoid the problems arising from substitution reactions of both chlorine atoms at the Si atom leading to the formation of bisaryldimethylsilyl compounds as heavier byproducts as detected by GC/MS analysis in some reactions. Therefore, cleaner reactions and better yields were only achieved when using a large excess of dichlorodimethylsilane.



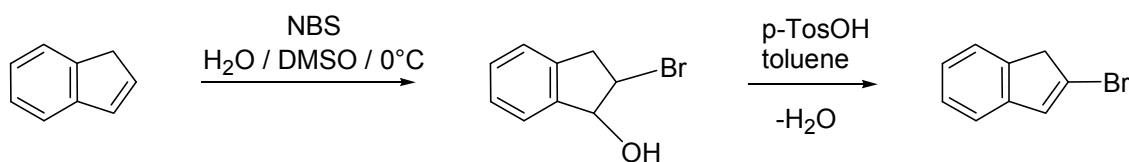
**Scheme 5:** Preparation of silane precursors **1-4** and potential ligands **5-8**.

**Table 1:** Overview of the silyl compounds 1-8

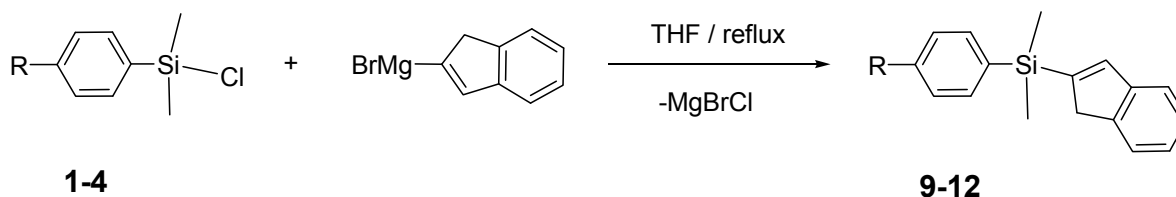
Compound	R	Structure
1	Methyl	
2	Methoxy	
3	Fluoro	
4	Trifluoro	
5	Methyl	
6	Methoxy	
7	Fluoro	
8	Trifluoro	

### 2.1.3 Preparation of the 2-substituted silylindenyl compounds 9-12

The 2-silyl substituted indenyl compounds **9-12** were readily prepared via a synthetic route that comprises the reaction of the Grignard reagent of 2-bromoindene and the corresponding aryldimethylchlorosilanes **1-4**. Therefore, 2-bromoindene, prepared according to the literature<sup>[76]</sup> by the reaction of indene with N-bromosuccinimide (NBS) followed by dehydration (Scheme 6), was reacted with magnesium powder in THF to yield the corresponding deep red Grignard reagent. Subsequent addition of a THF solution of an equivalent amount of the aryldimethylchlorosilanes **1-4** afforded the 2-substituted silylindenyl compounds **9-12** in 65-80% yields (Scheme 7).



**Scheme 6:** Preparation of 2-bromoindene.

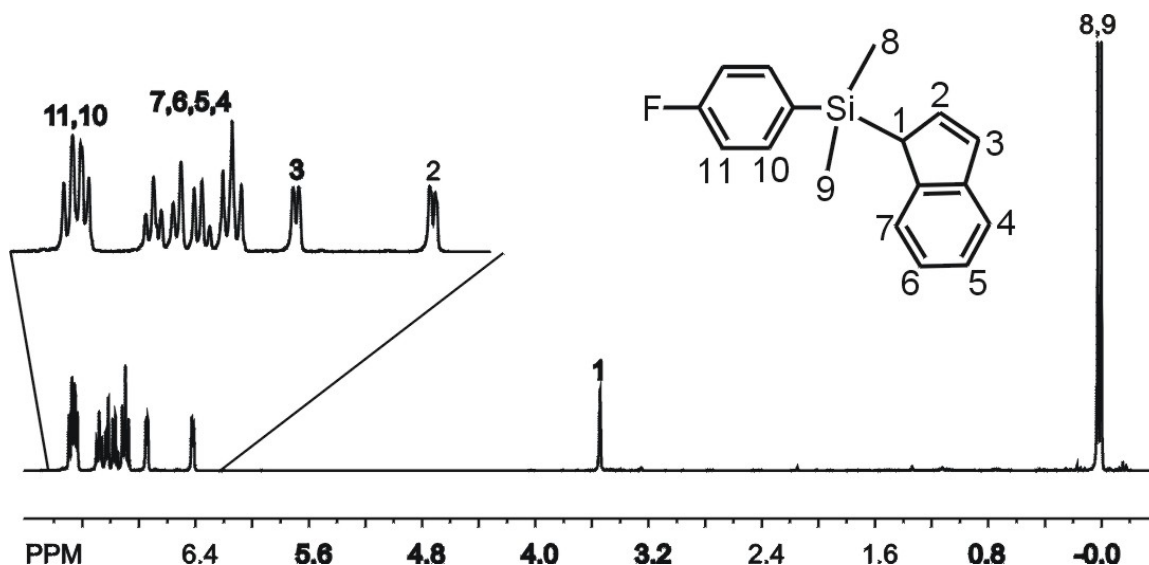


No.	R
<b>9</b>	Me
<b>10</b>	OMe
<b>11</b>	F
<b>12</b>	CF <sub>3</sub>

**Scheme 7:** Preparation of the ligand precursors **9-12**.

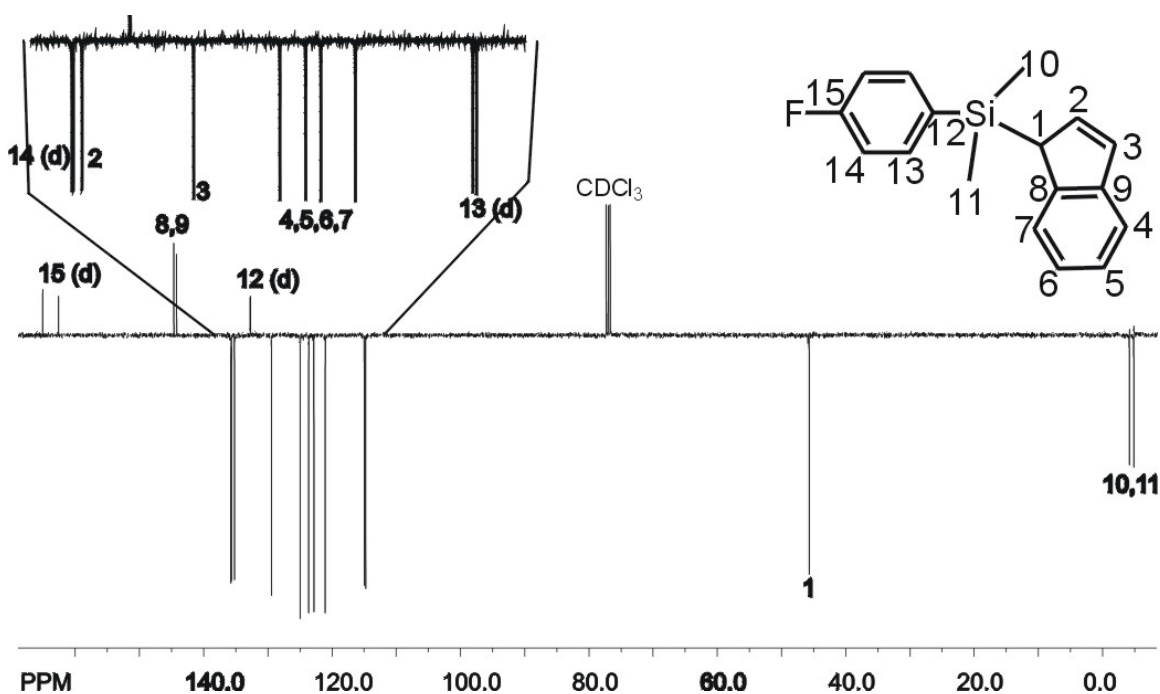
### 2.1.4 Characterization of compounds 1-12

Silyl substituted indenenes **5-12** and their parent chlorosilanes **1-4** were characterized by  $^1\text{H}$  and  $^{13}\text{C}$  NMR spectroscopy, the complete data are given in Table 2. The  $^1\text{H}$  and  $^{13}\text{C}$  NMR spectra of compounds **7** and **9** are discussed as examples. The  $^1\text{H}$  NMR spectrum of compound **7** (Scheme 8) shows two doublets at  $\delta = 7.28$  (d,  $^3J = 8.3$  Hz, 2H) and  $\delta = 7.24$  (d,  $^3J = 7.2$  Hz, 2H) ppm which can be assigned to the aromatic protons H11 and H10. The indene six-membered ring protons H7, H6, H5 and H4 display signals at  $\delta = 7.09$  (t, 1H), 7.03 (d,  $^3J = 7.4$  Hz, 1H), 6.98 (d,  $^3J = 7.3$  Hz, 1H) and 6.90 (t, 1H) ppm. The two doublets at  $\delta = 6.75$  ppm ( $^3J = 5.2$  Hz, 1H) and 6.42 ppm ( $^3J = 5.2$  Hz, 1H) are assigned to the protons H3 and H2 of indene, while the signal corresponding to the proton at the 1-position of indene (H1) appears at  $\delta = 3.54$  ppm (s, 1H). The six protons of the methyl groups (H8 and H9) produce the two singlets at  $\delta = 0.03$  and 0.00 ppm (6H,  $\text{Si}(\text{CH}_3)_2$ ).



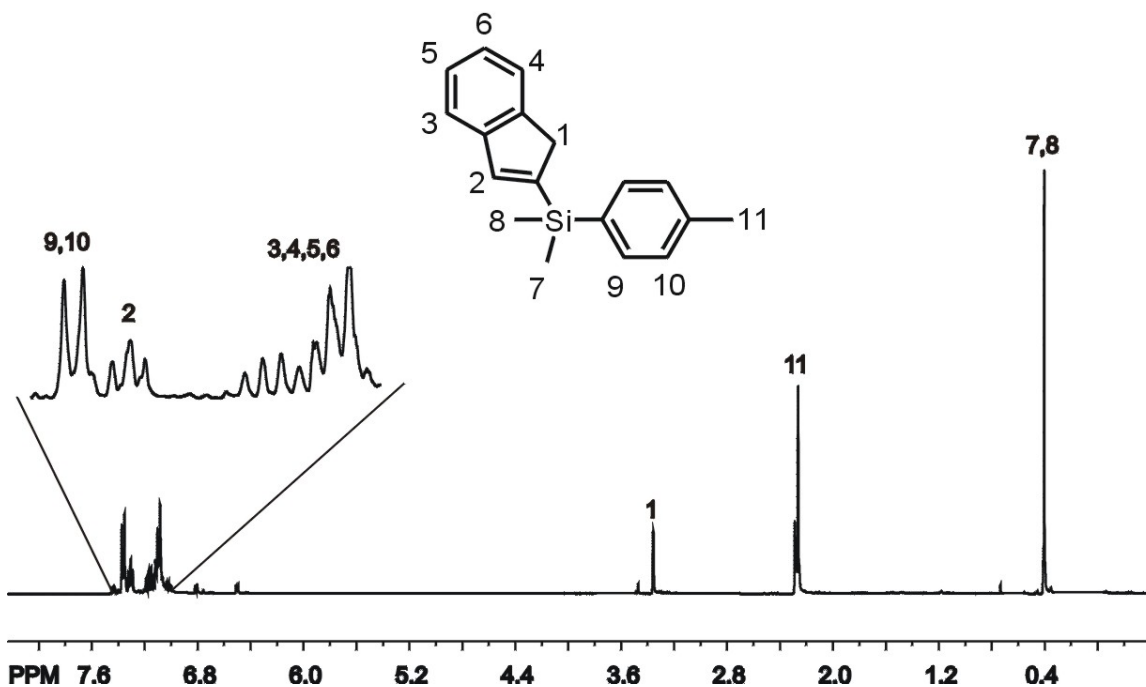
**Scheme 8:**  $^1\text{H}$  NMR spectrum of compound **7**.

The  $^{13}\text{C}$  NMR spectrum of compound **7** (Scheme 9) shows a doublet signal at  $\delta = 163.9$  ppm identifying the quaternary carbon atom C15 bearing the fluorine atom; the splitting of the signal is due to the  $^1J$  coupling with the fluorine atom [ $^1J(^{19}\text{F}-^{13}\text{C}) = 249$  Hz] which was observed also for C12, C13, and C14. The other quaternary carbon atoms in the molecule (C8, C9 and C12 (d)) display signals at  $\delta = 144.6$ , 144.2 and 132.7(d) ppm. The signals arising at  $\delta = 135.7$ , 135.2, 129.4, 125.0, 123.6, 122.8, 121.1, 114.9 ppm are assigned for the CH-type carbon atoms (C14 (d), C2, C3, C4, C5, C6, C7, and C13 (d)). The signal at  $\delta = 45.7$  ppm corresponds to the carbon atom at the 1-position of the indenyl moiety (C1) while the silyl methyl groups (C10 and C11) display the high field shifted signals at  $\delta = -4.2$  and  $-4.8$  ppm.



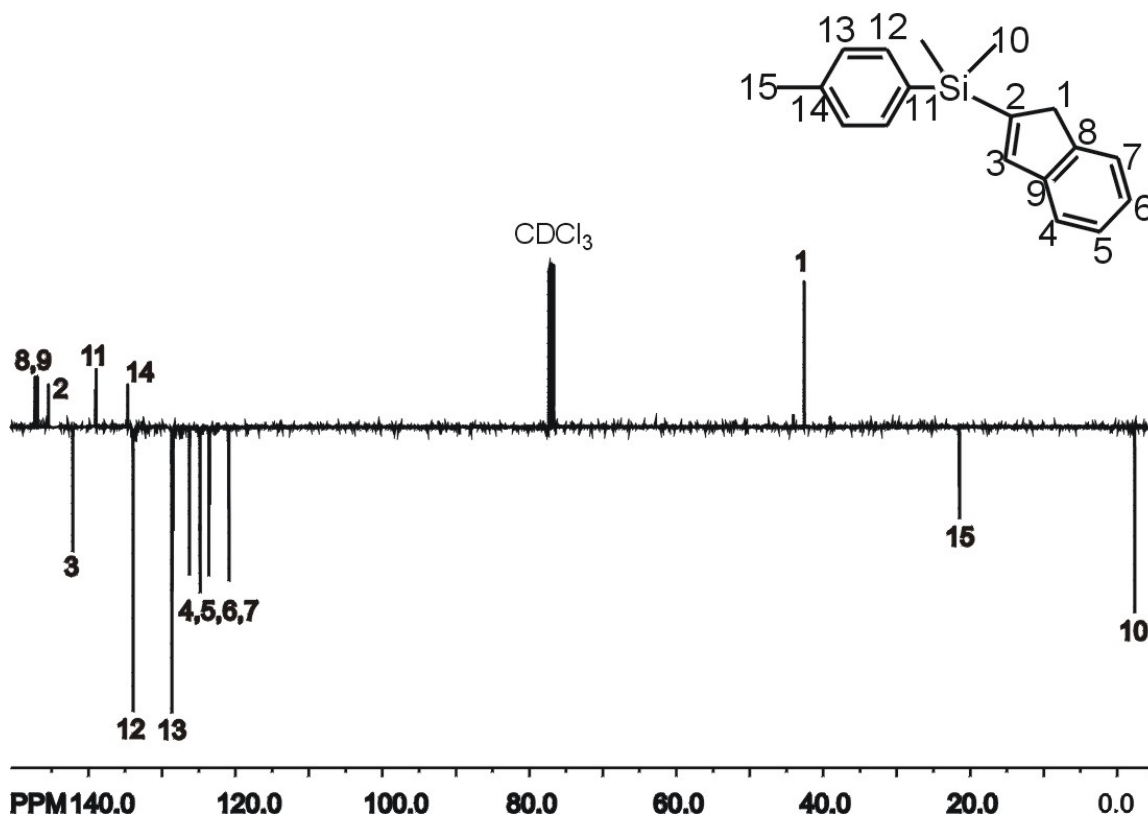
**Scheme 9:**  $^{13}\text{C}$  NMR spectrum of compound **7**.

The  $^1\text{H}$  NMR spectrum of compound **9** (Scheme 10) shows two signals at  $\delta = 7.36$  (br, 2H) and 7.32 (br, 2H) ppm corresponding to the aryl aromatic protons H9 and H10 while the proton attached at the 3-position of indene (H2) gives a multiplet at  $\delta = 7.29$  ppm. The four aromatic protons of indene (H3, H4, H5, and H6) display a multiplet at  $\delta = 7.12$ -7.07 (m, 4H) ppm while the protons at the 1-position of indene (H1) give rise to the singlet at  $\delta = 3.36$  (s, 2H) ppm. At  $\delta = 2.26$  ppm, the methyl group protons (H11) appear (s, 3H) while the two equivalent methyl groups attached to the silicon atom (H7, H8) display a singlet at  $\delta = 0.40$  ppm. A set of signals appearing beside the main signals (H1-H11) is assigned to the 1-substituted isomer which exists in approximately 10-15%.



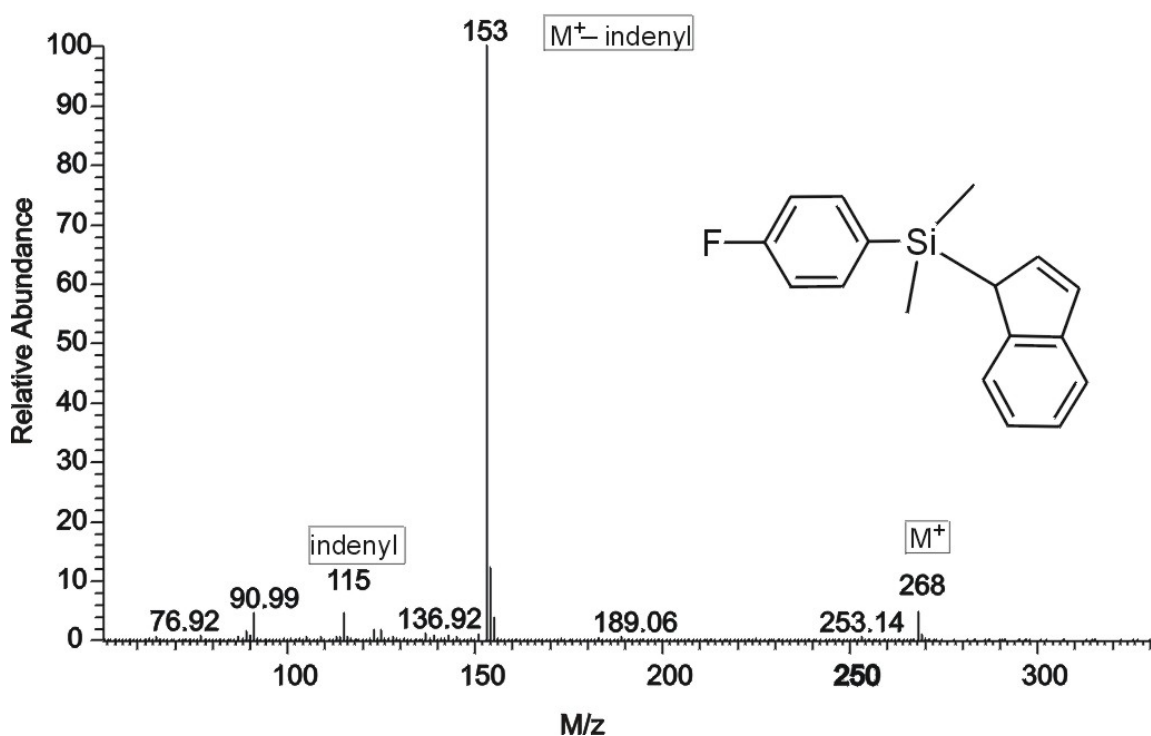
**Scheme 10:**  $^1\text{H}$  NMR spectrum of compound **9**.

The  $^{13}\text{C}$  NMR spectrum of compound **9** (Scheme 11) shows three signals shifted to down field at  $\delta = 147.3$ ,  $146.9$  and  $145.4$  ppm that correspond to the quaternary carbon atoms in the indenyl moiety (C8, C9, and C2) while the signals resulting from the phenyl ring, the quaternary carbon atoms (C11 and C14) appear at  $\delta = 138.9$  and  $134.6$  ppm. The signal at  $\delta = 142.1$  ppm is assigned to the carbon atom C3. The CH groups' carbon atoms in the phenyl ring (C12 and C13) are characterized by the doubly intensive signals appearing at  $\delta = 133.9$  and  $128.6$  ppm. The four signals at  $\delta = 126.2$ ,  $124.8$ ,  $123.6$ , and  $120.9$  ppm can be assigned to the aromatic CH carbon atoms in the indene six membered ring (C4, C5, C6, and C7). The signal at  $\delta = 42.6$  ppm corresponds to the indenyl  $\text{CH}_2$  group (C1). The signal at  $\delta = 21.5$  ppm is assigned to the tolyl carbon atom C15 while the signal at  $\delta = -2.4$  ppm represents the two identical methyl groups attached to the silicon atom (C10).



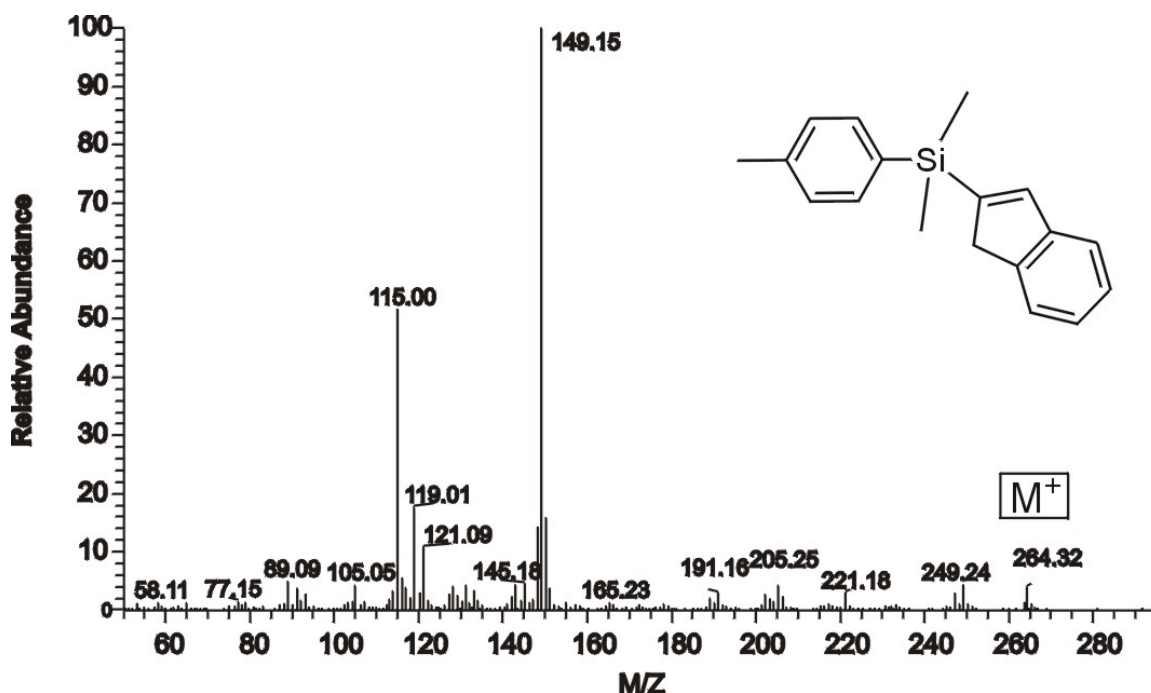
Scheme 11:  $^{13}\text{C}$  NMR spectrum of compound **9**.

Compounds **1-12** were also characterized by GC/MS. The complete data are given in Table 2. As examples, the mass spectra of compounds **7** and **9** were discussed. In the mass spectrum of compound **7** (Scheme 12), the molecular ion peak appears at  $m/z = 268.1$  with 7% intensity relative to base peak while the fragment resulting from the loss of one methyl group [ $M^+ - \text{Me}$ ] generates the peak at  $m/z = 253$  (intensity: 2%). The base peak which appears at  $m/z = 153$  corresponds to the loss of the indenyl group [ $M^+ - \text{indenyl}$ ]. The indenyl fragment gives rise to the peak at  $m/z = 115$  with 8% intensity.



**Scheme 12:** Mass spectrum of compound **7**.

In the mass spectrum of compound **9** (Scheme 13), the molecular ion peak appears at  $m/z = 264.3$  with 6% intensity. The loss of a methyl group leads to the peak at  $m/z = 249.2$  with 5% intensity. The base peak at  $m/z = 149.1$  can be explained by the loss of the indenyl moiety. The free indenyl fragment appears at  $m/z = 115$  with 38% intensity relative to the base peak.



Scheme 13: Mass spectrum of compound **9**.

**Table 2:** NMR<sup>a</sup> and MS data of compounds **1-12**.

No.	<sup>1</sup> H NMR	<sup>13</sup> C NMR	MS [m/z] (%)
<b>1</b>	7.61 d ( <sup>3</sup> J =5.6 Hz, 2H-Ar) 7.31 d ( <sup>3</sup> J =5.6 Hz, 2H-Ar) 2.46 s (3H, CH <sub>3</sub> ) 0.76 s (6H, Si(CH <sub>3</sub> ) <sub>2</sub> )	140.4 (C <sub>q</sub> ) 133.1 (CH) 132.6 (C <sub>q</sub> ) 128.8 (CH) 21.5 (CH <sub>3</sub> ) 2.1 (Si(CH <sub>3</sub> ) <sub>2</sub> )	n.d.
<b>2</b>	7.44 d ( <sup>3</sup> J =8.5 Hz, 2H-Ar) 6.78 d ( <sup>3</sup> J =9.0 Hz, 2H-Ar) 3.29 s (3H, O-CH <sub>3</sub> ) 0.47 s (6H, Si(CH <sub>3</sub> ) <sub>2</sub> )	161.9 (C <sub>q</sub> ) 135.1 (CH) 127.3 (C <sub>q</sub> ) 114.1 (CH) 54.5 (O-CH <sub>3</sub> ) 2.1 (Si(CH <sub>3</sub> ) <sub>2</sub> )	n.d.
<b>3</b>	7.61-7.57 m (2H-Ar) 7.09 t (2H-Ar) 0.66 s (6H, Si(CH <sub>3</sub> ) <sub>2</sub> )	164.4 d (C <sub>q</sub> ) 135.3 d (CH) 131.8 d (C <sub>q</sub> ) 115.3 d (CH) 2.1 (Si(CH <sub>3</sub> ) <sub>2</sub> )	188 M <sup>+</sup> (17) 173 M <sup>+</sup> -Me (100) 153 (8)
<b>4</b>	7.75 d ( <sup>3</sup> J =7.0 Hz, 2H-Ar) 7.65 d ( <sup>3</sup> J =7.0 Hz, 2H-Ar) 0.70 s (6H, Si(CH <sub>3</sub> ) <sub>2</sub> )	142.0 (C <sub>q</sub> ) 134.5 q (CH) 126.3 m (C <sub>q</sub> ) 125.7 q (CH) 123.5 m (C <sub>q</sub> , CF <sub>3</sub> ) 2.9 (Si(CH <sub>3</sub> ) <sub>2</sub> )	238 M <sup>+</sup> (10) 223 M <sup>+</sup> -Me (100)
<b>5</b>	7.33-7.27 m (4H, Ar-H) 7.13-7.08 m (4H, Ind-H) 6.85 m (1H, C <sub>3</sub> -Ind) 6.50 m (1H, C <sub>2</sub> -Ind) 3.63 s (1H, C <sub>1</sub> -Ind) 2.28 s (3H, Ar-CH <sub>3</sub> ) 0.06 s (3H, Si-CH <sub>3</sub> ) 0.00 s (3H, Si-CH <sub>3</sub> )	144.9, 144.2, 139.2 (C <sub>q</sub> ) 135.6 (CH, 2C) 133.9 (C <sub>q</sub> ) 133.8, 129.1, 128.6, 124.8, 123.5, 122.9 (CH) 120.9 (CH, 2C) 45.8 (CH, C <sub>1</sub> -Ind) 21.5 (Ar-CH <sub>3</sub> ) -4.4, -5.0 (Si(CH <sub>3</sub> ) <sub>2</sub> )	264 M <sup>+</sup> (8) 249 M <sup>+</sup> -Me (3) 149 M <sup>+</sup> -Ind (100) 115 Indenyl (5)
<b>6</b>	7.40-6.80 m (8H, Ar-H, Ind-H) 6.75 m (1H, C <sub>3</sub> -Ind) 6.48 m (1H, C <sub>2</sub> -Ind) 3.55 m (1H, C <sub>1</sub> -Ind) 3.28 s (3H, O-CH <sub>3</sub> ) 0.01 s (3H, Si-CH <sub>3</sub> ) 0.00 s (3H, Si-CH <sub>3</sub> )	161.3, 145.4, 144.7, 135.7 (C <sub>q</sub> ) 135.5 (CH, 2C) 129.6, 128.2, 125.3, 124.0, 123.3, 121.4 (CH) 114.0 (CH, 2C) 54.5 (O-CH <sub>3</sub> ) 46.5 (CH, C <sub>1</sub> -Ind) -4.0, -5.0 (Si(CH <sub>3</sub> ) <sub>2</sub> )	280 M <sup>+</sup> (4) 265 M <sup>+</sup> -Me (2) 165 M <sup>+</sup> -Ind (100) 115 Indenyl (7)

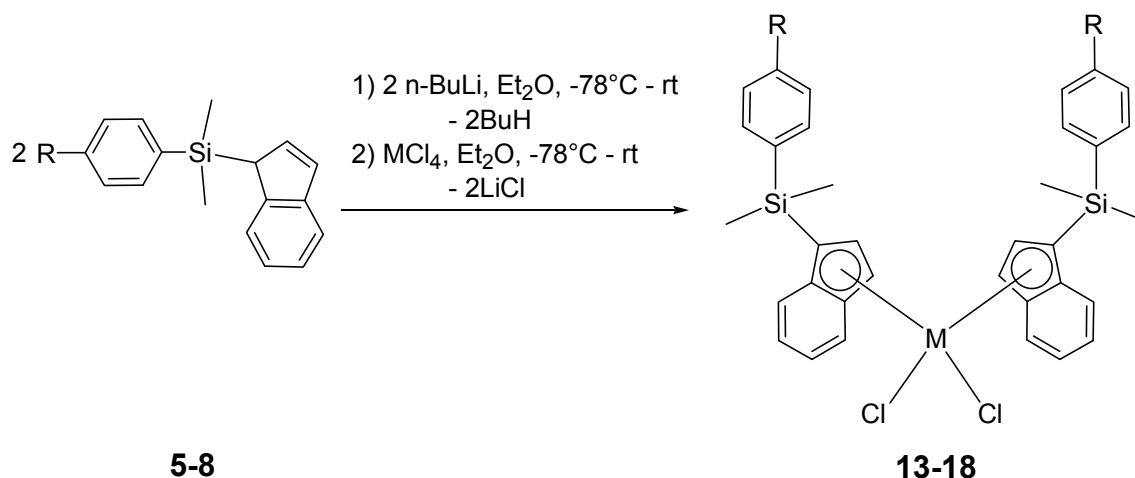
<b>7</b>	7.28 d ( $^3J = 8.3\text{Hz}$ , 2H, Ar-H) 7.24 d ( $^3J = 7.2\text{Hz}$ 2H, Ar-H) 7.09-6.90 m (4H, Ind-H) 6.75 d ( $^3J = 5.2\text{ Hz}$ , 1H, C <sub>3</sub> -Ind) 6.42 d ( $^3J = 5.2\text{ Hz}$ , 1H, C <sub>2</sub> -Ind) 3.54 s (1H, C <sub>1</sub> -Ind) 0.03 s (3H, Si-CH <sub>3</sub> ) 0.00 s (3H, Si-CH <sub>3</sub> )	163.9 d ( $^1J_{\text{C-F}} = 249\text{ Hz}$ C <sub>q</sub> , C-F) 144.6, 144.2 (C <sub>q</sub> ) 135.7 d ( $^3J_{\text{C-F}} = 7\text{ Hz}$ , CH, 2C) 135.2 (CH) 132.7 d ( $^4J_{\text{C-F}} = 4\text{ Hz}$ , C <sub>q</sub> ) 129.4, 125.0, 123.6, 122.8, 121.1(CH) 114.9 d ( $^2J_{\text{C-F}} = 20\text{ Hz}$ , CH, 2C) 45.7 (CH, C <sub>1</sub> -Ind) -4.2, -4.8 (Si(CH <sub>3</sub> ) <sub>2</sub> )	268 M <sup>+</sup> (7) 253 M <sup>+</sup> -Me (2) 153 M <sup>+</sup> -Ind (100) 115 Indenyl (8)
<b>8</b>	7.51-7.44 m (4H, Ar-H) 7.31-7.23 m (4H, Ind-H) 6.92 m (1H, C <sub>3</sub> -Ind) 6.60 m (1H, C <sub>2</sub> -Ind) 3.44 s (1H, C <sub>1</sub> -Ind) 0.46 s (3H, Si-CH <sub>3</sub> ) 0.44 s (3H, Si-CH <sub>3</sub> )	144.0 (C <sub>q</sub> ) 134.5 q (2C), 133.3, 132.5 (CH) 132.0, 131.5 (C <sub>q</sub> ) 126.8 (CH) 125.9 m (C <sub>q</sub> ) 124.5, 124.4 (CH) 124.3 m (C <sub>q</sub> , CF <sub>3</sub> ) 122.7, 121.0 q (2C), 39.0 (CH) 0.6 (Si(CH <sub>3</sub> ) <sub>2</sub> )	218 M <sup>+</sup> (5) 299 M <sup>+</sup> -F (1) 203 M-Ind (100) 115 Indenyl (12)
<b>9</b>	7.36 br (2H, Ar-H) 7.32 br (2H, Ar-H) 7.29 m (1H, C <sub>3</sub> -Ind) 7.12-7.07 m (4H) 3.36 s (2H, C <sub>1</sub> -Ind) 2.26 s (3H, Ar-CH <sub>3</sub> ) 0.40 br (6H, Si(CH <sub>3</sub> ) <sub>2</sub> )	147.3, 146.9, 145.4 (C <sub>q</sub> ) 142.1 CH (C <sub>3</sub> -Ind) 138.9, 134.6 (C <sub>q</sub> ) 133.9 (CH, 2C) 128.6 (CH, 2C) 126.2, 124.8, 123.6, 120.9 (CH) 42.6 (CH <sub>2</sub> , C <sub>1</sub> -Ind) 21.5 (Ar-CH <sub>3</sub> ) -2.4 (Si(CH <sub>3</sub> ) <sub>2</sub> )	264 [M <sup>+</sup> ] (6) 249 M <sup>+</sup> -Me (5) 149 M <sup>+</sup> -Ind (100) 115 Indenyl (38)
<b>10</b>	7.56-7.49 m (2H, Ar-H) 7.45 m (1H, C <sub>3</sub> -Ind) 7.33-7.16 (4H, Ind-H) 7.00-6.93 m (2H, Ar-H) 3.87 s (2H, C <sub>1</sub> -Ind) 3.85 s (3H, O-CH <sub>3</sub> ) 0.53 s (3H, Si-CH <sub>3</sub> ) 0.35 s (3H, Si-CH <sub>3</sub> )	160.6, 147.5, 145.4 (C <sub>q</sub> ) 142.0, 135.4 (2C) (CH) 130.9, 127.0 (C <sub>q</sub> ) 124.7 (2C), 124.5, 123.5, 122.9, 113.6 (CH) 54.9 (O-CH <sub>3</sub> ) 42.5 (CH <sub>2</sub> , C <sub>1</sub> -Ind) 0.9, -2.3 (Si(CH <sub>3</sub> ) <sub>2</sub> )	280 M <sup>+</sup> (3) 265 M <sup>+</sup> -Me (4) 165 M <sup>+</sup> -Ind (100) 115 Indenyl (20)

<b>11</b>	7.52 m (2H, Ar-H) 7.48 m (2H, Ar-H) 7.35 s (1H, C <sub>3</sub> -Ind) 7.28-7.24 m (2H) 7.16-7.10 m (2H) 3.51 s (2H, C <sub>1</sub> -Ind) 0.58 s (6H, Si(CH <sub>3</sub> ) <sub>2</sub> )	165.3 d, 146.8, 145.2, 146.6 (C <sub>q</sub> ) 142.4 (CH) 135.8 d (2C, CH) 134.9 d (C <sub>q</sub> ) 126.3 d (2C, CH) 125.0, 123.6, 121.0, 115.0 (CH) 42.5 (CH <sub>2</sub> , C <sub>1</sub> -Ind) -2.4 (Si(CH <sub>3</sub> ) <sub>2</sub> )	268 M <sup>+</sup> (20) 253 M <sup>+</sup> -Me (10) 152 M <sup>+</sup> -Ind (100) 114 Indenyl (11)
<b>12</b>	7.73-7.63 dd (4H, Ar-H) 7.60-7.46 m (2H) 7.35-7.26 m (2H) 7.25 s (1H, C <sub>3</sub> -Ind) 3.49 d ( <sup>3</sup> J = 1.7 Hz, 2H) 0.59 s (6H, Si(CH <sub>3</sub> ) <sub>2</sub> )	146.8, 145.6, 145.1, 141.1 (C <sub>q</sub> ) 142.9 (CH) 134.1 q (2C, CH) 132.4 q (C <sub>q</sub> ) 128.0 m (C <sub>q</sub> , CF <sub>3</sub> ) 126.4, 125.1, 124.3, 123.6 (CH) 121.0 q (2C, CH) 42.5 (CH <sub>2</sub> , C <sub>1</sub> -Ind) -2.7 (Si(CH <sub>3</sub> ) <sub>2</sub> )	318 M (5) 303 M <sup>+</sup> -Me (2) 203 M <sup>+</sup> -Ind (100) 115 Indenyl (7)

<sup>a</sup>  $\delta$  (ppm) rel. CHCl<sub>3</sub> (7.24 ppm, <sup>1</sup>H NMR) and rel. CDCl<sub>3</sub> (77.0 ppm, <sup>13</sup>C NMR) at 298 K.

### 2.1.5 Synthesis of the transition metal complexes

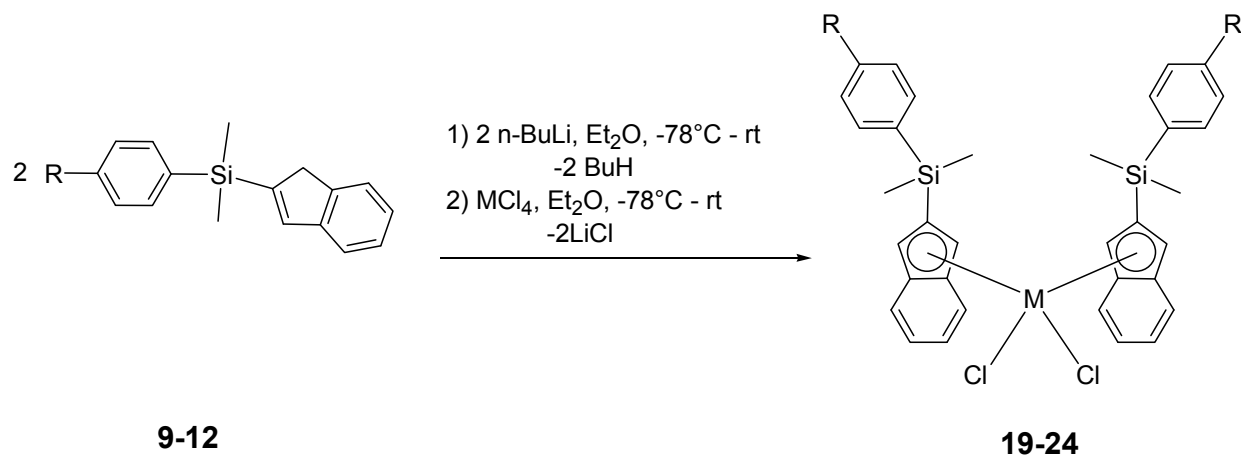
Two equivalents of the indenyl ligand precursors **5-8** were deprotonated by the addition of two equivalents of n-butyllithium (n-BuLi) in diethyl ether. Subsequent metallation reactions of the resulting lithiated ligands with one equivalent of zirconium tetrachloride or hafnium tetrachloride in diethyl ether yielded the desired metallocene complexes **13-18**. The general synthesis of these complexes is shown in Scheme 14.



No.	R	M
<b>13</b>	Me	Zr
<b>14</b>	Me	Hf
<b>15</b>	OMe	Zr
<b>16</b>	OMe	Hf
<b>17</b>	F	Zr
<b>18</b>	F	Hf

**Scheme 14:** Synthesis of the metallocene complexes **13-18**.

The 2-substituted silylindenyl complexes **19-24** were synthesized similarly. Thus, two equivalents of the 2-substituted indenyl compounds **9-12** were transformed to their lithium salts via deprotonation with n-BuLi. Following reactions with Zr(IV) or Hf(IV) chlorides in diethyl ether provided the desired complexes (Scheme 15). The complexes were obtained in moderate to high yields as fine powders. Reactions of the potential ligands **8** and **12** bearing trifluoromethyl substituents at the silyl groups with zirconium tetrachloride were futile and failed to yield the desired complexes under various reaction conditions. Instead, extremely air sensitive substances were obtained. The attempts to identify these residues were unsuccessful because of their insolubility in common organic solvents.



No.	R	M
<b>19</b>	Me	Zr
<b>20</b>	Me	Hf
<b>21</b>	OMe	Zr
<b>22</b>	OMe	Hf
<b>23</b>	F	Zr
<b>24</b>	F	Hf

**Scheme 15:** Synthesis of the metallocene complexes **19-24**.

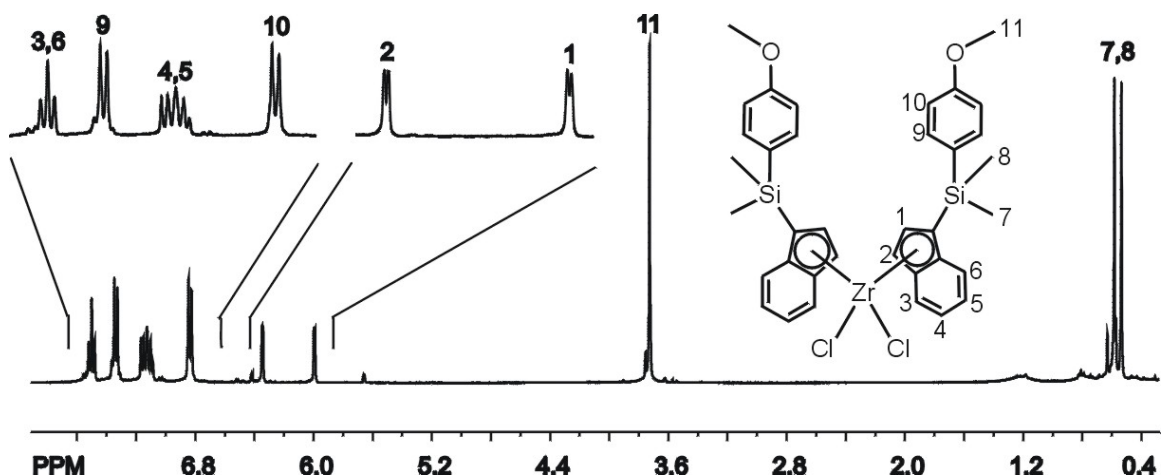
### 2.1.6 Characterization of the complexes

The complexes **13-24** were characterized with NMR spectroscopy, mass spectroscopy, and elemental analysis (see experimental part).

The silyl substituted bis(indenyl) metallocene complexes were characterized with  $^1\text{H}$  and  $^{13}\text{C}$  NMR spectroscopy (Table 3). The NMR spectra of few complexes exhibited the existence of two or more isomers. The  $^1\text{H}$  and  $^{13}\text{C}$  NMR spectra of complexes **15** and **20** are discussed as examples.

The  $^1\text{H}$  NMR spectrum of complex **15** (Scheme 16) shows two overlapping doublets at  $\delta = 7.50$  ppm [ $^3J = 7.8$  Hz, 4H] corresponding to the indene six-membered ring protons H3 and H6, while the signals of protons H4 and H5 appear at  $\delta = 7.16$ -7.10 ppm (dd, 4H). The aromatic phenyl protons H9 and H10 exhibit two signals: a doublet at  $\delta = 7.33$

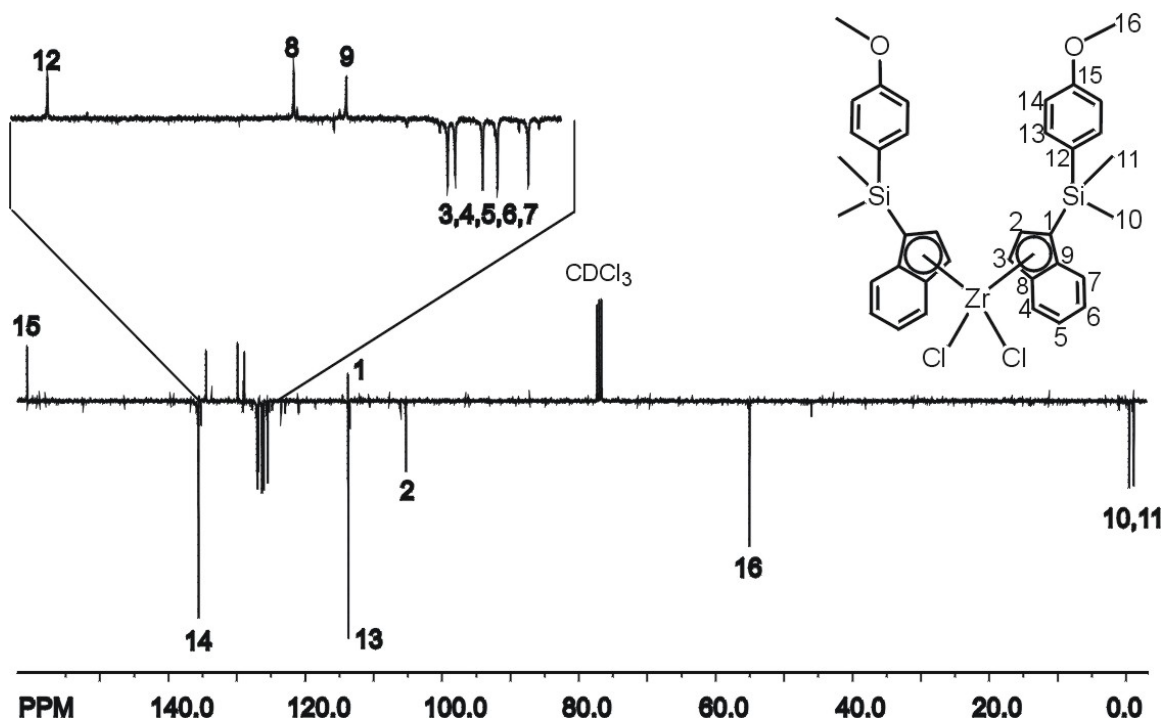
ppm ( $^3J = 7.9$  Hz, 4H) corresponding to H9 and a doublet at  $\delta = 6.83$  ppm ( $^3J = 7.9$  Hz, 4H) which could be assigned to H10. The protons at the 2-position of the indene ring (H1) gives rise to the doublet appearing at  $\delta = 6.34$  ppm ( $^3J = 3.0$  Hz, 2H) and the proton at the 3-position of the indene ring (H2) produces the doublet at  $\delta = 6.00$  ppm ( $^3J = 3.0$  Hz, 2H). The methoxy protons (C11) can be associated with the singlet that appears at  $\delta = 3.72$  ppm (6H), while the silyl methyl groups (H7 and H8) can be detected as two singlets appearing further upfield at  $\delta = 0.60$  and  $\delta = 0.53$  ppm (each with 6H intensity).



**Scheme 16:**  $^1\text{H}$  NMR spectrum of complex **15**.

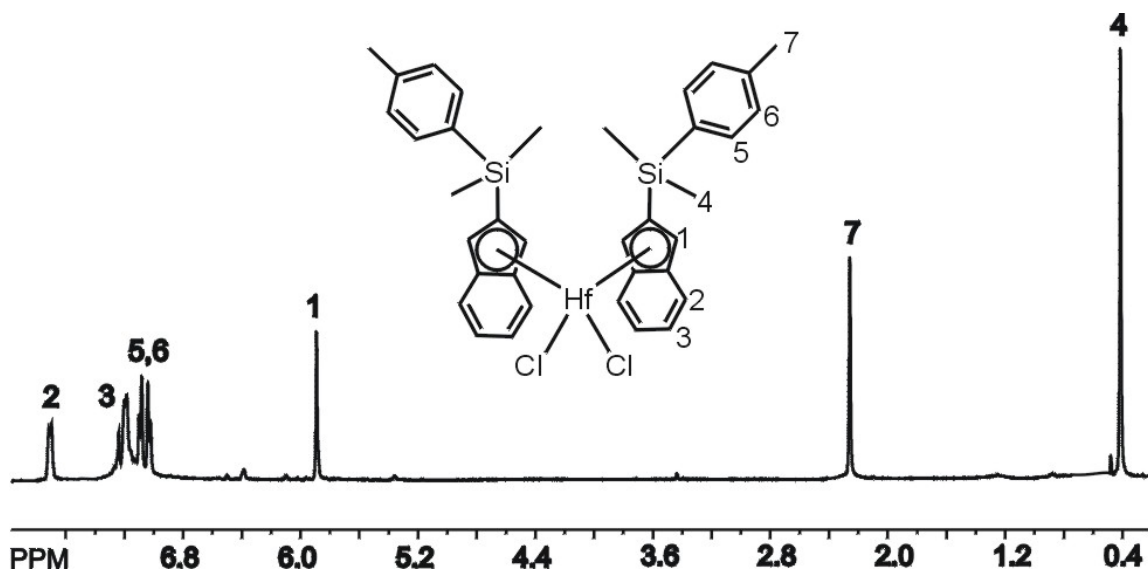
The  $^{13}\text{C}$  NMR spectrum of complex **15** (Scheme 17) exhibits sixteen resonance signals interpreted as followed: the signal far downfield at  $\delta = 160.6$  ppm is assigned to the quaternary carbon atom C15 bonded to the methoxy group. The doubly intensive signal appearing at  $\delta = 135.6$  ppm results from C14. The remaining quaternary carbon atoms C12, C8 and C9 afford the signals at  $\delta = 134.5$ , 129.9 and 128.9 ppm. At  $\delta = 127.0$ , 126.8, 126.3, 126.1, and 125.5 ppm, the CH-type carbon atoms C3, C4, C5, C6, and C7 appear, while the CH-type carbon atom C13 affords the signal at 113.7 ppm. The signal associated with the carbon atom at the 1-position of the indenyl moiety (C1) arises at  $\delta = 113.8$  ppm while the carbon atom at the 2-position of the indene ring (C2) is identified by the signal at  $\delta = 105.3$  ppm. The methoxy carbon atom (C16) is characterized by the

signal at  $\delta = 55.1$  ppm, while the two methyl groups attached to the silicon atom (C10 and C11) appear at  $\delta = -0.5$  and  $-1.1$  ppm.



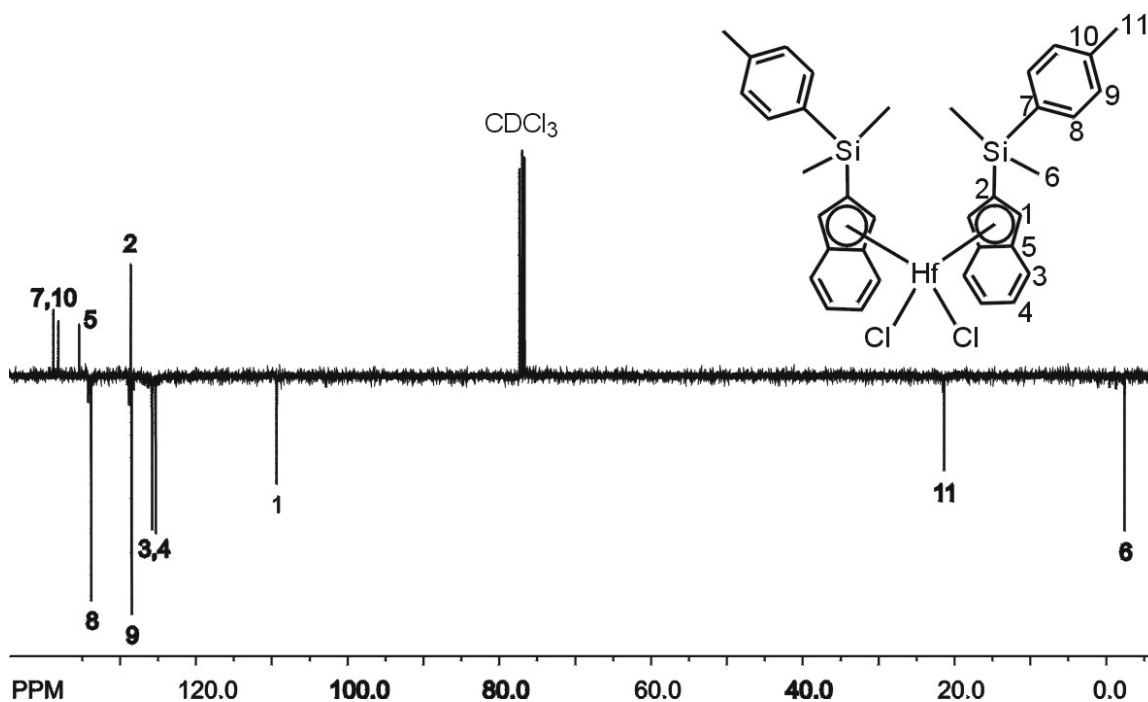
**Scheme 17:**  $^{13}\text{C}$  NMR spectrum of complex 15.

The  $^1\text{H}$  NMR spectrum of complex 20 (Scheme 18) shows a multiplet signal at  $\delta = 7.71$ - $7.69$  (4H) and a multiplet signal at  $\delta = 7.20$ - $7.18$  (4H) ppm assigned to the protons H2 and H3 of the 6-membered indene ring. The aromatic protons H5 and H6 give rise to two doublets which appear at  $\delta = 7.10$  ppm (d,  $^3J = 7.2$  Hz, 4H) and  $\delta = 7.02$  ppm (d,  $^3J = 7.2$  Hz, 4H). The singlet at  $\delta = 5.90$  ppm (s, 4H) is characteristic for the proton H1 at the indenyl moiety. The tolyl  $\text{CH}_3$  protons (H7) produce the signal at  $\delta = 2.25$  ppm (s, 6H) while the six equivalent protons of the silyl methyl groups (H4) appear further upfield at  $\delta = 0.41$  ppm (s, 12H).



**Scheme 18:** <sup>1</sup>H NMR spectrum of complex **20**.

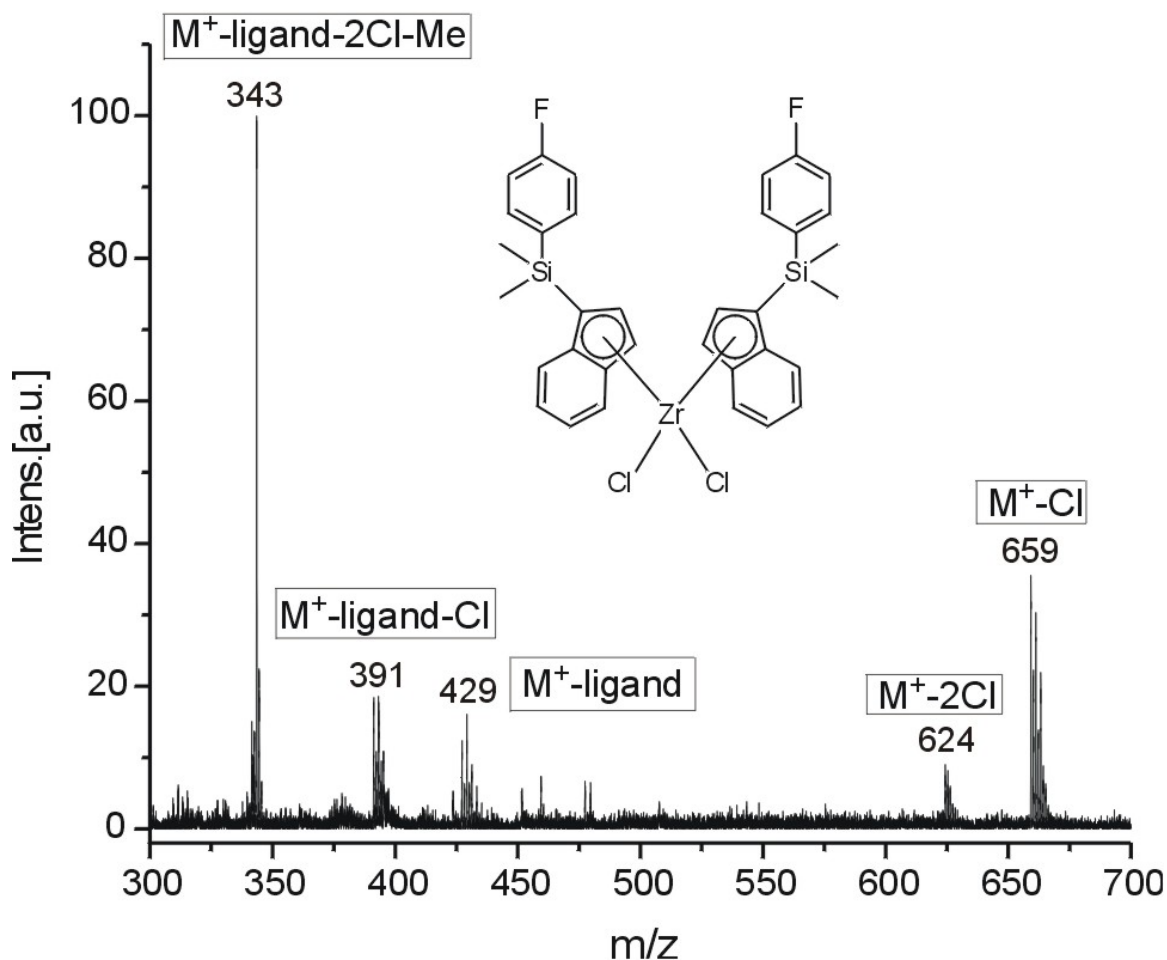
The <sup>13</sup>C NMR spectrum of complex **20** (Scheme 19) shows three signals downfield at  $\delta = 138.8$ ,  $138.1$  and  $135.4$  ppm assigned to the quaternary carbon atoms C7, C10, and C5. The two signals at  $\delta = 133.8$  and  $128.4$  ppm are associated with the CH-type carbon atoms of the phenyl ring of the silyl group (C8 and C9) while the CH-type carbons of the indene six-membered ring (C3 and C4) display signals at  $\delta = 125.8$  and  $125.3$  ppm. The quaternary carbon atom C2 gives rise to the signal at  $\delta = 128.6$  ppm. The signal at  $\delta = 109.3$  ppm is characteristic for the CH group carbon atom C1 located at the 1-position of the indenyl moiety. The methyl group at the para position to the silicon atom (C11) produces the signal at  $\delta = 21.3$  ppm, while the signal at  $\delta = -2.4$  ppm arises from the methyl groups attached to the silicon atom (C6). Due to the high symmetry of the complex (as well as for the other 2-indenyl substituted complexes), the NMR spectra are easier to evaluate compared with the spectra of the 1-substituted bis(indenyl) complexes.



**Scheme 19:**  $^{13}\text{C}$  NMR spectrum of complex **20**.

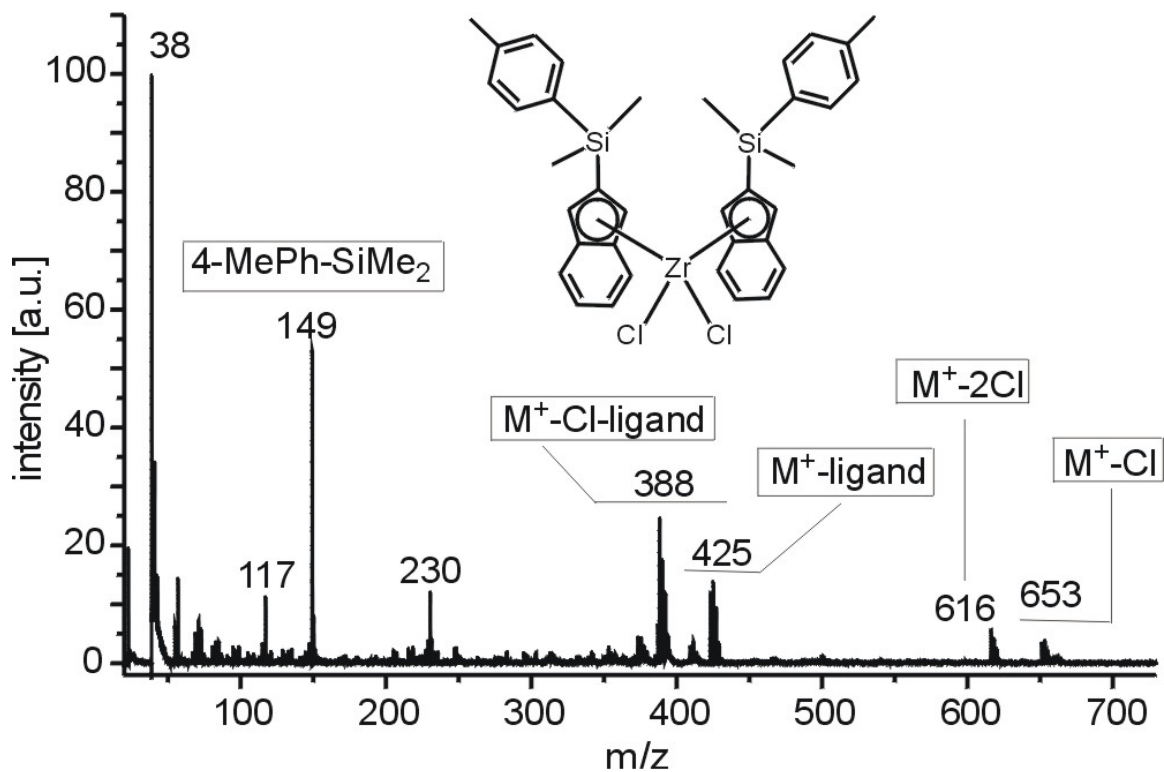
The mass spectrometrical characterization of 1- and 2-substituted bis(silylindenyl) complexes using a direct inlet mass spectrometer (EI, 70 eV) was unsuccessful. Using this high energy (70 eV) ionization technique, the molecules proved to break into smaller fragments. For instance, complex **17** when analyzed by mass spectroscopy (70 eV) exhibited only peaks corresponding to the fragment from the loss of one ligand ( $m/z = 425$ ). Accordingly, matrix-assisted laser desorption ionization (MALDI-TOF) was used as a milder ionization technique for mass spectra measurements.

The MALDI-TOF mass spectra of complexes **17** and **19** are discussed as representative examples. In the mass spectrum of the zirconium complex **17** (Scheme 20), the molecular ion peak is not observed. The ion formed by the loss of one chlorine atom  $[\text{M}^+ - \text{Cl}]$  produces the peak at  $m/z = 659$  with 36% intensity. Further loss of a second chlorine atom  $[\text{M}^+ - 2\text{Cl}]$  gives the peak at  $m/z = 624$  (intensity: 10%). The loss of one indenyl ligand from the complex molecule gives a peak at  $m/z = 429$  with 16% intensity, while further loss of a chlorine atom results in the peak at  $m/z = 391$  with 18% intensity. The base peak appears at  $m/z = 343$ .



**Scheme 20:** Mass spectrum of complex **17** obtained from MALDI-TOF analysis.

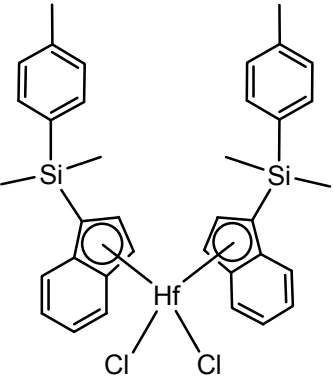
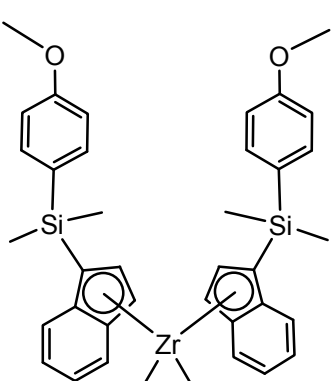
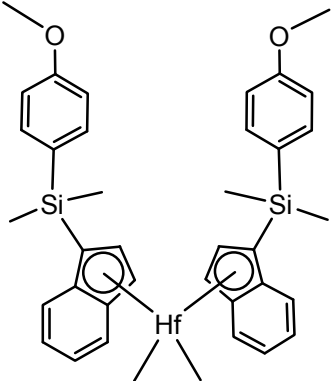
In the mass spectrum of complex **19** (Scheme 21) the molecular ion peak was again not observed. The peak at  $m/z = 653.1$  with 4% intensity could be explained by the loss of one chlorine atom from the molecule, while the peak at  $m/z = 616.4$  (6% intensity) is generated from the loss of two chlorine atoms. The loss of a ligand molecule gives rise to the peak at  $m/z = 425.3$  (15% intensity), further loss of a chlorine atom generates the peak at  $m/z = 388.3$  (25% intensity). The 4-tolyldimethylsilyl fragment gives the peak at  $m/z = 149.38$  with 55% intensity.

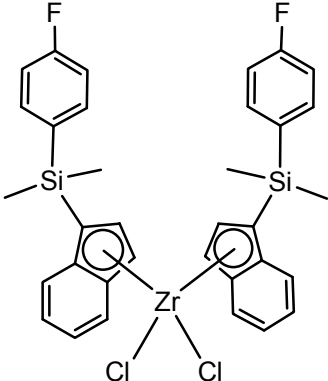
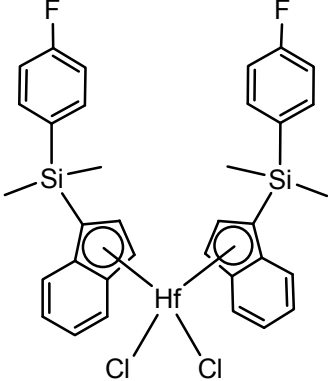
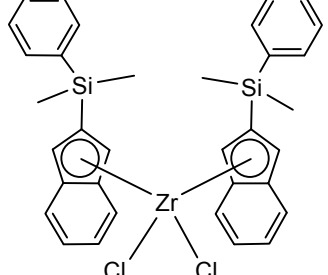
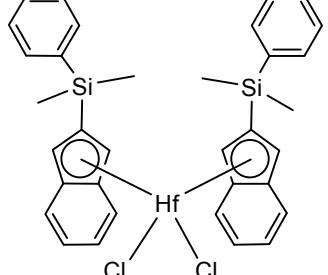


Scheme 21: Mass spectrum of complex 19.

Table 3:  $^1\text{H}$  and  $^{13}\text{C}$  NMR<sup>a</sup> spectra of complexes 13-24.

No.	Structure	$^1\text{H}$ NMR	$^{13}\text{C}$ NMR
13		7.52-7.46 m (4H) 7.30-7.28 m (4H) 7.13-7.06 m (8H) 6.3 br (2H, C <sub>3</sub> -Ind) 6.0 br (2H, C <sub>2</sub> -Ind) 2.3 s (6H, Ar-CH <sub>3</sub> ) 0.58 s (6H, Si-CH <sub>3</sub> ) 0.53 s (6H, Si-CH <sub>3</sub> )	139.3, 134.5, 134.4 (C <sub>q</sub> ) 134.2 (2C, Ar-CH) 130.0 (C <sub>q</sub> ) 128.8, 127.0, 126.8, 126.4, 126.1 (CH), 125.5 (2C, Ar-CH) 113.5 (C <sub>q</sub> , C <sub>1</sub> -Ind) 105.3 (CH, C <sub>2</sub> -Ind) 21.5 (Ar-CH <sub>3</sub> ) -0.6, -1.3 (Si(CH <sub>3</sub> ) <sub>2</sub> )

14		7.49-7.43 m (4H) 7.31-7.29 m (4H) 7.13-7.08 m (8H) 6.3 d ( $^3J = 2.8$ Hz, 2H, C <sub>3</sub> -Ind) 5.8 d ( $^3J = 2.8$ Hz, 2H, C <sub>2</sub> -Ind) 2.3 s (6H, Ar-CH <sub>3</sub> ) 0.6 s (6H, Si-CH <sub>3</sub> ) 0.5 s (6H, Si-CH <sub>3</sub> )	139.3, 134.5 (C <sub>q</sub> ) 134.2 (2C, Ar-CH) 133.5, 130.1 (C <sub>q</sub> ) 128.8, 126.9, 126.4, 126.3, 125.9 (CH), 125.5 (2C, Ar-CH) 110.1 (C <sub>q</sub> , C <sub>1</sub> -Ind) 102.8 (CH, C <sub>2</sub> -Ind) 21.5 (Ar-CH <sub>3</sub> ) -0.4, -1.2 (Si(CH <sub>3</sub> ) <sub>2</sub> )
15		7.50 d ( $^3J = 7.8$ Hz, 4H) 7.33 d ( $^3J = 7.9$ Hz, 4H, Ar-H) 7.16-7.10 dd (4H) 6.83 d ( $^3J = 7.9$ Hz, 4H, Ar-H) 6.33 d ( $^3J = 3.0$ Hz, 2H, C <sub>3</sub> -Ind) 6.00 d ( $^3J = 3.0$ Hz, 2H, C <sub>2</sub> -Ind) 3.72 s (6H, O-CH <sub>3</sub> ) 0.60 s (6H, Si-CH <sub>3</sub> ) 0.53 s (6H, Si-CH <sub>3</sub> )	160.6 (C <sub>q</sub> ) 135.6 (2C, CH) 134.5, 129.9, 128.9 (C <sub>q</sub> ) 127.0, 126.8, 126.3, 126.1, 125.5 (CH) 113.8 (C <sub>q</sub> , C <sub>1</sub> -Ind) 113.7 (2C, CH) 105.3 (CH, C <sub>2</sub> -Ind) 55.1 (O-CH <sub>3</sub> ) -0.5, -1.1 (Si(CH <sub>3</sub> ) <sub>2</sub> )
16		7.56-7.47 m (4H) 7.35 m (4H, Ar-H) 7.21 m (4H) 6.91 m (4H, Ar-H) 6.38 br (2H, C <sub>3</sub> -Ind) 6.05 br (2H, C <sub>2</sub> -Ind) 3.74 s (6H, O-CH <sub>3</sub> ) 0.61 s (6H, Si-CH <sub>3</sub> ) 0.53 s (6H, Si-CH <sub>3</sub> )	160.9 (C <sub>q</sub> ) 135.8 (2C, CH) 134.6, 129.7, 129.0 (C <sub>q</sub> ) 127.2, 126.9, 126.6, 126.3, 125.9 (CH) 111.2 (C <sub>q</sub> , C <sub>1</sub> -Ind) 113.9 (2C, CH) 102.7 (CH, C <sub>2</sub> -Ind) 55.1 (O-CH <sub>3</sub> ) -0.5, -1.0 (Si(CH <sub>3</sub> ) <sub>2</sub> )

17 <sup>b</sup>	 <p>Chemical structure of ZrCl<sub>2</sub>(Ind)<sub>2</sub>(SiMe<sub>2</sub>PhF)<sub>2</sub>. The zirconium center is coordinated to two chlorine atoms and two indenyl ligands. Each indenyl ligand is substituted with a dimethylsilyl group, which is further substituted with a p-fluorophenyl group.</p>	<p>7.46 br (4H, Ar-H)  7.30 br (4H, Ar-H)  7.10 m (2H)  6.89 m (2H)  6.34 m (2H)  6.20 m (2H)  6.03 m (2H, C<sub>3</sub>-Ind)  5.63 m (2H, C<sub>2</sub>-Ind)  0.53 s (6H, Si-CH<sub>3</sub>)  0.49 s (6H, Si-CH<sub>3</sub>)</p>	<p>163.9 d (C<sub>q</sub>, <sup>1</sup>J<sub>C-F</sub> = 247 Hz)  136.0 d (<sup>2</sup>J<sub>C-F</sub> = 7.3, CH-Ar, 2C)  133.6 d (C<sub>q</sub>, <sup>4</sup>J<sub>C-F</sub> = 3.8 Hz, C-F)  130.0, 128.5 (C<sub>q</sub>)  127.6, 127.0, 126.3, 125.8, 125.3 (CH)  114.9 d (<sup>3</sup>J<sub>C-F</sub> = 19.8 Hz, CH-Ar, 2C)  113.8 (C<sub>q</sub>, C<sub>1</sub>-Ind)  106.1 (CH, C<sub>2</sub>-Ind)  -0.5, -0.9 (Si(CH<sub>3</sub>)<sub>2</sub>)</p>
18	 <p>Chemical structure of HfCl<sub>2</sub>(Ind)<sub>2</sub>(SiMe<sub>2</sub>PhF)<sub>2</sub>. The hafnium center is coordinated to two chlorine atoms and two indenyl ligands. Each indenyl ligand is substituted with a dimethylsilyl group, which is further substituted with a p-fluorophenyl group.</p>	<p>7.50 dd (4H)  7.32 t (4H)  7.13 d (4H)  6.95 t (4H)  6.25 d (<sup>3</sup>J = 3.2 Hz, 2H, C<sub>3</sub>-Ind)  5.94 d (<sup>3</sup>J = 2.8 Hz, 2H, C<sub>2</sub>-Ind)  0.58 s (6H, Si-CH<sub>3</sub>)  0.57 s (6H, Si-CH<sub>3</sub>)</p>	<p>163.8 d (C<sub>q</sub>, <sup>1</sup>J<sub>C-F</sub> = 248 Hz, C-F)  136.0 d (<sup>2</sup>J<sub>C-F</sub> = 7.3, Ar-CH, 2C)  133.9 d (C<sub>q</sub>, <sup>4</sup>J<sub>C-F</sub> = 3.8 Hz, C-F)  133.4, 128.6 (C<sub>q</sub>)  127.2, 126.9, 126.4, 126.0, 125.3 (CH)  115.0 d (<sup>3</sup>J<sub>C-F</sub> = 19.5 Hz, Ar-CH, 2C)  110.7 (C<sub>q</sub>, C<sub>1</sub>-Ind)  102.8 (CH, C<sub>2</sub>-Ind)  0.6, -1.1 (Si(CH<sub>3</sub>)<sub>2</sub>)</p>
19	 <p>Chemical structure of ZrCl<sub>2</sub>(Ind)<sub>2</sub>(SiMe<sub>2</sub>PhMe)<sub>2</sub>. The zirconium center is coordinated to two chlorine atoms and two indenyl ligands. Each indenyl ligand is substituted with a dimethylsilyl group, which is further substituted with a p-tolyl group.</p>	<p>7.65-7.63 m (4H)  7.11-7.09 m (4H)  7.04-6.95 dd (8H, Ar-H)  5.96 s (4H, C<sub>1</sub>-Ind)  2.19 s (6H, Ar-CH<sub>3</sub>)  0.35 s (12H, Si-CH<sub>3</sub>)</p>	<p>138.7, 138.4, 135.2 (C<sub>q</sub>)  133.7 (CH)  129.3 (C<sub>q</sub>)  128.4, 125.7, 125.4, 112.3 (CH)  21.3 (Ar-CH<sub>3</sub>)  -2.5 (CH<sub>3</sub>, Si(CH<sub>3</sub>)<sub>2</sub>)</p>
20	 <p>Chemical structure of HfCl<sub>2</sub>(Ind)<sub>2</sub>(SiMe<sub>2</sub>PhMe)<sub>2</sub>. The hafnium center is coordinated to two chlorine atoms and two indenyl ligands. Each indenyl ligand is substituted with a dimethylsilyl group, which is further substituted with a p-tolyl group.</p>	<p>7.71-7.69 m (4H)  7.20-7.18 m (4H)  7.10 d (<sup>3</sup>J = 7.2 Hz, 4H, Ar-H)  7.02 d (<sup>3</sup>J = 7.2 Hz, 4H, Ar-H)  5.90 s (4H, C<sub>1</sub>-Ind)  2.25 s (6H, Ar-CH<sub>3</sub>)  0.41 s (12H, SiCH<sub>3</sub>)</p>	<p>138.8, 138.1, 135.4 (C<sub>q</sub>)  133.8 (CH)  128.6 (C<sub>q</sub>)  128.4, 125.8, 125.3, 109.3 (CH)  21.3 (Ar-CH<sub>3</sub>)  -2.4 (Si(CH<sub>3</sub>)<sub>2</sub>)</p>

21		7.34-7.27 m (8H) 7.00-6.92 m (8H) 6.11 s (4H, C <sub>1</sub> -Ind) 3.84 s (6H, O-CH <sub>3</sub> ) 0.10 s (12H, SiCH <sub>3</sub> )	159.7, 144.9, 144.0 (C <sub>q</sub> ) 129.4 (CH) 129.2 (C <sub>q</sub> ) 126.3, 126.0, 120.6, 113.9 (CH) 55.1 (O-CH <sub>3</sub> ) 2.1 (Si(CH <sub>3</sub> ) <sub>2</sub> )
22		7.40-7.32 m (8H) 7.09-7.01 m (8H) 6.16 s (4H, C <sub>1</sub> -Ind) 3.84 s (6H, O-CH <sub>3</sub> ) 0.11 s (12H, SiCH <sub>3</sub> )	160.0, 145.0, 144.1 (C <sub>q</sub> ) 129.7 (CH) 129.1 (C <sub>q</sub> ) 126.4, 126.0, 120.8, 114.3 (CH) 55.2 (O-CH <sub>3</sub> ) 2.1 (Si(CH <sub>3</sub> ) <sub>2</sub> )
23 <sup>b</sup>		7.42 m (4H, Ar-H) 7.29-7.13 m (8H) 7.07 m (4H, Ar-H) 6.20 s (4H, C <sub>1</sub> -Ind) 0.08 s (12H, SiCH <sub>3</sub> )	164.1 d ( <sup>1</sup> J <sub>C-F</sub> = 253 Hz, C <sub>q</sub> ) 144.7 d ( <sup>4</sup> J <sub>C-F</sub> = 3.6 Hz, C <sub>q</sub> ) 143.4 (C <sub>q</sub> ) 135.7 d ( <sup>2</sup> J <sub>C-F</sub> = 7.9 Hz, Ar-CH) 132.8 (C <sub>q</sub> ) 129.4, 125.0 (CH) 115.0 d ( <sup>3</sup> J <sub>C-F</sub> = 19.5 Hz, Ar-CH) 105.3 (CH, C <sub>1</sub> -Ind) -4.0 (Si(CH <sub>3</sub> ) <sub>2</sub> )
24 <sup>b</sup>		7.43 m (4H, Ar-H) 7.28-7.16 m (8H) 7.05 m (4H, Ar-H) 5.90 s (4H, C <sub>1</sub> -Ind) 0.45 s (12H, SiCH <sub>3</sub> )	163.5 d ( <sup>1</sup> J <sub>C-F</sub> = 254 Hz, C <sub>q</sub> ) 138.2 d ( <sup>4</sup> J <sub>C-F</sub> = 3.6 Hz, C <sub>q</sub> ) 136.0 d ( <sup>2</sup> J <sub>C-F</sub> = 6.9 Hz, Ar-CH) 133.5, 128.6 (C <sub>q</sub> ) 126.0, 125.7 (CH) 115.0 d ( <sup>3</sup> J <sub>C-F</sub> = 19.5 Hz, CH) 109.1 (CH, C <sub>1</sub> -Ind) -2.3 (Si(CH <sub>3</sub> ) <sub>2</sub> )

<sup>a</sup>  $\delta$  (ppm) rel. CHCl<sub>3</sub> (7.24 ppm, <sup>1</sup>H NMR) and rel. CDCl<sub>3</sub> (77.0 ppm, <sup>13</sup>C NMR) at 298 K.

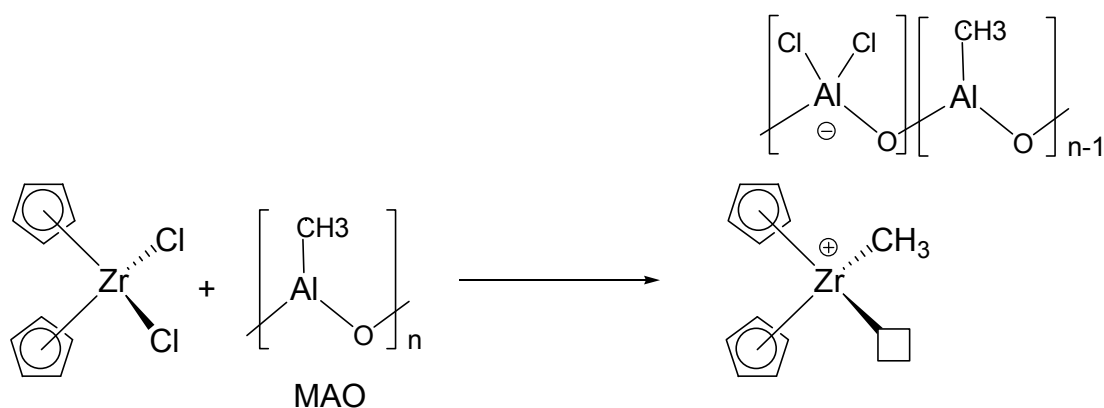
<sup>b</sup> Two isomers.

## 2.1.7 Ethylene polymerization experiments

### 2.1.7.1 General aspects and mechanism

Metallocene dichloride complexes of group (IV) metals are very important candidates in catalysis because they can facilitate the polymerization of olefins when treated with a suitable activator. Methylaluminoxane (MAO), among other activators, is the most commonly used cocatalyst for this purpose.

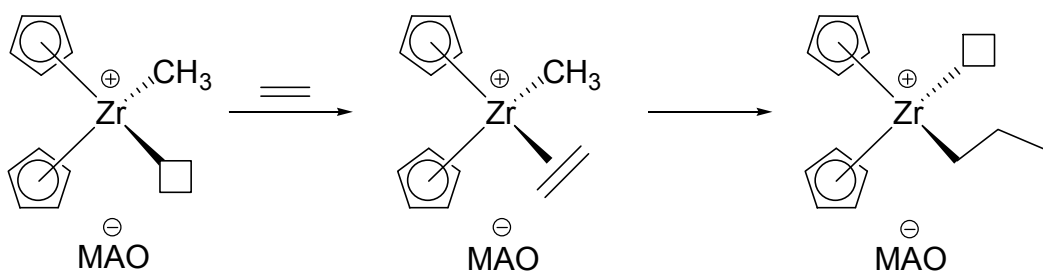
The activation of a metallocene precatalyst proceeds by substitution of one chloro ligand with a methyl group followed by abstraction of the remaining chloro ligand. Consequently, an active metal center with a vacant coordination site (14 electron species) is generated which is often assumed to be  $(L)_2M^+-R$  ( $L$  = cyclopentadienyl, indenyl, fluorenyl). The latter is considered as the active species and can react as a strong Lewis acid capable to react with  $\pi$ -electrons of the incoming ethylene monomer.<sup>[19]</sup>



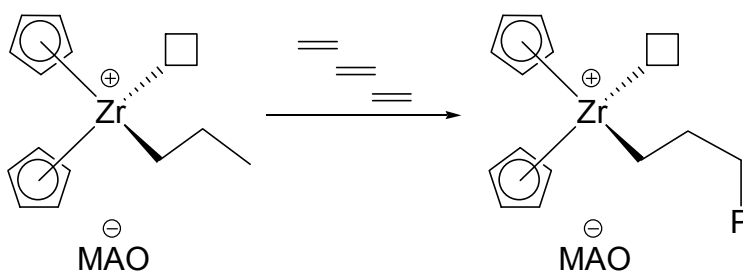
**Scheme 22:** Activation of a metallocene catalyst with MAO.

The homogeneous metallocene-based polymerization of olefins using methylaluminoxane (MAO) as a cocatalyst can be explained by a mechanism first reported by Cossee<sup>[21]</sup> and Arlman<sup>[22,23]</sup> for mechanistic studies of the traditional Ziegler-Natta catalysts. The proposed mechanism involves three steps: initiation, propagation and chain termination (Scheme 23).

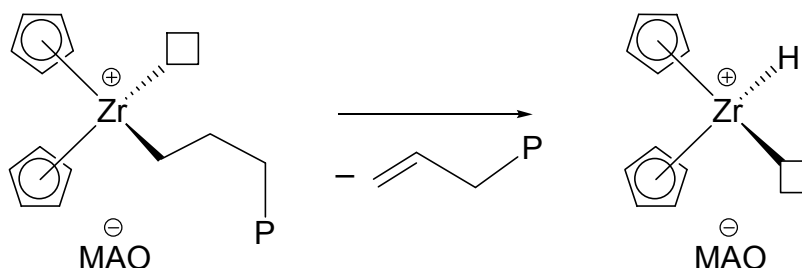
The initiation step essentially represents the insertion of the first ethylene molecule into the M–CH<sub>3</sub> bond of the catalyst cation. The ethylene molecule coordinates to the metal through its  $\pi$ -electrons giving rise to an  $\eta^2$ -ethylene complex. The propagation step starts with further insertions of ethylene molecules followed by migration of the chain to the newly  $\pi$ -coordinated ethylene providing a new vacant site to repeat the insertion process. Finally, the growth of the polymer chain is terminated by  $\beta$ -hydrogen elimination or chain transfer to the cocatalyst.



a) Initiation step



b) Chain propagation



c) Chain termination

**Scheme 23:** Cossee-Arlman mechanism of ethylene polymerization: a) initiation step, b) chain propagation, and c) chain termination.

### 2.1.7.2 Ethylene polymerization activities of complexes 13-18

The catalyst precursors **13-18** are unbridged indenyl metallocene complexes bearing phenyl substituted silyl groups at the 1-position of the indenyl ligands. Ethylene polymerization reactions were carried out in a 1 liter Büchi steel reactor using 250 ml of pentane and MAO as co-catalyst (M:Al = 1:2000) at a polymerization temperature of 60°C and 10 bar ethylene pressure. The catalytic activities of complexes **13-18** are shown in Table 4.

**Table 4:** Ethylene polymerization activities of complexes **13-18**.

Structure	No.	M	R	Activity <sup>a</sup>
	<b>13</b>	Zr	Me	3980
	<b>14</b>	Hf	Me	1760
	<b>15</b>	Zr	MeO	490
	<b>16</b>	Hf	MeO	50
	<b>17</b>	Zr	F	4475
	<b>18</b>	Hf	F	1755

<sup>a</sup> (kg PE/mol cat. h)

In the catalysts series **13-18**, the zirconium catalyst **17** bearing fluoro substituents at the phenyl silyl groups was the most active catalyst (4475 kg PE/mol cat. h), whereas the hafnium catalyst **16** containing a methoxy phenyl silyl group showed the lowest activity (50 kg PE/mol cat. h). The variation in the activities of **13-18** correlates well with the steric bulk of the substituents (Me, MeO, and F) rather than their electronic properties. For instance, the complexes **13** and **17** showed comparable activities despite the big difference in the electronic nature of methyl and fluoro groups. This trend is even more obvious for complexes **14** and **18**. This can give an indication that the electronic nature of methyl and fluoro substituents seems to have a minor effect on the activity of the corresponding catalysts and that only their similar steric contribution accounts for their comparable activities. In a similar trend, a study carried out by Grimmer<sup>[72]</sup> has

demonstrated that the activity variation in ethylene polymerization of a series of 1- and 2-substituted indenyl complexes can be mainly rationalized by steric reasons. The activities observed for the complexes **13-18** were, as anticipated, lower than the activity recorded for the unsubstituted metallocene complex  $\text{Ind}_2\text{ZrCl}_2$  [29300 kg PE/mol Zr h] under similar polymerization conditions<sup>[77]</sup>. However, the activities in the homopolymerization of ethylene of **14** and **17** are significantly higher than the activities recently reported<sup>[73]</sup> for similar metallocene catalysts comprising silyl-substituted ligands;  $[\text{1-(SiMe}_3\text{)indenyl}]_2\text{ZrCl}_2$  (300 kg PE/mol Zr h) and  $[\text{1-(Me}_2\text{SiPh)indenyl}]_2\text{ZrCl}_2$  (2570 kg PE/mol Zr h). This behaviour reveals that the electronic effect of the aromatic phenyl ring of the synthesized catalysts enhances their activity.

The polymerization activities of the 1-substituted catalysts **13-18** (Table 4) are generally lower than the activity values observed for the analogous 1-benzyl substituted catalyst<sup>[78]</sup> and the 1-(4-fluorobenzyl) substituted catalyst.<sup>[55]</sup>

The hafnium complexes in this series of catalysts exhibited significantly lower activities compared with their zirconium analogues which could be explained by the thermodynamically more stable metal carbon  $\sigma$ -bond between hafnium and the polymer chain (Hf-C) or due to kinetic reasons.<sup>[79]</sup>

The catalysts **15** and **16** bearing methoxy groups exhibited comparatively lower activities compared with the other catalysts. However, these activity values are consistent and comparable with the activity values noted for other similar catalysts incorporating heteroatom substituted ligands<sup>[80]</sup>. The inefficiency of these types of catalysts can be attributed to the poisoning effect resulting from intermolecular interactions of the lone pair electrons at the heteroatoms with the cationic metal centers or the cocatalyst (Lewis base-Lewis acid interaction).

### 2.1.7.3 Ethylene polymerization activities of complexes 19-24

Complexes **19-24** are a series of unbridged symmetrical 2-substituted silylindenyl complexes of zirconium and hafnium. The bulky silyl substituents bear an electron withdrawing atom (F), an electron donating group (Me), and an electron donating group with lone pair of electrons (O-Me) at the para position to the silicon atom. Ethylene polymerization reactions were carried out in a 1 liter Büchi steel reactor using 250 ml of

pentane and MAO as the cocatalyst (M:Al = 1:2000) at a polymerization temperature of 60°C and 10 bar ethylene pressure. The catalytic activities of complexes **20-25** are presented in Table 5.

**Table 5:** Ethylene polymerization activities of complexes **19-24**.

Structure	No.	M	R	Activity <sup>a</sup>
	<b>19</b>	Zr	Me	870
	<b>20</b>	Hf	Me	770
	<b>21</b>	Zr	MeO	940
	<b>22</b>	Hf	MeO	60
	<b>23</b>	Zr	F	510
	<b>24</b>	Hf	F	3700

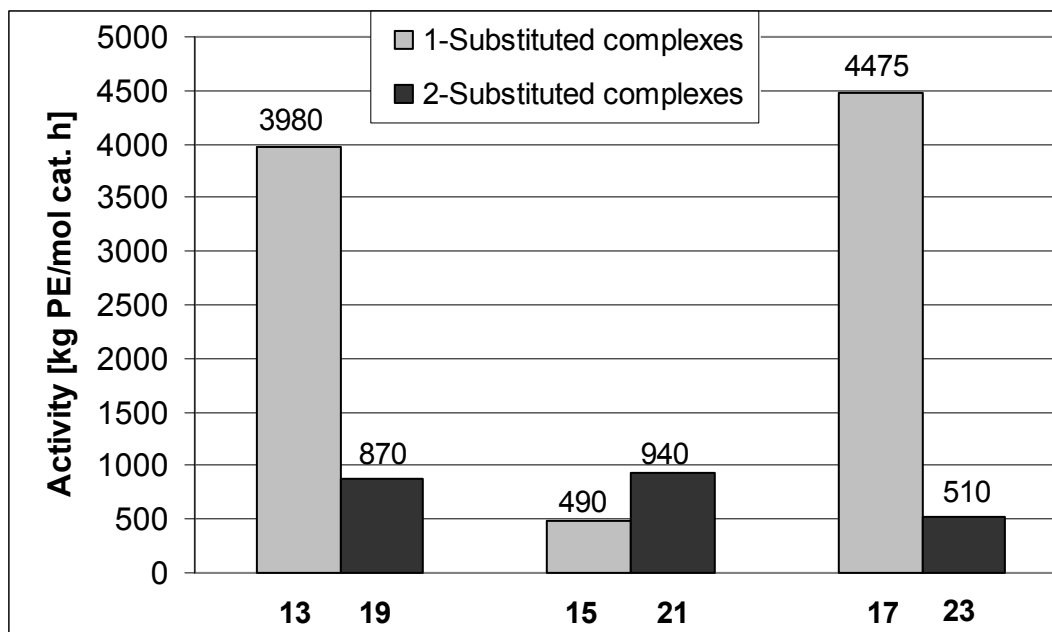
<sup>a</sup> (kg PE/mol cat. h)

Among this series, the highest activity was achieved by the hafnium complex **24** containing a fluorine atom at the silyl group, while complex **22** bearing a methoxy group showed the lowest activity (60 kg PE/ mol cat. h). This result can again be explained by the fact that the methoxy group attached to the silicon atom is a Lewis base due to the presence of free electron pairs at the oxygen atom. These lone pairs of electrons can interact with the metal centers resulting in blocking the active sites and substantial deactivation of the catalyst.<sup>[80]</sup> It is worthy to note that the hafnium complex **24** is, surprisingly, seven times more active than the zirconium complex **23** of the same ligand. The zirconium and hafnium complexes **19** and **20** displayed almost similar activities. This unusual catalytic behaviour is very different from the general recognition that Zr-based catalysts show higher activities and could be attributed to the high bulkiness of the silyl groups at the 2-positions, making the other parameter, such as the nature of central metal, less dominant in activity reasons. Among the synthesized 2-substituted catalysts, catalyst **24**/MAO exhibited a higher activity compared with the previously reported 2-trimethylsilyl and 2-dimethylphenylsilyl substituted catalysts<sup>[73]</sup>, but was

significantly lower active than the 2-benzyl and 2-alkyl substituted catalysts<sup>[72]</sup>. In a comparison with the unsubstituted metallocene catalyst  $\text{Ind}_2\text{ZrCl}_2$  the catalyst precursors **19-24**, demonstrated lower polymerization activities.<sup>[77]</sup>

#### 2.1.7.4 Comparison between the polymerization activities of 1- and 2-substituted zirconocenes

The zirconium complexes **19**, **21** and **23** bear different silyl groups at position 2 of the indenyl moiety. On the other hand, the zirconium complexes **13**, **15** and **17** bear the same silyl groups at position 1 of the indenyl framework. Among this series of catalysts, the position at which the substituents are attached to the indenyl rings has proved to possess a significant influence on the activities. For instance, catalyst **13**/MAO bearing a methyl phenyl substituted silyl group at position 1 displayed an almost five times higher activity than the catalyst **19**/MAO bearing the same substituent at position 2. The same trend was observed for complexes **23** and **17** bearing a fluoro substituted phenyl silyl group.



**Scheme 24:** Comparison of the polymerization activities of 1- and 2-substituted zirconocene complexes bearing the same silyl substituents.

This pattern indicates that 1-substituted indenyl complexes are much more active in ethylene polymerization than their 2-substituted counterparts. This behavior may be explained in the way that the same silyl substituent in position 2 can exert more steric hindrance around the metal center compared to the 1-substituted analogues.

### 2.1.7.5 Polymer analysis

The produced polyethylene samples were analyzed by differential scanning calorimetry (DSC) and viscosimetry. The results of the polymer analyses are summarized in Table 6.

**Table 6:** DSC and viscosimetry molecular weight analysis of polyethylenes produced with complexes **13-24**

Complex	$\Delta H_m$ [J/g]	$T_m$ [°C]	Crystallinity [ $\alpha$ ]	$M_n$ [g/mol]
<b>13</b>	162.3	135.4	0.56	292000
<b>14</b>	151.2	136.2	0.52	355000
<b>15</b>	141.9	135.5	0.49	n.d.
<b>16</b>	142.0	136.2	0.49	n.d.
<b>17</b>	152.7	136.9	0.53	270000
<b>18</b>	141.7	135.9	0.49	535000
<b>19</b>	169.2	135.4	0.58	265000
<b>20</b>	144.9	135.2	0.50	445000
<b>21</b>	158.5	137.5	0.55	350000
<b>22</b>	138.9	135.0	0.48	n.d.
<b>23</b>	151.1	135.4	0.52	385000
<b>24</b>	130.8	137.3	0.45	n.d.

From DSC analyses of the polyethylene samples no significant differences in the melting points were observed. However, molecular weight measurements showed that the molecular weights of polymers produced with hafnium complexes are significantly higher than those of the polymers produced with the analogous zirconium complexes.

This could be attributed to the thermodynamically more stable bond between hafnium and the polymer chain.<sup>[79]</sup>

The crystallinity values were obtained from the following equation:  $\alpha = \Delta H_m / \Delta H_{m,0}$  with  $\Delta H_{m,0} = 290$  J/g extrapolated for 100% crystalline polyethylene.<sup>[81]</sup> While the molecular weights of the hafnium catalyzed polyethylene samples were higher compared with the zirconium catalyzed polymers, the opposite trend could be observed for the crystallinity values.

## 2.2 1,2-Bis(dimethylsilyl)phenylidene-bridged zirconocene and hafnocene dichloride complexes

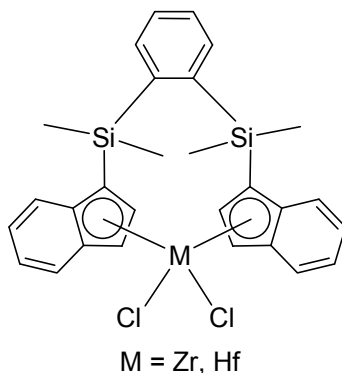
### 2.2.1 General remarks

A wide range of bridged bis(indenyl) metallocene complexes has been synthesized and tested as catalyst precursors for olefin polymerization. These complexes include different bridging-type moieties. However, the most commonly used bridges are the dimethylsilylene, ethylene, isopropylidene, and methylene units.<sup>[26,28,82-86]</sup>

The structure of the bridging unit in ansa metallocene complexes has a strong influence on the catalyst activity and the molecular weight of the generated polymers.<sup>[87]</sup> The activity can be improved by enlarging the reaction space around the metal center, mainly by increasing the metal-centroid distance and the dihedral angle between the two indenyl based  $\pi$ -ligands.

In contrast to silylene and alkylidene bridged metallocene complexes, few examples of ansa-metallocene complexes are known containing bulky aromatic groups as bridges. For instance, *o*-xylidene- and naphthylidene-bridged catalysts have recently been synthesized and evaluated as catalysts for ethylene and propylene polymerization after activation with MAO.<sup>[88,89]</sup>

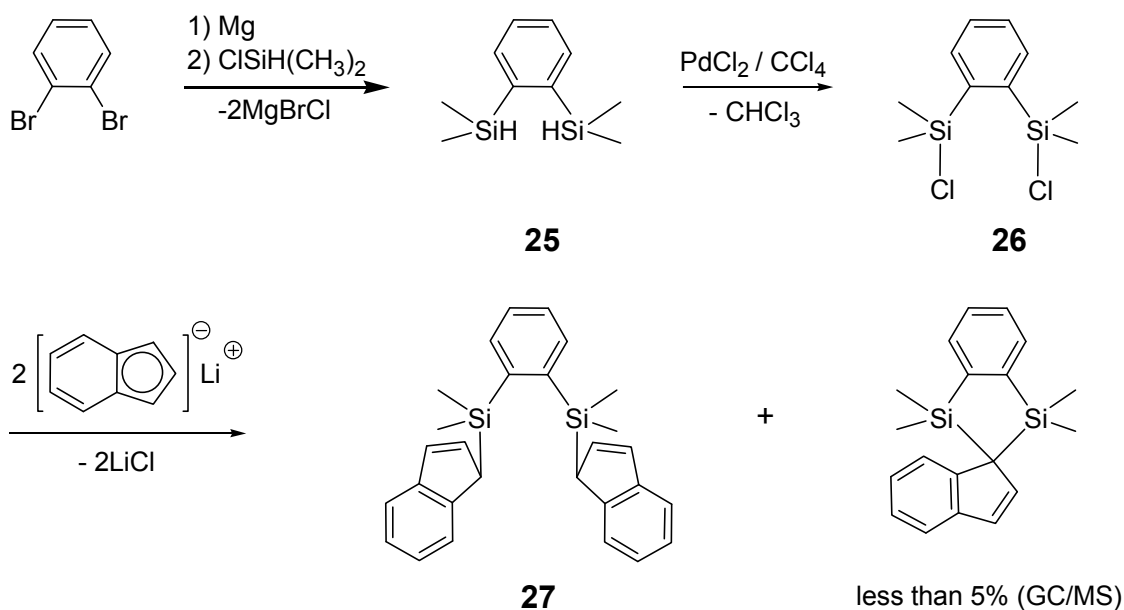
Herein, a synthesis of new ansa-complexes of zirconium and hafnium is described, which possess two indenyl ligands that are linked through a 1,2-bis(dimethylsilyl)phenylidene bridge (Scheme 25), together with a study of their catalytic behavior in the homogeneous polymerization of ethylene.



**Scheme 25:** General structural formula of the metallocene complexes **34** and **35**.

### 2.2.2 Synthesis of the ligand precursor

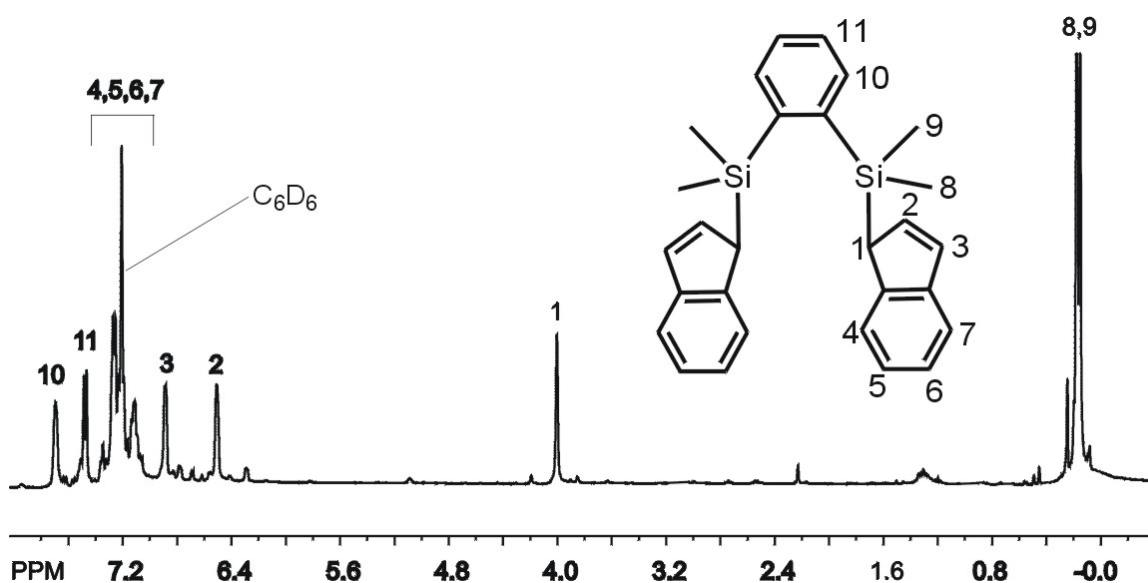
1,2-Bis(inden-1-yl)dimethylsilyl)benzene **27** was prepared via a three steps method that comprises a Grignard coupling of 1,2-dibromobenzene with chlorodimethylsilane to give 1,2-bis(dimethylsilyl)benzene (**25**), followed by chlorination with carbon tetrachloride in the presence of a catalytic amount of palladium dichloride to obtain 1,2-bis(chlorodimethylsilyl)benzene (**26**).<sup>[90]</sup> The desired compound was readily prepared by the reaction of compound **26** with two equivalents of indenyllithium (prepared separately via reaction of indene and n-butyllithium in ether) (Scheme 26). This reaction was necessarily conducted in ether at room temperature. If another solvent such as THF is used, the undesired monoindenyl spiro compound is formed as a side product. This proceeds by the deprotonation at the C1-position in the already silyl-bonded indene followed by an intramolecular reaction with the chlorine atom of the same molecule leading to the formation of the cyclic mono substituted indenyl derivative with a  $sp^3$ -hybridized carbon atom. Compound **27** was initially obtained with trace amounts of the monoindenyl-substituted derivative as side product. Thus, the purity was improved via prolonged evacuation at elevated temperature.



**Scheme 26:** Three-step synthesis of compound **27**.

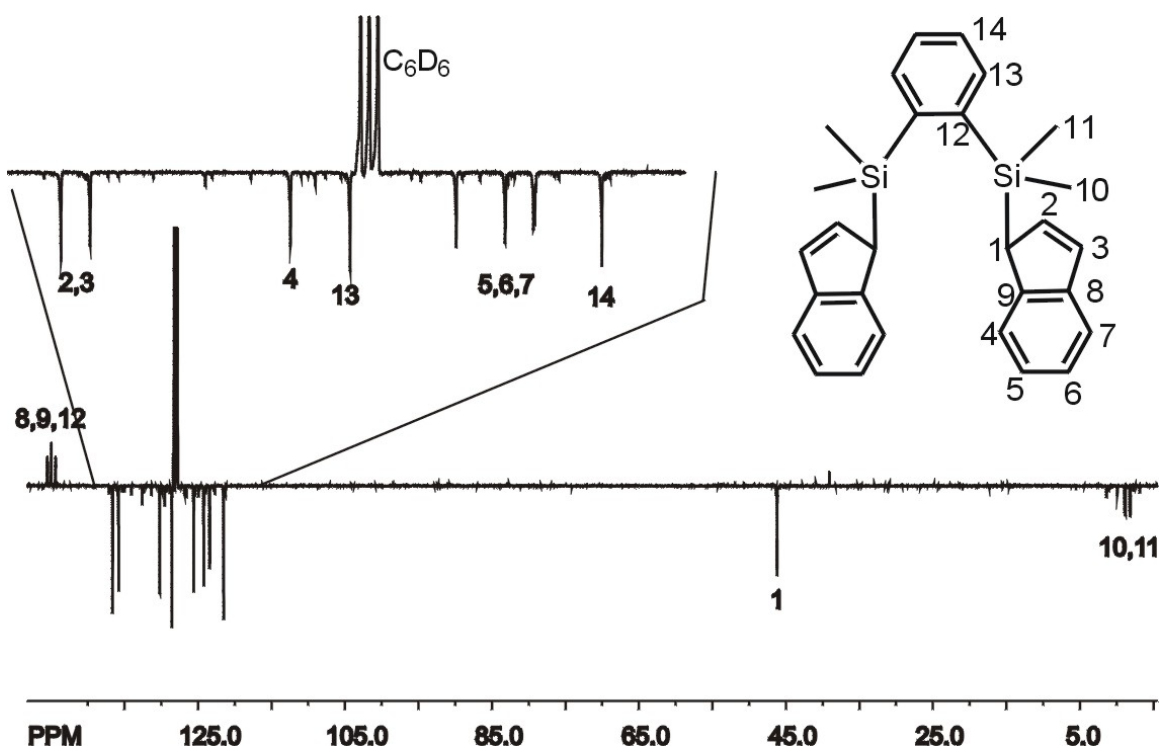
### 2.2.3 Characterization of compound 27

Compound **27** was characterized by  $^1\text{H}$  NMR,  $^{13}\text{C}$  NMR and GC/MS (Table 7). The  $^1\text{H}$  NMR spectrum of compound **27** (Scheme 27) shows multiplet signals at  $\delta = 7.76\text{-}7.73$  (m, 2H),  $7.50\text{-}7.46$  (m, 2H),  $7.29\text{-}7.26$  (m, 4H) and  $7.14\text{-}7.09$  ppm (m, 4H) for the aromatic protons of both the bridge and the indenyl moiety (H10, H11, H4, H5, H6 and H7). The two signals appearing at  $\delta = 6.96$  (d,  $^3J(\text{H,H}) = 5.2$  Hz, 2H) and  $6.57$  ppm (dd, 2H) can be attributed to the protons at the 3- and 2-positions of the indenyl moiety (H3 and H2). The protons at the 1-positions of the indenyl moieties (H1) produce the signal at  $\delta = 4.00$  ppm (s, 2H) while the signal for the silyl protons (H8 and H9) appears at  $\delta = 0.20$  ppm (s, 12H).



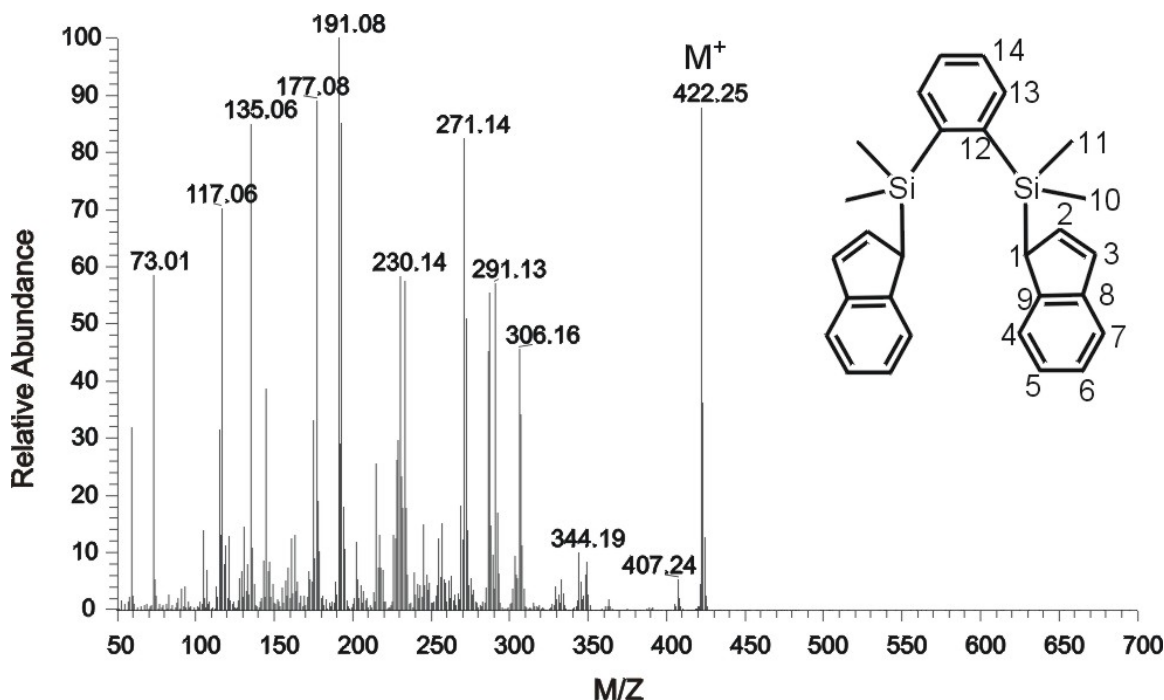
Scheme 27:  $^1\text{H}$  NMR spectrum of compound **27**.

The  $^{13}\text{C}$  NMR spectrum of compound **27** (Scheme 28) shows three resonance signals at  $\delta = 145.0$ ,  $144.4$  and  $144.0$  ppm attributed to the quaternary carbon atoms C8, C9, and C12. The two signals at  $\delta = 136.2$  and  $135.7$  ppm correspond to C2 and C3 of the indene five membered ring, while the CH-type carbon atoms in the indenyl moiety (C4, C5, C6 and C7) give signals at  $\delta = 129.7$ ,  $125$ ,  $123.6$ , and  $123.0$  ppm. The two signals at  $\delta = 128.3$  and  $121.0$  ppm can be assigned to the carbon atoms of the phenyl ring (C13 and C14). The carbon atom at the 1-position of the indenyl ligand (C1) shows a signal at  $\delta = 45.8$  ppm while the silyl methyl groups (C10 and C11) show signals at  $\delta = -1.3$  and  $-1.9$  ppm.



**Scheme 28:**  $^{13}\text{C}$  NMR spectrum of compound **27**.

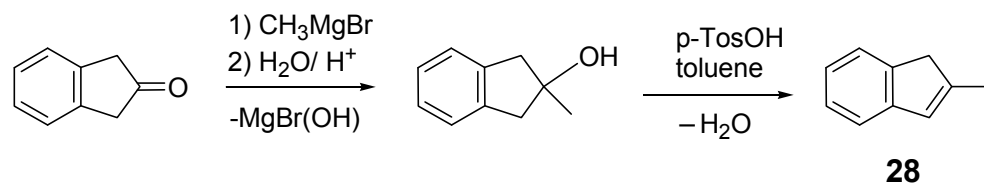
The mass spectrum of compound **27** (Scheme 29) shows the molecular ion peak at  $m/z = 422$  with 88% intensity. The ion formed by the loss of one indenyl unit [ $M^+$ -indenyl] generates the peak at  $m/z = 306$  (intensity 45%) while the loss of two indenyl units from the molecule gives rise to the base peak at  $m/z = 191$ .



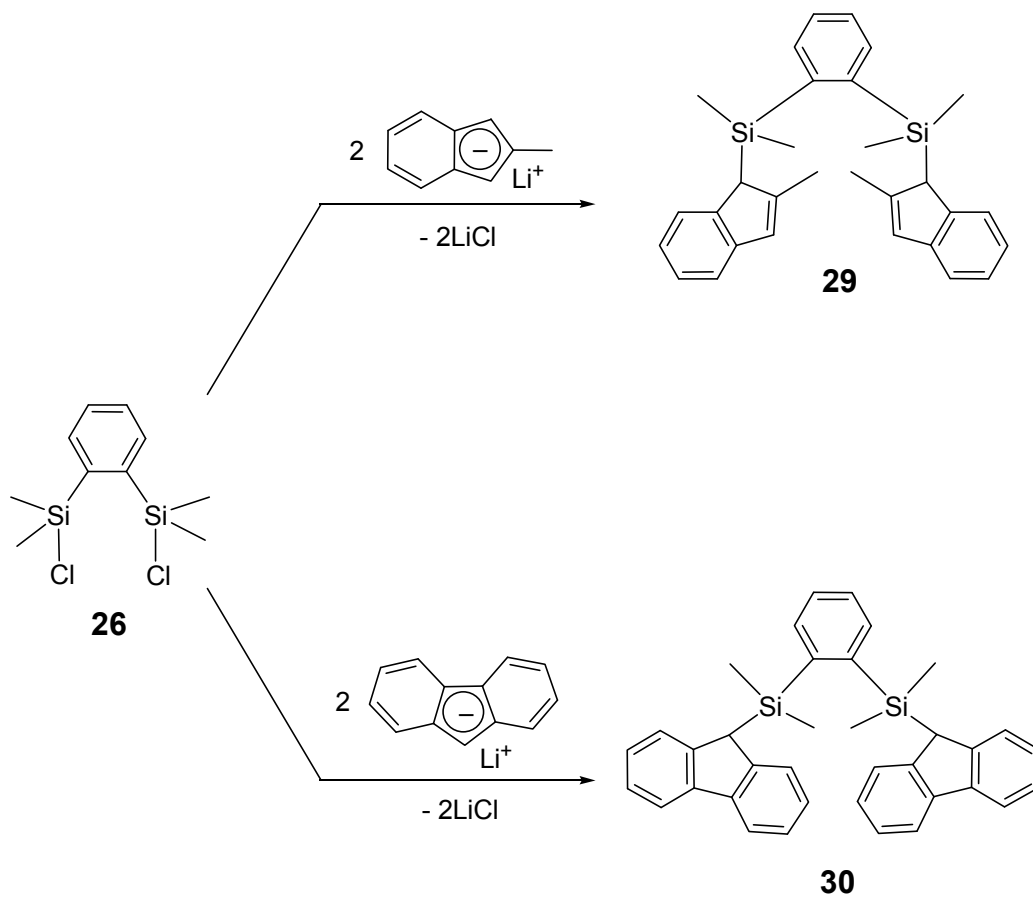
**Scheme 29:** Mass spectrum of compound **27**.

#### 2.2.4 Synthesis and characterization of compounds **29** and **30**

Compounds **29** and **30** were synthesized by the reactions of one equivalent of 1,2-bis(chlorodimethylsilyl)benzene (**26**) with two equivalents of 2-methylindenyllithium and fluorenyllithium, respectively (Scheme 31). Both reactions were conducted in ether at room temperature. Fluorenyllithium was prepared by the reaction of fluorene and *n*-butyllithium in diethylether, while 2-methylindene (**28**) was prepared by the reaction of 2-indanone with methyl magnesium bromide in diethyl ether followed by a water elimination reaction of the resulting carbinol intermediate with *para*-toluenesulfonic acid in toluene (Scheme 30).<sup>[91]</sup>



**Scheme 30:** Preparation of 2-methylindene.

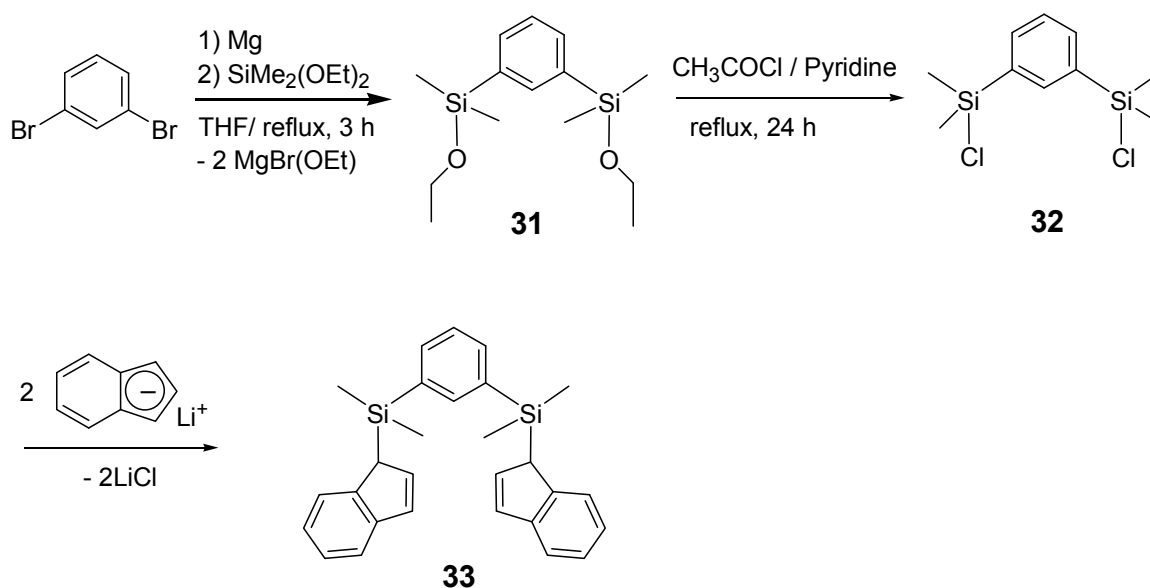


**Scheme 31:** Preparation of compounds **29** and **30**.

Compounds **29** and **30** were characterized by  $^1\text{H}$  NMR and  $^{13}\text{C}$  NMR spectroscopy (Table 7).

### 2.2.5 Synthesis and characterization of the 1,3-bis(dimethylsilyl)phenylidene bridged bis(indenyl) compound **33**

The reaction of 1,3-dibromobenzene with magnesium powder in the presence of two equivalents of diethoxydimethylsilane in refluxing THF afforded 1,3-bis(ethoxydimethylsilyl)benzene **31**. Ethoxy – chlorine exchange at compound **31** was achieved via reaction with excess acetyl chloride in the presence of a catalytic amount of pyridine to yield compound **32**.<sup>[90]</sup> A subsequent reaction of one equivalent of compound **32** with two equivalents of indenyllithium in diethylether at room temperature, afforded the desired bis(indenyl) compound **33** in 70% overall yield (Scheme 32).



**Scheme 32:** Preparation of compound **33**.

Compound **33** was fully characterized by means of  $^1\text{H}$  NMR,  $^{13}\text{C}$  NMR and GC/MS. The full spectral data are given in Table 7.

**Table 7:**  $^1\text{H}$ ,  $^{13}\text{C}$  NMR and GC/MS data for compounds **25-33**

No.	$^1\text{H}$ NMR	$^{13}\text{C}$ NMR	MS [m/z] (%)
<b>25<sup>a</sup></b>	7.64-7.60 m (2H) 7.44-7.38 m (2H) 4.78-4.72 m (2H) 0.43 s (6H, Si-CH <sub>3</sub> ) 0.41 s (6H, Si-CH <sub>3</sub> )	144.3 (C <sub>q</sub> ) 134.3, 128.4 (CH) -2.6 (Si(CH <sub>3</sub> ) <sub>2</sub> )	194 [M <sup>+</sup> ] (10) 179 M <sup>+</sup> -Me (46) 134 (100)
<b>26<sup>a</sup></b>	7.90-7.88 m (2H) 7.47-7.45 m (2H) 0.80 s (12H, Si(CH <sub>3</sub> ) <sub>2</sub> )	141.7 (C <sub>q</sub> ) 135.5, 129.3 (CH) 5.2 (Si(CH <sub>3</sub> ) <sub>2</sub> )	247.0 M <sup>+</sup> -Me (100) 211 M <sup>+</sup> -HCl (38) 119 (23)
<b>27<sup>b</sup></b>	7.76-7.73 m (2H) 7.50-7.46 m (4H) 7.29-7.26 m (2H) 7.14-7.09 m (4H) 6.96 d ( $^3J = 5.2$ Hz, 2H, C <sub>3</sub> -Ind) 6.57 dd (2H, C <sub>2</sub> -Ind) 4.00 s (2H, C <sub>1</sub> -Ind) 0.22 s (6H, Si-CH <sub>3</sub> ) 0.20 s (6H, Si-CH <sub>3</sub> )	145.0, 144.4, 144.0 (C <sub>q</sub> ) 136.2 (CH, C <sub>2</sub> -Ind) 135.7 (CH, C <sub>3</sub> -Ind) 129.7, 128.3, 125.0, 123.6 123.0, 121.0 (CH) 45.8 (CH, C <sub>1</sub> -Ind) -1.3, -1.9 (Si(CH <sub>3</sub> ) <sub>2</sub> )	422 M <sup>+</sup> (88) 306 M <sup>+</sup> -Ind (45) 135 (85) 191 M <sup>+</sup> -2Ind (100)
<b>28<sup>a</sup></b>	7.43-7.40 d (1H) 7.31-7.24 m (2H) 7.17-7.12 m (1H) 6.54 s (1H) 3.34 s (2H) 2.21 s (3H)	145.9, 145.8, 143.3 (C <sub>q</sub> ) 127.1, 126.1, 123.4, 123.2, 119.6 (CH) 42.6 (CH <sub>2</sub> ) 16.7 (CH <sub>3</sub> )	130 M <sup>+</sup> (100) 115 M <sup>+</sup> -Me (92)
<b>29<sup>a</sup></b>	7.75-7.71 m (2H) 7.46-7.43 m (2H) 7.33 d (2H) 7.20-7.16 m (2H) 7.00-6.89 m (4H) 6.59 s (2H, C <sub>3</sub> -Ind) 3.83 s (2H, C <sub>1</sub> -Ind) 1.97 s (J = 4.0 Hz, 6H, CH <sub>3</sub> ) 0.26 s (6H, Si-CH <sub>3</sub> ) 0.21 s (6H, Si-CH <sub>3</sub> )	145.1, 144.8, 144.7, 144.2 (C <sub>q</sub> ) 136.5, 128.1, 126.3, 125.0, 123.1, 122.4, 119.6, 48.5 (CH) 17.6 (CH <sub>3</sub> ) -1.2 (Si(CH <sub>3</sub> ) <sub>2</sub> )	450 M <sup>+</sup> (1) 321 (70) 191 (100)
<b>30<sup>b</sup></b>	7.72-7.69 m (4H, Ar-H) 7.24-7.05 m (16H) 4.22 s (2H, C <sub>9</sub> -Flu) 0.00 s (12H, Si(CH <sub>3</sub> ) <sub>2</sub> )	145.6, 144.3, 141.3 (C <sub>q</sub> ) 137.2, 128.4, 126.3, 125.9, 124.7, 120.3, 42.4 (CH) -1.5 (Si(CH <sub>3</sub> ) <sub>2</sub> )	n.d.

<b>31<sup>b</sup></b>	8.08 s (1H) 7.63 d (2H) 7.30 t (1H) 3.56 q (4H, CH <sub>2</sub> ) 1.10 t (6H, CH <sub>3</sub> ) 0.30 m (12H, Si(CH <sub>3</sub> ) <sub>2</sub> )	n.d.	282 M <sup>+</sup> (2) 267 M <sup>+</sup> -Me (100) 223 (28) 179 (25)
<b>32<sup>b</sup></b>	8.01 s (1H) 7.53 d (2H) 7.15 t (1H) 0.42 s (12H, Si(CH <sub>3</sub> ) <sub>2</sub> )	n.d.	n.d.
<b>33<sup>a</sup></b>	7.51-7.47 m (1H) 7.40-7.36 m (2H) 7.26-7.07 m (9H) 6.83-6.81 m (2H, C <sub>3</sub> -Ind) 6.50-6.47 m (2H, C <sub>2</sub> -Ind) 3.58 d ( <sup>3</sup> J = 1.9Hz, 2H, C <sub>1</sub> -Ind) 0.08 s (6H, Si-CH <sub>3</sub> ) 0.07 s (6H, Si-CH <sub>3</sub> )	144.7, 144.2 (C <sub>q</sub> ) 139.1 (CH) 136.2 (C <sub>q</sub> ) 135.4, 134.7, 129.3, 126.9, 124.9, 123.5, 122.9, 121.0, 45.7 (CH) -4.1, -5.0 (Si(CH <sub>3</sub> ) <sub>2</sub> )	422 M <sup>+</sup> (7) 307 M <sup>+</sup> -Ind (100) 233 (70) 115 (56)

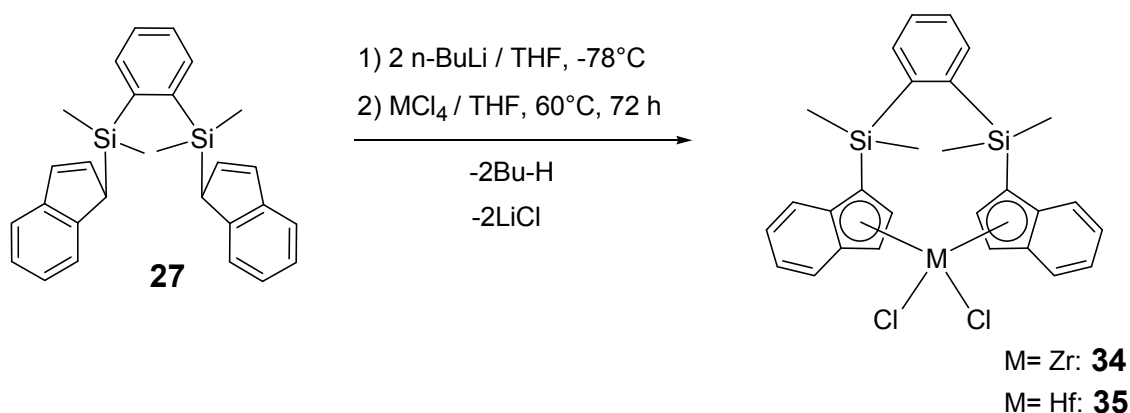
<sup>a</sup> δ (ppm) rel. CDCl<sub>3</sub> (7.24 ppm, <sup>1</sup>H NMR and 77.0 ppm, <sup>13</sup>C NMR) at 298 K.

<sup>b</sup> δ (ppm) rel. C<sub>6</sub>D<sub>6</sub> (7.16 ppm, <sup>1</sup>H NMR and 128.0 ppm, <sup>13</sup>C NMR) at 298 K.

## 2.2.6 Synthesis of 1,2-phenylene-bis(inden-1-yl)dimethylsilyl complexes of zirconium (34) and hafnium (35)

The 1,2-phenylenedisilyl bridged bis(indenyl) complexes of zirconium and hafnium were synthesized by a method that comprises the deprotonation of the bridged bis(indenyl) compound **27** with two equivalents of *n*-butyllithium (*n*-BuLi) in ether at  $-78^{\circ}\text{C}$ . A subsequent reaction of the resulting dilithium salt with one equivalent of zirconium (IV) chloride or hafnium (IV) chloride in THF at  $-78^{\circ}\text{C}$  afforded the mononuclear zirconocene dichloride **34** and the hafnocene dichloride **35**. The general synthetic method is illustrated in Scheme 33.

Reactions of  $\text{ZrCl}_4$  and  $\text{HfCl}_4$  with the ligand precursor **27** proceeded successfully to afford the corresponding ansa metallocene complexes. However, the reaction of  $\text{TiCl}_4$  with compound **27** under various reaction conditions was unsuccessful.

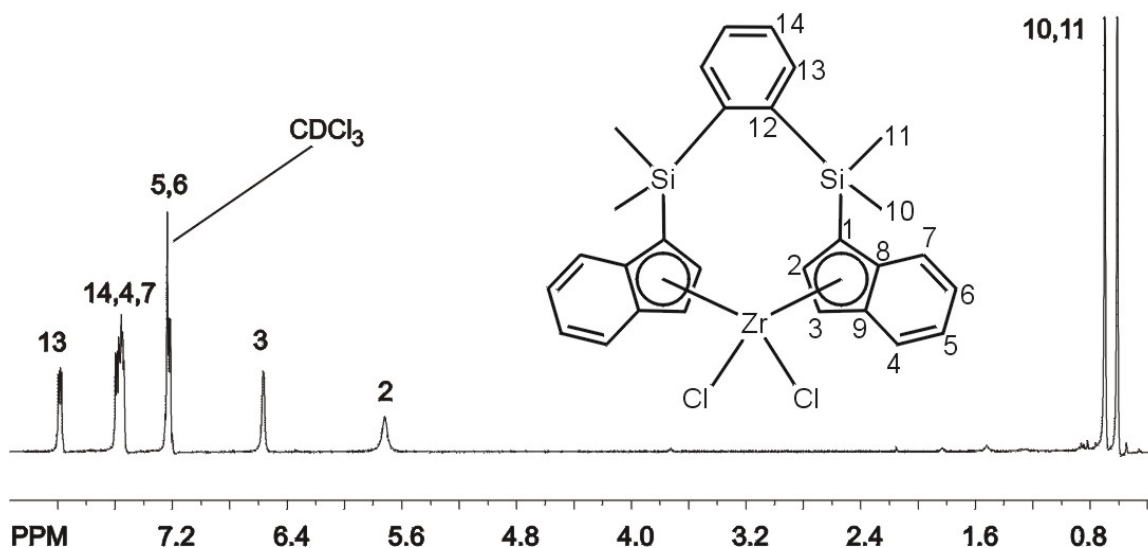


**Scheme 33:** Synthesis of the complexes **34** and **35**.

## 2.2.7 Characterization of the complexes 34 and 35

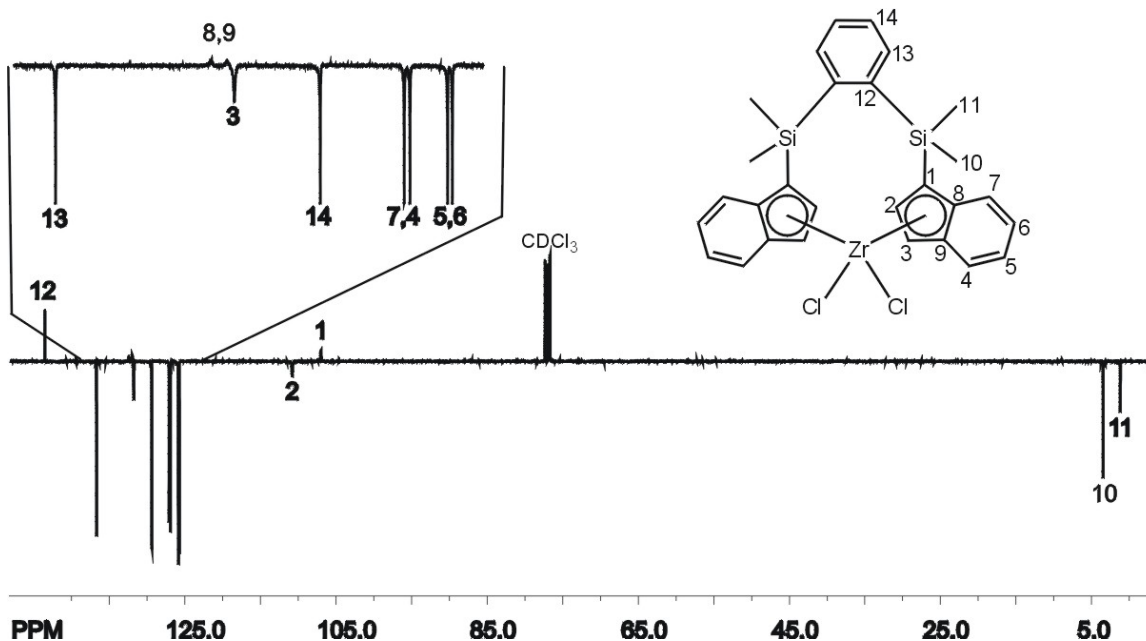
The synthesized metallocene dichloride complexes were characterized by  $^1\text{H}$  NMR,  $^{13}\text{C}$  NMR, mass spectroscopy (Table 8), and elemental analysis (see experimental part). The molecular structures of both complexes were determined with single crystal X-ray diffraction (Schemes 37 and 38).

The  $^1\text{H}$  and  $^{13}\text{C}$  NMR spectra of complex **34** are discussed as examples. The  $^1\text{H}$  NMR spectrum of complex **34** (Scheme 34) shows a multiplet at  $\delta = 7.99\text{--}7.97$  ppm (2H) which is assigned to the aromatic protons H13. The overlapping signal appearing at  $\delta = 7.59\text{--}7.53$  ppm (m, 6H) can be assigned to the protons H14, H4 and H7 while the multiplet signal appearing at  $\delta = 7.23\text{--}7.20$  ppm (m, 4H) is attributed to the protons H5 and H6 at the six-membered ring of the indenyl ligands. The protons at the 3- and 2-positions of the indenyl moieties (H3 and H2) are characterized by the signals at  $\delta = 6.56$  ppm (br, 2H) and  $\delta = 5.72$  ppm (br, 2H). The methyl groups (H10 and H11) produce the two singlets at  $\delta = 0.70$  (6H) and  $\delta = 0.61$  ppm (6H).



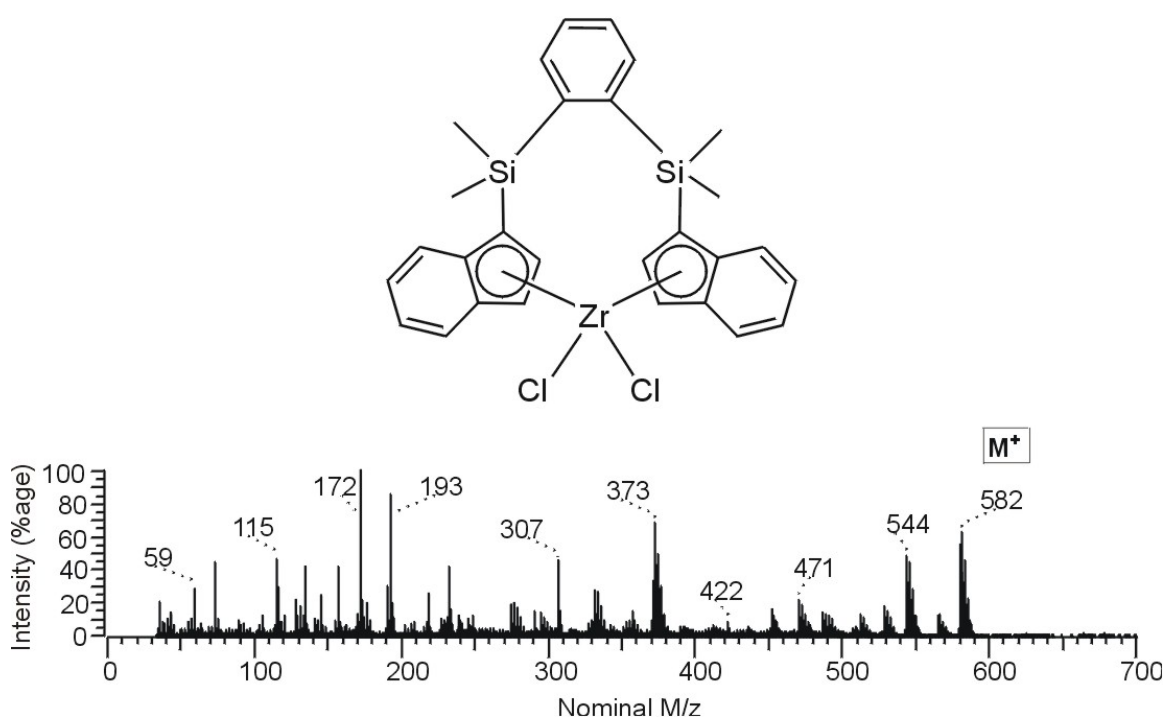
**Scheme 34:**  $^1\text{H}$  NMR spectrum of complex **34**.

The  $^{13}\text{C}$  NMR spectrum for complex **34** (Scheme 35) shows a signal at  $\delta = 143.5$  ppm corresponding to the quaternary carbon atom C12. The aromatic carbon atoms C13 and C14 give the two signals at  $\delta = 136.7$  and 129.4 ppm. The two signals appearing at  $\delta = 132.4$  and 131.9 ppm are generated by the quaternary carbon atoms of the indenyl moiety (C8 and C9). The signal at  $\delta = 131.7$  ppm is assigned to C3 while the four resonances at 127.1, 126.9, 125.8 and 125.7 ppm are attributed to the CH-type carbon atoms of indene C7, C4, C5, and C6. The signal which appears at  $\delta = 110.8$  ppm is assigned to C2 while the signal at  $\delta = 107.0$  ppm is characteristic for the quaternary carbon atom C1 at the 1-position of the indenyl moiety. The two signals appearing at  $\delta = 3.4$  and 1.2 ppm are attributed to the silyl methyl groups C10 and C11.



Scheme 35:  $^{13}\text{C}$  NMR spectrum of complex **34**.

The mass spectrum of the zirconium complex **34** (Scheme 36) shows the molecular ion peak at  $m/z = 582$  with 62% intensity. Due to the presence of isotopes (Zr, Cl), a characteristic distribution of  $M^+$  peaks are observed. The ion formed by the loss of one chloro ligand or one HCl molecule produces the peaks around  $m/z = 544$  with 58% intensity. The ionized ligand molecule gives a 10% intensity peak at  $m/z = 422$ , while the loss of one indenyl unit from the ligand [ligand-Ind] produces the peak at  $m/z = 306$  with 45% intensity. The base peak at  $m/z = 172$  results from a fragment containing an indenyldimethylsilyl unit.



**Scheme 36:** Mass spectrum of complex **34**.

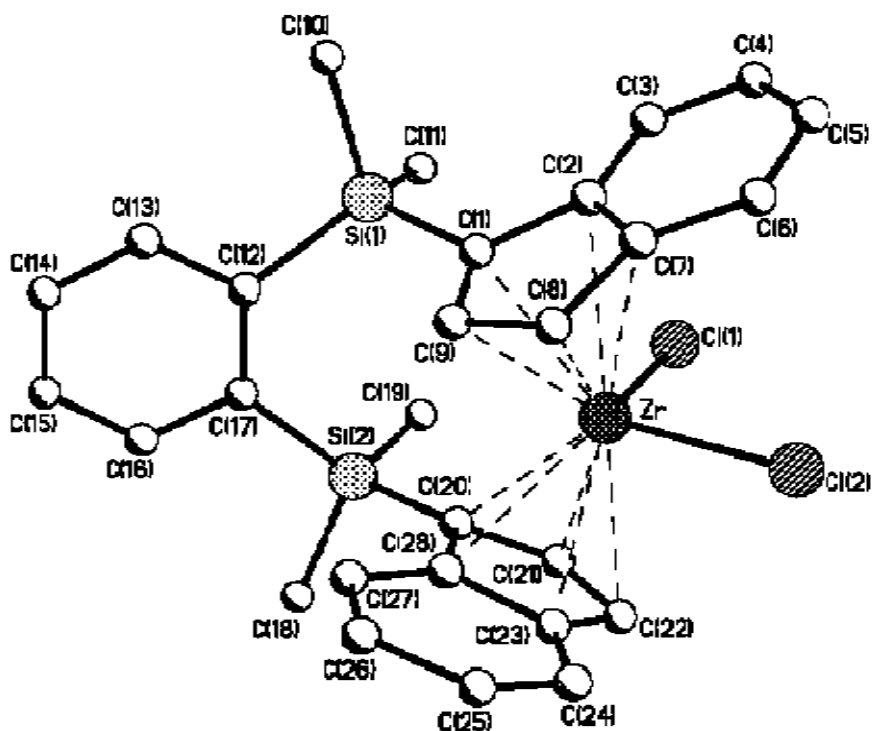
**Table 8:**  $^1\text{H}$ ,  $^{13}\text{C}$  NMR and MS data for complexes **34** and **35**.

Complex	$^1\text{H}$ -NMR	$^{13}\text{C}$ -NMR	MS [m/z] (%)
<b>34<sup>a</sup></b>	7.99-7.97 m (2H) 7.59-7.53 m (6H) 7.23-7.20 m (4H) 6.56 br (2H, C <sub>3</sub> -Ind) 5.72 br (2H, C <sub>2</sub> -Ind) 0.70 s (6H, Si-CH <sub>3</sub> ) 0.61 s (6H, Si-CH <sub>3</sub> )	143.5 (C <sub>q</sub> ) 136.7 (CH) 132.4, 131.9 (C <sub>q</sub> ) 131.7 (CH, C <sub>3</sub> -Ind) 129.4, 127.1, 126.9, 125.8, 125.7 (CH) 110.8 (CH, C <sub>2</sub> -Ind) 107.0 (C <sub>q</sub> , C <sub>1</sub> -Ind) 3.4, 1.2 (Si(CH <sub>3</sub> ) <sub>2</sub> )	582 M <sup>+</sup> (62) 544 M <sup>+</sup> -HCl (58) 422 M <sup>+</sup> -ZrCl <sub>2</sub> (10) 307 (46) 172 (100)
<b>35<sup>a</sup></b>	7.98-7.95 q (2H) 7.57-7.48 m (6H) 7.20-7.17 q (4H) 6.54 br (2H, C <sub>3</sub> -Ind) 5.58 br (2H, C <sub>2</sub> -Ind) 0.68 s (6H, Si-CH <sub>3</sub> ) 0.59 s (6H, Si-CH <sub>3</sub> )	143.7 (C <sub>q</sub> ) 136.6 (CH) 131.9 (C <sub>q</sub> ) 131.5 CH (C <sub>3</sub> -Ind) 131.1 (C <sub>q</sub> ) 129.4, 127.0, 126.9, 125.7, 125.5 (CH) 108.0 (CH, C <sub>2</sub> -Ind) 103.8 (C <sub>q</sub> , C <sub>1</sub> -Ind) 3.5, 1.0 (Si(CH <sub>3</sub> ) <sub>2</sub> )	670 M <sup>+</sup> (85) 634 M <sup>+</sup> -HCl (10) 421 M <sup>+</sup> -HfCl <sub>2</sub> -H (30) 172 (100)

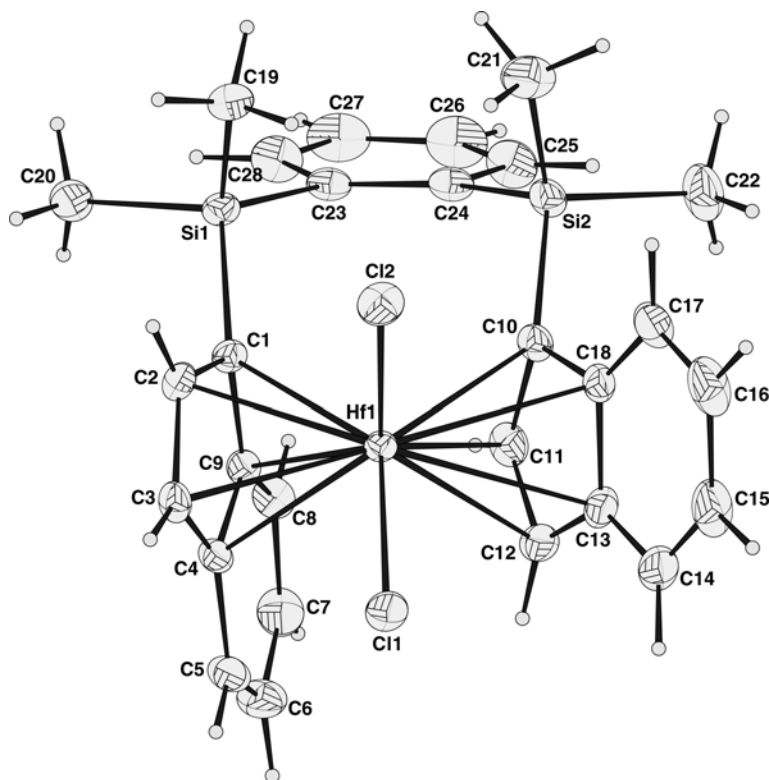
<sup>a</sup>)  $\delta$  (ppm) rel. CDCl<sub>3</sub> (7.24 ppm,  $^1\text{H}$  NMR and 77.0 ppm,  $^{13}\text{C}$  NMR) at 298 K.

### 2.2.8 Crystal structures of complexes **34** and **35**

Single crystals suitable for the X-ray diffraction analyses of complexes **34** and **35** were obtained by slow solvent evaporation from concentrated solutions of pentane/toluene mixtures in an approximately 9:1 ratio. The molecular structures of the complexes have been established by single crystal X-ray diffraction analyses. The ORTEP diagrams of **34** and **35** are displayed in Schemes 37 and 38. Table 9 summarizes the crystal data and structural refinement of complex **34**, while the crystal data and structural refinement of **35** is given in Table 10. Selected bond lengths and angles for complexes **34** and **35** are presented in Tables 11 and 12.



**Scheme 37:** ORTEP diagram of complex **34**, ellipsoids are drawn in 30% probability level. Hydrogen atoms are omitted for clarity.



**Scheme 38:** ORTEP diagram of complex **35**, along with atom numbering scheme, ellipsoids are drawn in 30% probability level. Hydrogen atoms are drawn as spheres with fixed small radius. Hydrogen atom names are omitted for clarity.

The solid state crystal structure analysis shows that the metallocene dichloride complexes **34** and **35** are isostructural and adopt a pseudotetrahedral coordination geometry around the metal atom formed by two chlorine atoms and two  $\eta^5$ -coordinated indenyl ligands. As both complexes have closely equivalent bond lengths and angles, the following description of complex **34** is also valid for **35**. One of the important features is that the indenyl ligand planes in the molecule are twisted from being perfectly  $C_2$ -symmetric thus leading to a distorted rac orientation. In **34**, the angle Cl(1)-Zr-Cl(2) is  $96.81^\circ$  which is comparable to that of the unbridged zirconocene complex  $\text{Ind}_2\text{ZrCl}_2$  ( $94.71^\circ$ )<sup>[92]</sup> and the  $\text{Me}_2\text{Si}$  bridged metallocene complex  $\text{Me}_2\text{Si}(\text{Ind})_2\text{ZrCl}_2$  ( $98.76^\circ$ ).<sup>[93]</sup> The angle that comprises the zirconium atom and the two five membered ring planes, Cen-Zr-Cen, is  $130.45^\circ$  which is larger than that of  $\text{Ind}_2\text{ZrCl}_2$  ( $128.3^\circ$ ) and the bridged  $\text{Me}_2\text{Si}(\text{Ind})_2\text{ZrCl}_2$  ( $127.8^\circ$ ). The Zr-C bond distances are different; the

quaternary carbon atoms between the five- and six-membered rings, C(2), C(7), C(23), and C(28), are apparently further away from the zirconium atom compared to the three remaining carbon atoms. These two common carbon atoms are covalently bonded to three other carbon atoms, which reduces their bonding ability to zirconium.<sup>[94]</sup> The value of the dihedral angle between the two planes of the five ring centroids is  $51.37^\circ$  which is smaller than that of  $\text{Me}_2\text{Si}(\text{Ind})_2\text{ZrCl}_2$  with a difference of  $\Delta = 10.57^\circ$ . For metallocene complexes prepared for catalytic functions, the greater dihedral angle allows better access of the monomer molecules to the cationic metal center. Therefore, catalysts with wider dihedral angles should show comparatively higher activities. The distance between the zirconium and the Cen1 plane is  $2.2513 \text{ \AA}$  being slightly longer than the Zr-Cen2 distance ( $2.2114 \text{ \AA}$ ), the distance between the two centroids is  $4.05 \text{ \AA}$  and the zirconium atom is located  $0.935 \text{ \AA}$  out of this Cen1-Cen2 vector.

**Table 9:** Crystal data and structure refinement for **34**.

Empirical formula	$\text{C}_{28} \text{H}_{28} \text{Cl}_2 \text{Si}_2 \text{Zr}$
Formula weight	582.80
Temperature	293(2) K
Wavelength	$0.71073 \text{ \AA}$
Space group	P-1; Triclinic
<i>a</i> (Å)	9.1925(18)
<i>b</i> (Å)	10.110(2)
<i>c</i> (Å)	15.726(3)
$\alpha$ (°)	91.63(3)
$\beta$ (°)	100.26(3)
$\gamma$ (°)	111.24(3)
Volume	$1333.6(5) \text{ \AA}^3$
Z	2
Density (calculated)	$1.451 \text{ Mg/m}^3$
Absorption coefficient	2.65 to $26.01^\circ$ .
F(000)	596
Crystal size	$0.28 \times 0.18 \times 0.16 \text{ mm}^3$
Theta range for data collection	$0.718 \text{ mm}^{-1}$

Index ranges	-10<=h<=9, 9<=k<=12, -19<=l<=19
Reflections collected	6271
Independent reflections	4372 [R(int) = 0.0396]
Completeness to theta = 26.01°	83.0 %
Absorption correction	None
Refinement method	Full-matrix least- squares on F <sup>2</sup>
Data / restraints / parameters	4372 / 0 / 298
Goodness-of-fit on F <sup>2</sup>	0.938
Largest diff. peak and hole	R1 = 0.0398, wR2 = 0.0956
R indices (all data)	0.534 and -0.314 e.Å <sup>-3</sup>
Final R indices [I>2sigma(I)]	R1 = 0.0547, wR2 = 0.1022

**Table 10:** Crystal data for the hafnium complex **35**.

Formula	C <sub>28</sub> H <sub>28</sub> Cl <sub>2</sub> Si <sub>2</sub> Hf
Space group	P-1, Triclinic
Z	2
<i>a</i> (Å)	10.0503(18)
<i>b</i> (Å)	9.1624(16)
<i>c</i> (Å)	15.643(3)
$\alpha$ (°)	91.567(19)
$\beta$ (°)	100.285(18)
$\gamma$ (°)	111.167(8)
Volume (Å <sup>3</sup> )	1315.0(4)
<i>F</i> (000)	660
Temperature (K)	293
Wave length (Å)	0.71069
Crystal dimensions (mm <sup>3</sup> )	0.3 × 0.2 × 0.2
<i>R</i> <sub>int</sub>	0.056

$[\text{Sin}(\theta)/\lambda]_{\text{max}}$ ( $\text{\AA}^{-1}$ )	0.8709
Density ( $\text{g cm}^{-3}$ )	1.6918
Absorption coefficient ( $\text{mm}^{-1}$ )	4.276
Observed Criteria	$I > 3\sigma(I)$
No. of observed/all reflections	8001/ 11018
$wR_F(\text{obs/all})$	0.0395/0.0663
$R_F(\text{obs/all})$	0.0422/0.0446
$\Delta\rho_{\text{max}}/\Delta\rho_{\text{min}}$ ( $\text{e}\text{\AA}^{-3}$ )	1.61/1.79
$GoF(\text{obs/all})$	1.01/-0.87

**Table 11:** Selected Bond lengths and angles of **34**.

<u>Selected bond lengths [<math>\text{\AA}</math>]</u>			
		Si(1)-C(1)	1.867(4)
Zr-Cl(1)	2.4230(14)	Si(2)-C(20)	1.872(4)
Zr-Cl(2)	2.4398(11)	Cen1-Zr	2.2513
Zr-C(1)	2.499(3)	Cen2-Zr	2.2114
Zr-C(2)	2.634(3)	Cen1-Cen2	4.0520
Zr-C(7)	2.654(3)	<u>Selected bonds angles [<math>^\circ</math>]</u>	
Zr-C(8)	2.506(4)	Cl(1)-Zr-Cl(2)	96.81(5)
Zr-C(9)	2.490(3)	C(1)-Si(1)-C(12)	111.68(18)
Zr-C(20)	2.491(3)	C(20)-Si(2)-C(17)	114.49(16)
Zr-C(21)	2.465(3)	C(2)-C(1)-Si(1)	126.2(3)
Zr-C(22)	2.479(3)	C(28)-C(20)-Si(2)	129.1(3)
Zr-C(23)	2.565(4)	Dihedral angle	51.368
Zr-C(28)	2.617(4)	Cen1-Zr-Cen2	130.453

**Table 12:** Selected Bond lengths and angles of **35**.

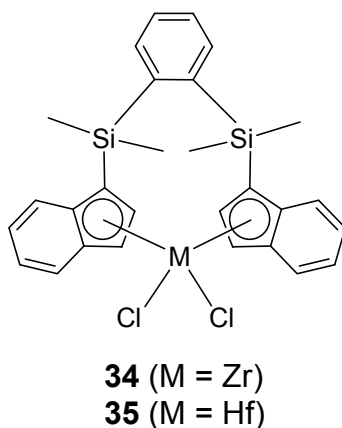
<u>Selected bond lengths [Å]</u>		Si(1)-C(1)	1.868(4)
Hf-Cl(1)	2.4095(14)	Si(2)-C(10)	1.855(4)
Hf-Cl(2)	2.3921(14)	Cen1-Hf	2.194(4)
Hf-C(1)	2.469(4)	Cen2-Hf	2.231(5)
Hf-C(2)	2.449(4)	Cen1-Cen2	4.024(8)
Hf-C(3)	2.464(4)	<u>Selected bonds angles [°]</u>	
Hf-C(4)	2.549(4)	Cl(1)-Hf-Cl(2)	95.91(4)
Hf-C(9)	2.596(4)	C(1)-Si(1)-C(23)	113.77(15)
Hf-C(10)	2.473(4)	C(10)-Si(2)-C(24)	111.32(19)
Hf-C(11)	2.452(4)	C(9)-C(1)-Si(1)	129.7(3)
Hf-C(12)	2.485(4)	C(18)-C(10)-Si(2)	125.8(3)
Hf-C(13)	2.644(4)	Dihedral angle	51.478(150)
Hf-C(18)	2.625(4)	Cen1-Hf-Cen2	130.813(10)

### 2.2.9 Reactions of compounds **29**, **30** and **33** with zirconium tetrachloride

Many futile attempts were made to prepare the zirconium complexes derived from compounds **29**, **30** and **33**. The titled compounds were reacted with  $ZrCl_4$  by a similar method used in Scheme 29. The attempts to characterize the obtained powders with NMR spectroscopy were unsuccessful due to their insolubility in common organic solvents. In the mass spectra, the molecular ion peak or any of the cracking patterns relevant to the targeted complexes were not detected. Instead, a peak for the dilithium salt appeared [ $m/z = 435$  corresponding to the compound **33** dilithium salt]. The use of different solvents such as toluene or diethyl ether, besides THF, and prolonged heating failed to drive these reactions towards completion.

### 2.2.10 Ethylene polymerization experiments with complexes **34** and **35**

Complexes **34** and **35** are ansa bis(1-indenyl) metallocene dichloride complexes, the two indenyl ligands are tethered via a 1,2-bis(dimethylsilyl) phenylene bridge. (Scheme 39).



**Scheme 39:** Structural formula of complexes **34** and **35**.

The catalytic activities of complexes **34** and **35** in the homogeneous polymerization of ethylene along with the results of the polymer analyses are summarized in Table 13. Methylaluminoxane (MAO) was used as a cocatalyst (M:Al = 1:2000), the experiments were conducted at a polymerization temperature of 60°C, 10 bar ethylene pressure, and in 250 ml of pentane for one hour. The produced polyethylene samples were analyzed by DSC and viscosimetry.

**Table 13:** Ethylene polymerization activities and analyses of the polymers produced with complexes **34/MAO** and **35/MAO**.

Complex No.	M	Activity <sup>a</sup>	DSC			M <sub>n</sub> [g/mol]
			ΔH <sub>m</sub> [J/g]	T <sub>m</sub> [°C]	[α]	
<b>34</b>	Zr	7610	124.5	135.5	0.43	366000
<b>35</b>	Hf	3590	124.6	135.5	0.43	375000

<sup>a</sup> (kg PE/mol cat. h)

Both MAO-activated zirconium and hafnium catalysts were active in ethylene polymerization. The zirconium catalyst **34**/MAO gave a higher activity compared to the hafnium complex derived from the same ligand while the hafnium catalyst **35**/MAO produced polyethylene with apparently higher molecular weight. This result is consistent with the fact reported previously that zirconocene catalysts provide higher activities while the hafnocene analogues produce polyolefins with greater molecular weights.<sup>[95]</sup> The difference in the polymerization behavior between Zr- and Hf-based catalysts could be attributed to thermodynamically stronger  $\sigma$ -bonds between hafnium and the polymer chain (Hf-C), hindering not only the chain propagation but also the release of the chain, giving rise to less activities and higher molecular weight polyethylenes.<sup>[79]</sup> In line with this assumption, a recent study of hafnocene catalysts demonstrated that the activation energies for chain propagation and termination are significantly higher compared with zirconium catalysts.<sup>[96]</sup>

The catalytic activity of **34**/MAO in the homogeneous polymerization of ethylene is, as expected, lower, than the activities observed for the unbridged bis-indenyl metallocene complex<sup>[77]</sup> and that of the single atom bridged metallocene complexes such as  $-\text{CH}_2-$ <sup>[97,98]</sup>,  $-\text{Me}_2\text{C}-$ <sup>[97,99]</sup>, and  $-\text{Me}_2\text{Si}-$ <sup>[29,85]</sup> bridged species. Similar results are observed when comparing the activity of **34**/MAO with the widely known ethylidene bridged catalyst precursor,<sup>[100,101]</sup>  $\text{rac}[\text{Et}(\text{Ind})_2]\text{ZrCl}_2$  ("Brintzinger catalyst"). However, in terms of molecular weight, catalyst **34**/MAO produces the polyethylene with the highest molecular weight compared with the above mentioned catalysts (except the  $\text{Me}_2\text{Si}$ -bridged one). The comparatively lower activity of **34**/MAO can be rationalized by the existence of the 4 atoms-bridge, 1,2-bis(dimethylsilyl)phenylene, incorporating 2 C and 2 Si atoms. This rigid and long bridge resulted in a smaller dihedral angle and thus the zirconium center becomes more shielded.

From the crystal structure data of complex **34**/MAO (Scheme 37, Table 9), the value of the dihedral angle was determined to  $51.4^\circ$ , whereas the dihedral angle reported for  $\text{CH}_2-$ ,  $\text{Me}_2\text{C}-$ ,  $\text{Me}_2\text{Si}-$ , and  $\text{C}_2\text{H}_4$ -bridged metallocene complexes are  $72.4^\circ$ ,  $70.9^\circ$ ,  $61.6^\circ$  and  $62.1^\circ$ . A greater value of the dihedral angle between the ligand planes enhances the activity in olefin polymerization by increasing the reaction space of the metal center.<sup>[87]</sup>

Catalyst **34** exhibited a far better catalytic performance in terms of both activity and molecular weight compared with the known metallocene catalysts comprising 4-atom-bridges such as *o*-xylidene-bridged<sup>[88]</sup> and (-Me<sub>2</sub>Si-CH<sub>2</sub>-CH<sub>2</sub>-Me<sub>2</sub>Si-)-bridged<sup>[102]</sup> catalysts. This distinction could be explained by the favourable replacement of the two methylene groups with two dimethylsilyl groups in **34**.

Changing the metal centre in this catalyst system seems to have no influence on the melting points and crystallinity values of the polyethylenes.

## **2.3 2,2'-Bis(methylene)biphenylidene-bridged 1-indenyl complexes of group (IV) metals**

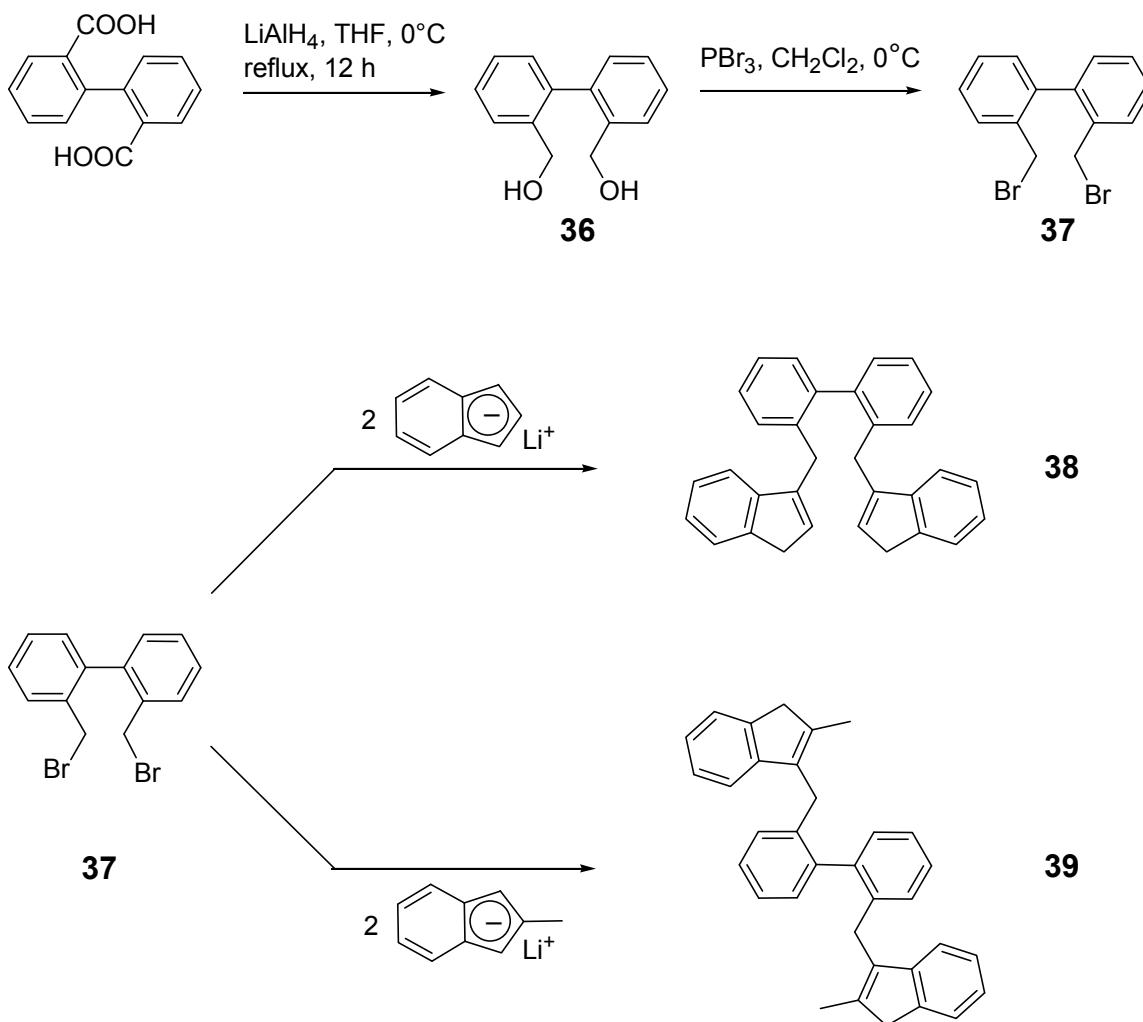
### **2.3.1 General remarks**

The activity and stereoselectivity of a metallocene-based catalyst in olefin polymerization can be significantly influenced by slight structural variations in the bridging unit (structure property relationship).<sup>[25]</sup> In this study, the synthesis of new ansa-titanocene, zirconocene, and hafnocene dichloride complexes is reported. The titled complexes comprise two indenyl or 3-methylindenyl ligands tethered, at the 1-position, via a 2,2'-bis(methylene)-1,1'-biphenylidene bridge. Moreover, the catalytic behavior of the prepared ansa-metallocene catalysts in the homopolymerization of ethylene was investigated after activation with MAO.

### **2.3.2 Preparation of the ligand precursors 38 and 39**

Diphenic acid was converted to the corresponding 2,2-bis(hydroxymethyl) biphenyl **36** according to a reported method.<sup>[103]</sup> Reduction of diphenic acid with lithium aluminium hydride in THF and purification by crystallization from a chilled methanol solution gave **36** in good yield. Treatment of the diol compound **36** with phosphorus tribromide in methylene chloride afforded 2,2'-bis(bromomethyl) biphenyl **37**.<sup>[104]</sup>

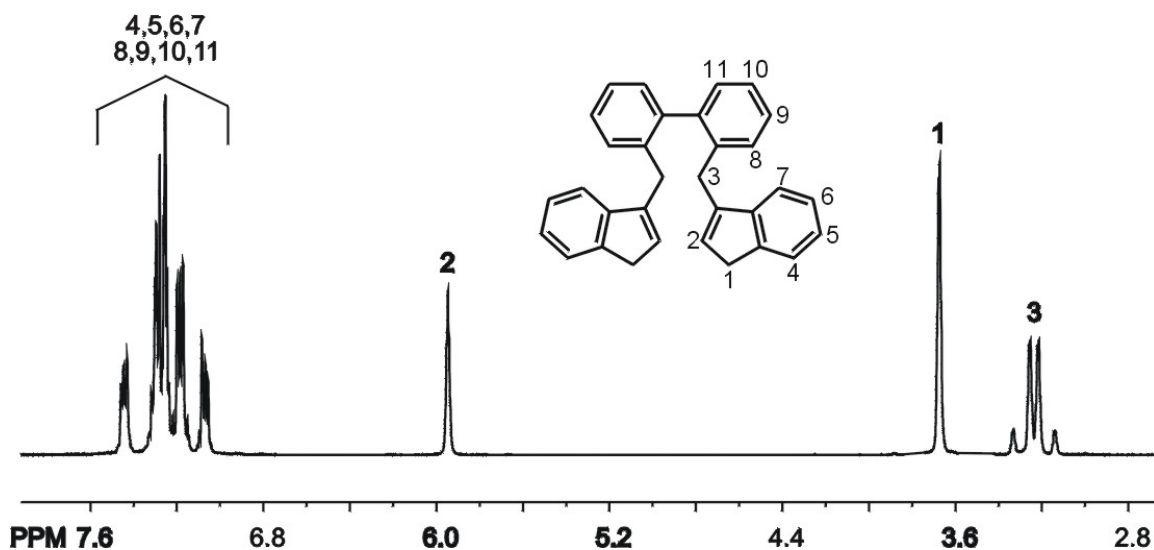
Compounds **38** and **39** were then obtained via reactions of 2,2'-bis(bromomethyl) biphenyl **37** with two equivalents of indenyllithium or 2-methylindenyllithium. Both reactions were carried out in THF at -78°C Thus the indenyl moieties were coupled through the 3-position (Scheme 40).



**Scheme 40:** Preparation of compounds **38** and **39** from 2,2'-bis(bromomethyl)-biphenyl.

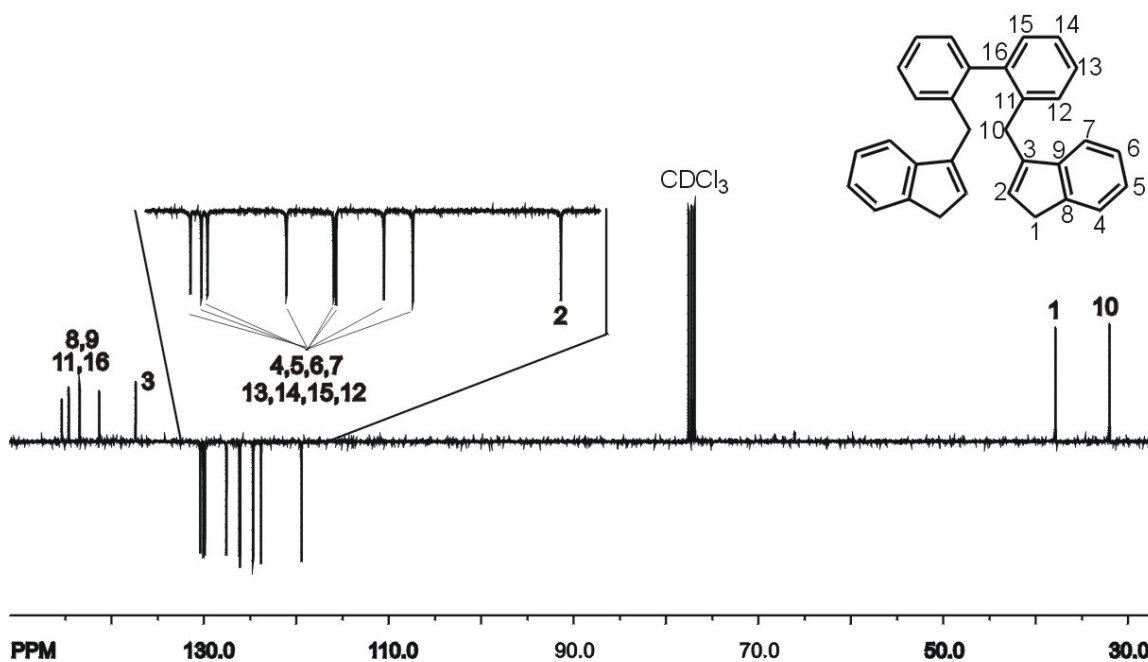
### 2.3.3 Characterization of compounds **38** and **39**

Compounds **38** and **39** and the intermediates were characterized by NMR spectroscopy. The complete data are given in Table 14. The  $^1\text{H}$  and  $^{13}\text{C}$  NMR spectra of compound **38** are discussed as examples. In the  $^1\text{H}$  NMR spectrum of compound **38** (Scheme 41), the four multiplet resonance signals appearing at  $\delta = 7.48 - 7.08$  ppm represent the 16 aromatic protons belonging to the indenyl and biphenylene bridge six-membered rings (H4-H7 and H8-H11). The protons at the 2-position of the indenyl moieties (H2) display the broad signal at  $\delta = 5.96$  ppm (2H) while the protons at the 1-position of the indenyl rings produce the broad signal at  $\delta = 3.68$  ppm (4H). The methylene group protons of the bridging element (H3) produce the signal at  $\delta = 3.22$  ppm (dd, 4H).



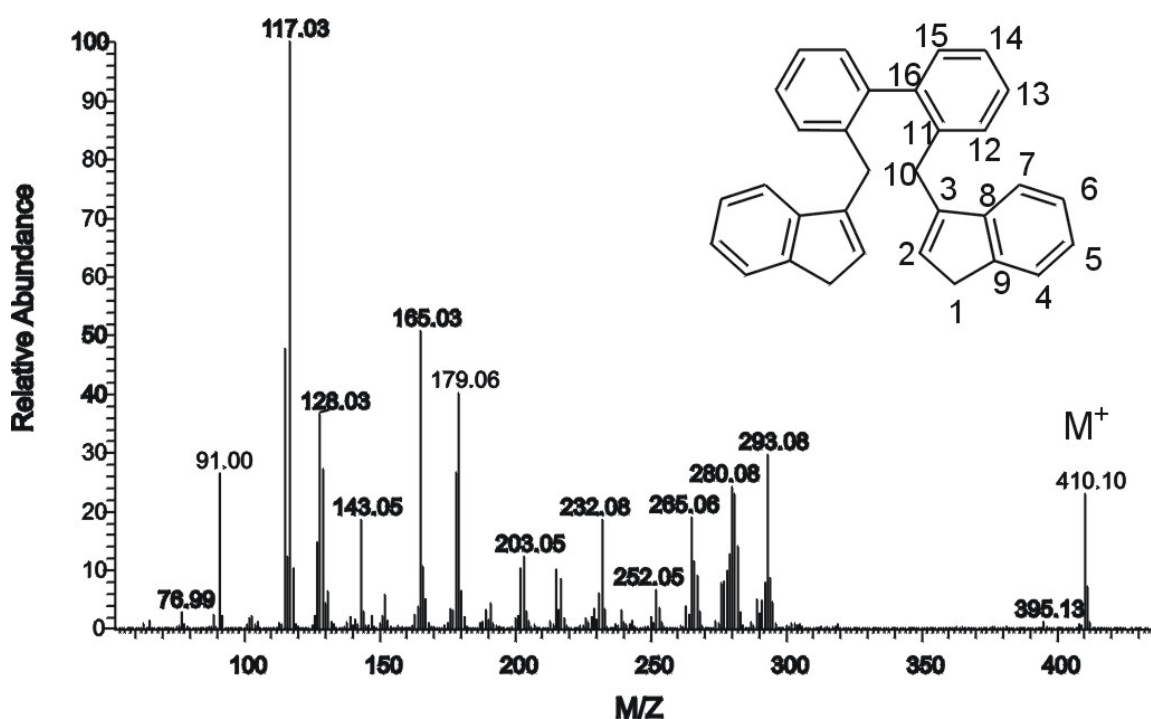
**Scheme 41:**  $^1\text{H}$  NMR spectrum of compound **38**.

The  $^{13}\text{C}$  NMR spectrum for compound **40** (Scheme 42) shows three sets of resonances: the five signals at  $\delta = 145.1, 144.4, 143.2, 141.1$  and  $137.2$  ppm are assigned to the five quaternary carbon atoms in the bridging biphenyl and indenyl moieties (C8, C9, C11, C16, and C3). The CH-type carbon atoms in the molecule (C4, C5, C6, C7, C13, C14, C15, C12, and C2) produce the signals at  $\delta = 130.2, 129.9, 129.7, 127.3, 125.9, 125.8, 124.4, 123.6$  and  $119.2$  ppm. The two signals appearing at  $\delta = 37.6$  and  $31.8$  ppm are assigned to the indenyl  $\text{CH}_2$  group carbon atoms (C1) and the benzylic carbon atoms of the bridging unit (C10).



Scheme 42:  $^{13}\text{C}$  NMR spectrum of compound **38**.

Compounds **38** and **39** were also characterized by GC/MS (Table 14). The mass spectrum of compound **38** is discussed as an example. The mass spectrum of compound **38** (Scheme 43) shows the molecular ion peak at  $m/z = 410$  with 25% intensity. The ion with the mass  $m/z = 293$  and 30% intensity can be explained by the loss of one indenyl fragment [ $M^+ - \text{Ind}$ ] and 2 H atoms. The indenyl fragments (+ 2 hydrogen atoms, probably as indanyl moieties) separated from the molecule give rise to the base peak at  $m/z = 117$ .



**Scheme 43:** Mass spectrum of compound **38**.

**Table 14:**  $^1\text{H}$ ,  $^{13}\text{C}$  NMR<sup>a</sup> and MS data for compounds **36-39**.

No.	$^1\text{H-NMR}$	$^{13}\text{C-NMR}$	MS [m/z] (%)
<b>36</b>	7.48 d ( $^3J = 7.5$ Hz, 2H) 7.43-7.32 m (4H) 7.15 d ( $^3J = 7.5$ Hz, 2H) 4.37-4.28 t (4H) 3.20 br (2H)	140.1, 138.6 ( $\text{C}_q$ ) 129.6, 129.5, 128.1, 127.6 (CH) 62.9 ( $\text{CH}_2$ )	196 (100) $\text{M}^+ - \text{H}_2\text{O}$ 165 (70) 152 (35)
<b>37</b>	7.57 d ( $^3J = 7.2$ Hz, 2H) 7.47-7.37 m (4H) 7.29 d ( $^3J = 7.2$ Hz, 2H) 4.38 d ( $^3J = 10$ Hz, 2H) 4.22 d ( $^3J = 10$ Hz, 2H)	139.4, 135.8 ( $\text{C}_q$ ) 130.6, 130.1, 128.6, 128.3 (CH) 32.0 ( $\text{CH}_2$ )	340 (2) $\text{M}^+$ 259 $\text{M}^+ - \text{Br}$ (12) 179 (100)
<b>38</b>	7.48-7.45 m (2H) 7.34-7.27 m (8H) 7.22-7.19 m (4H) 7.11-7.08 m (2H) 5.96 br (2H, $\text{C}_2\text{-Ind}$ ) 3.68 br (4H, $\text{C}_1\text{-Ind}$ ) 3.24 dd (4H, $\text{CH}_2$ )	145.1, 144.4, 143.2, 141.1, 137.2 ( $\text{C}_q$ ) 130.2, 129.9, 129.7, 127.3, 125.9, 125.8, 124.4, 123.6, 119.2 (CH) 37.6 ( $\text{Ind-CH}_2$ ) 31.8 ( $\text{CH}_2$ )	410 (25) $\text{M}^+$ 293 (30) 117 (100)
<b>39</b>	7.37 d ( $^3J = 6.9$ Hz, 2H) 7.29-7.25 m (4H) 7.22-7.06 (8H) 6.97 d ( $^3J = 6.9$ Hz, 2H) 3.69 s (4H, $\text{C}_1\text{-Ind}$ ) 3.34 s (4H, $\text{CH}_2$ ) 1.97 s (6H, $\text{CH}_3$ )	146.6, 142.4, 141.2, 140.6, 137.3, 134.8 ( $\text{C}_q$ ) 129.5, 128.3, 127.5, 126.0, 125.9, 123.5, 123.0, 118.9 (CH) 42.7, 29.1 ( $\text{CH}_2$ ) 14.1 ( $\text{CH}_3$ )	438 (22) $\text{M}^+$ 179 (79) 128 (100)

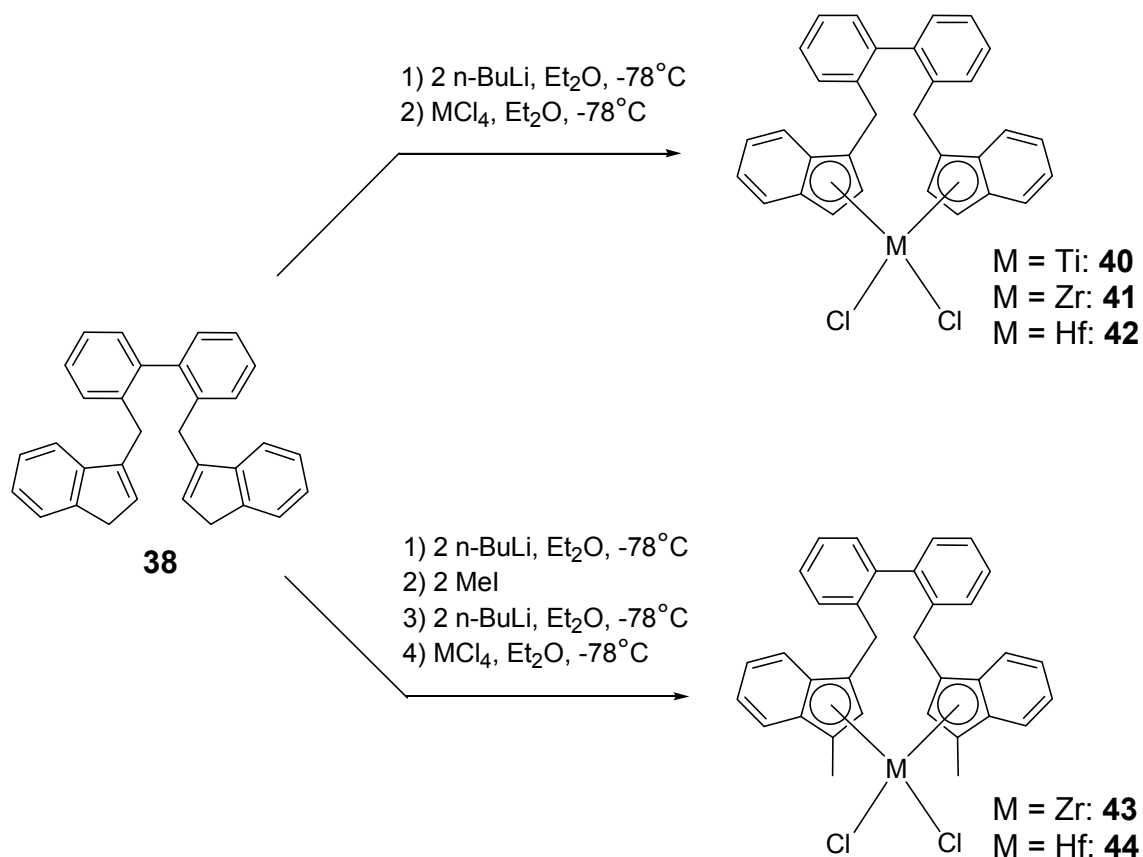
<sup>a</sup>  $\delta$  (ppm) rel.  $\text{CHCl}_3$  (7.24 ppm,  $^1\text{H}$  NMR) and rel.  $\text{CDCl}_3$  (77.0 ppm,  $^{13}\text{C}$  NMR) at 298 K.

### 2.3.4 Synthesis of the titanium, zirconium and hafnium complexes **40-42**

The bridged bis(indenyl) compound **38** was deprotonated by two equivalents of *n*-butyllithium (*n*-BuLi) at  $-78^\circ\text{C}$  in diethyl ether. Subsequently, reactions of the resulting dilithium salt of the ligand with one equivalent of either titanium tetrachloride, zirconium tetrachloride or hafnium tetrachloride yielded the desired metallocene dichlorides **40-42**. The general synthesis method is illustrated in Scheme 44.

For the synthesis of complexes **43** and **44**, compound **38** was deprotonated with two equivalents of *n*-butyllithium. A subsequent reaction of the resulting dilithium salt with two equivalents of methyl iodide furnished the 1,1'-dimethyl substituted ligand precursor

which was transformed simultaneously to its corresponding dilithium salt via reaction with two equivalents of *n*-BuLi in diethyl ether. The desired complexes **43** and **44** were obtained by the reactions of equimolar quantities of the dilithium salt and zirconium tetrachloride or hafnium tetrachloride (Scheme 44). Attempts to synthesize the titanium complex of compound **38** were futile.



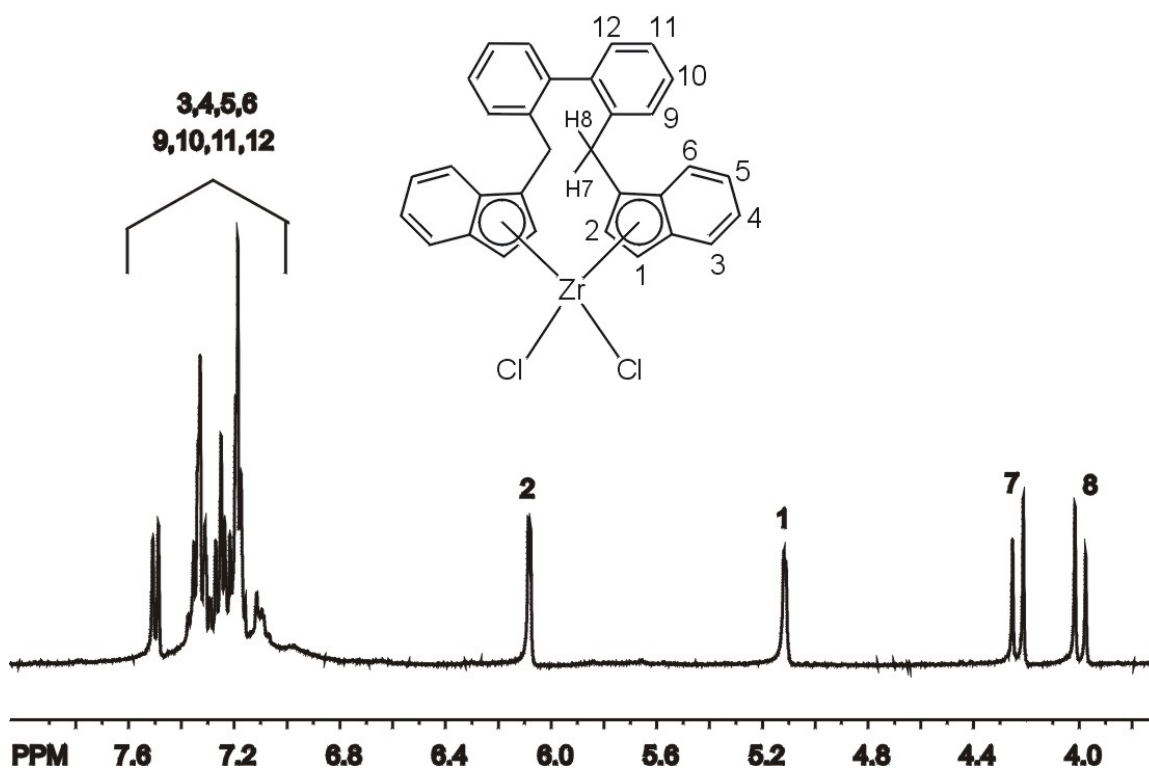
**Scheme 44:** Synthesis of the metallocene complexes **40-44**.

### 2.3.5 Characterization of the complexes **40-44**

The metallocene complexes **40-44** were characterized by NMR spectroscopy (Table 15), mass spectroscopy (Table 15), and elemental analysis (experimental part). Additionally, complex **41** was structurally characterized with single crystal x-rays diffraction (Scheme 48).

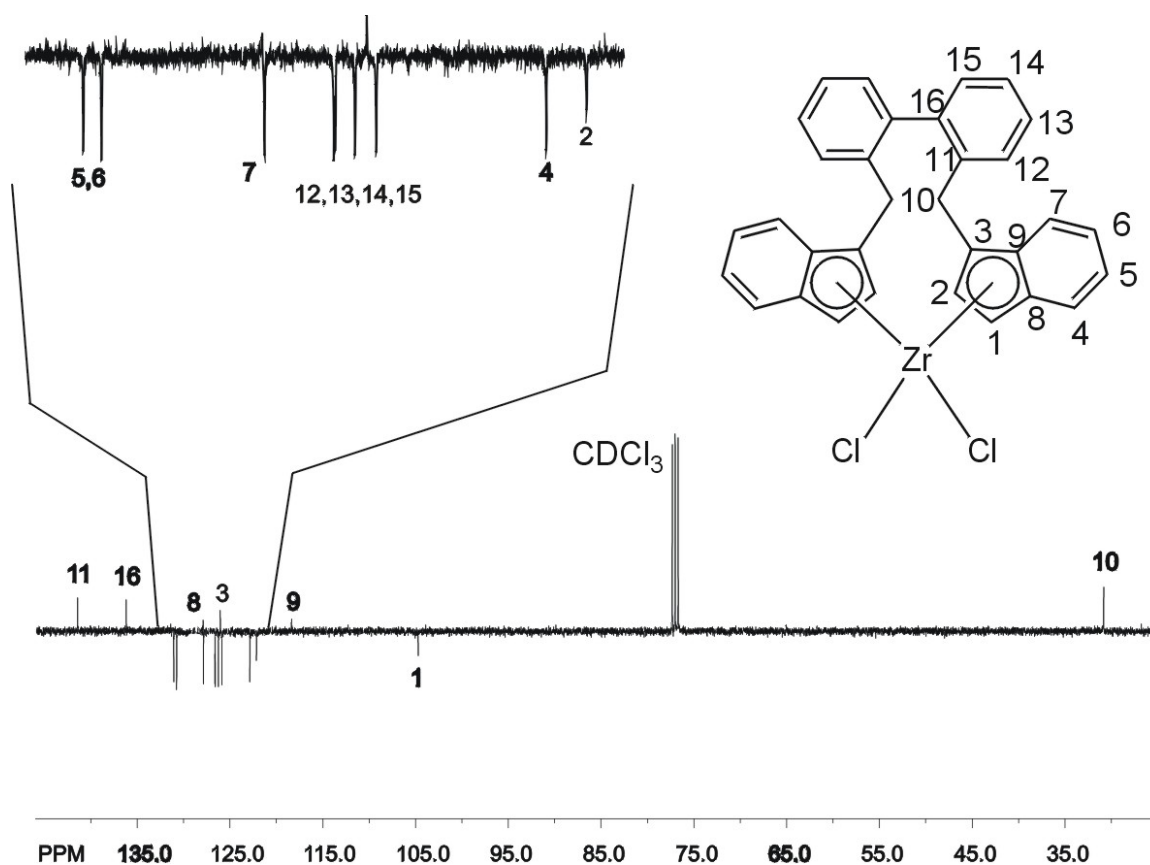
The <sup>1</sup>H and <sup>13</sup>C NMR spectra of complex **41** are discussed as examples. In the <sup>1</sup>H-NMR spectrum of compound **41** (Scheme 45) the 16 aromatic protons (H3-H6 and H9-H12)

display four signals at  $\delta = 7.50$  (d, 2H), 7.35-7.31 (m, 6H) 7.27-7.24 (t, 2H) and 7.22-7.17 (m, 6H) ppm. The protons located at the 2-positions of the indenyl rings (H2) generate the doublet at  $\delta = 6.08$  (d,  $^3J = 3.3$  Hz, 2H) ppm while the protons at the 1-positions of the indenyl rings (H1) produce the doublet at  $\delta = 5.11$  (d,  $^3J = 3.3$  Hz, 2H) ppm. The protons of the methylene group (H7, H8) give the two signals at  $\delta = 4.23$  (d,  $J = 15.9$  Hz, 2H) and 4.00 (d,  $J = 16.2$  Hz, 2H) ppm.



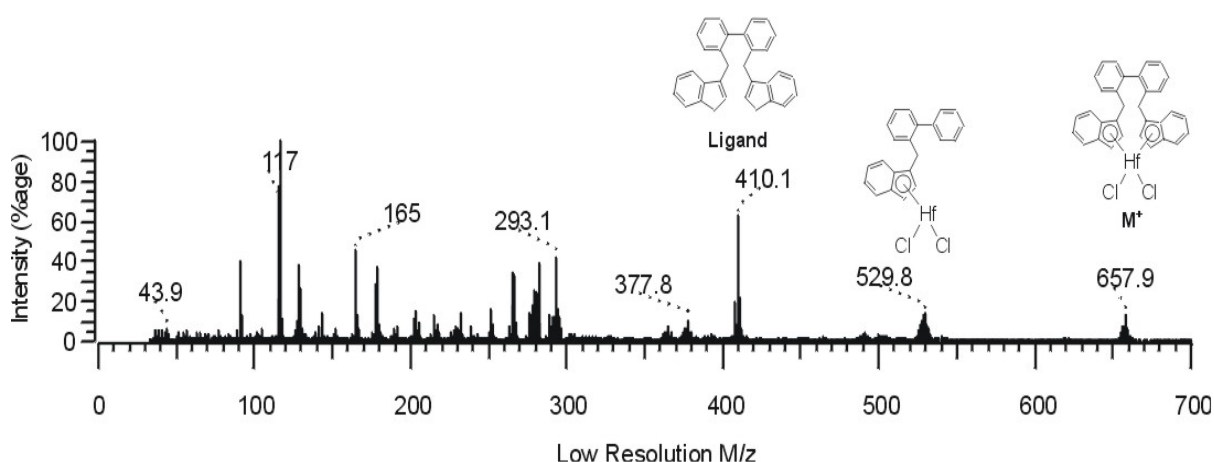
**Scheme 45:**  $^1\text{H}$  NMR spectrum of complex 41.

The  $^{13}\text{C}$  NMR spectrum of complex **41** (Scheme 46) shows two resonances at  $\delta = 141.4$  and 136.2 ppm attributed to the quaternary carbon atoms in the biphenyl bridging unit (C11 and C16). The two signals appearing at  $\delta = 131.1$  and 130.7 ppm are assigned to C5 and C6 of the indenyl rings. The remaining quaternary carbon atoms C8, C9 and C3 are identified with the signals appearing at  $\delta = 127.9$ , 126.0, and 118.4 ppm. The signal at  $\delta = 127.8$  ppm can be assigned to the CH carbon atom C7 while the carbon atom C4 corresponds to the chemical shift at  $\delta = 122.8$  ppm. The aromatic CH-type carbon atoms in the biphenyl moiety (C12, C13, C14, and C15) are associated with the signals at  $\delta = 126.6$ , 126.2, 125.9, and 124.9 ppm. The signal at  $\delta = 122.1$  ppm is assigned to the carbon atom at the 2-positions of the indenyl groups (C2) while the signal at  $\delta = 104.7$  ppm is characteristic for the carbon atom at the 1-position of the indenyl moieties (C1). The benzylic  $\text{CH}_2$  carbon atoms (C10) appear at  $\delta = 30.8$  ppm.



**Scheme 46:**  $^{13}\text{C}$  NMR spectrum of complex **41**.

The mass spectrum of complex **42** is also discussed as an example. In the mass spectrum of complex **42** (Scheme 47), the molecular ion peak appears at  $m/z = 658$  with 14% intensity. The ion with  $m/z = 530$  and 14% intensity can be explained by the loss of one methylene-indenyl fragment from the molecule, while the peak appearing at  $m/z = 410$  with 78% relative intensity arises from the free bis(indenyl) ligand. Further loss of one indenyl fragment from the ligand gives rise to the peak at  $m/z = 293$  with 47% intensity relative to the base peak. The base peak at  $m/z = 117$  is generated by indenyl fragments.



**Scheme 47:** Mass spectrum of complex **42**.

**Table 15:**  $^1\text{H}$ ,  $^{13}\text{C}$  NMR and MS data for complexes **40-44**.

No.	$^1\text{H}$ -NMR	$^{13}\text{C}$ -NMR	MS [ $m/z$ ] (%)
<b>40<sup>a</sup></b>	7.64-7.61 m (2H) 7.40-7.36 m (2H) 7.26-7.19 m (8H) 7.18-7.12 m (4H) 5.99 br (2H) 5.12 br (2H) 4.30 d ( $J = 15.4$ Hz, 2H) 4.14 d ( $J = 15.4$ Hz, 2H)	142.4, 141.3, 132.8 ( $\text{C}_q$ ) 131.5, 131.0, 129.6 (CH) 129.4 ( $\text{C}_q$ ) 128.8, 128.4, 128.3, 127.1, 125.8, 123.3 (CH) 120.9 ( $\text{C}_q$ ) 108.1 (CH) 32.6 ( $\text{CH}_2$ )	526 $\text{M}^+$ (12) 491 $\text{M}^+$ -Cl (52) 455 $\text{M}^+$ -Cl-HCl (15) 409 ligand-H (100) 293 (90)
<b>41<sup>b</sup></b>	7.50 d ( $^3J = 8.6$ Hz, 2H) 7.35-7.31 m (6H) 7.27-7.24 t (2H)	141.4, 136.2 ( $\text{C}_q$ ) 131.1, 130.7 (CH) 127.9 ( $\text{C}_q$ )	570 $\text{M}^+$ (45) 410 ligand (100) 293 (67)

	7.22-7.17 m (6H) 6.08 d ( $^3J = 3.3$ Hz, 2H, C <sub>2</sub> -Ind) 5.11 d ( $^3J = 3.3$ Hz, 2H, C <sub>1</sub> -Ind) 4.23 d (J = 15.9 Hz, 2H) 4.00 d (J = 16.2 Hz, 2H)	127.8, 126.6, 126.5, 126.2 (CH) 126.0 (C <sub>q</sub> ) 125.9, 122.8, 122.1 (CH) 118.4 (C <sub>q</sub> ) 104.7 (CH) 30.8 (CH <sub>2</sub> )	117 (96)
<b>42<sup>a)</sup></b>	7.52-7.49 m (2H) 7.40-7.38 m (2H) 7.28-7.21 m (8H) 7.17-7.12 m (4H) 6.10 d ( $^3J = 3.4$ Hz, 2H) 5.02 br (2H) 4.29 d (J = 16 Hz, 2H) 4.15 d (J = 16 Hz, 2H)	142.1, 137.0 (C <sub>q</sub> ) 131.7, 131.2, 128.3, 127.0, 126.9, 126.5, 126.3 (CH) 126.2 (C <sub>q</sub> ) 123.3, 122.2 (CH) 118.6, 116.5 (C <sub>q</sub> ) 101.8 (CH) 31.1 (CH <sub>2</sub> )	658 M <sup>+</sup> (14) 529 (14) 410 ligand (78) 293 (47) 117 (100)
<b>43<sup>a)c)</sup></b>	7.85-6.76 m (16H, Ar-H) 6.35 s (2H) 4.54 d (J = 15.8 Hz, 2H, CH <sub>2</sub> ) 4.03 d (J = 15.8 Hz, 2H, CH <sub>2</sub> ) 2.21 br (6H, CH <sub>3</sub> )	141.5, 138.3, 136.7 (C <sub>q</sub> ) 133.0, 131.1, 129.5 (CH) 129.1 (C <sub>q</sub> ) 127.7, 126.1, 125.8, 124.3, 123.0, 119.8 (CH) 117.0, 114.5 (C <sub>q</sub> ) 34.3 (CH <sub>2</sub> ) 21.8 (CH <sub>3</sub> )	599 M <sup>+</sup> (5) 527 M <sup>+</sup> -2Cl (13) 437 M <sup>+</sup> -ZrCl <sub>2</sub> -H (22) 307 (33) 131 (100)
<b>44<sup>a)c)</sup></b>	7.95-7.08 m (8H, Ar-H) 6.85 s (1H) 4.58 d (J = 16.3 Hz, 1H, CH <sub>2</sub> ) 4.07 d, (J = 16.3 Hz, 1H, CH <sub>2</sub> ) 2.32 br (3H, CH <sub>3</sub> )	144.0, 140.1, 137.7 (C <sub>q</sub> ) 134.8, 132.1, 130.1 (CH) 129.0 (C <sub>q</sub> ) 128.8, 126.9, 126.4, 124.9, 123.5, 121.0 (CH) 117.3, 115.9 (C <sub>q</sub> ) 34.7 (CH <sub>2</sub> ) 22.0 (CH <sub>3</sub> )	n.d.

<sup>a)</sup>  $\delta$  (ppm) rel. CD<sub>2</sub>Cl<sub>2</sub> (5.30 ppm, <sup>1</sup>H NMR and 54.0 ppm, <sup>13</sup>C NMR) at 298 K.

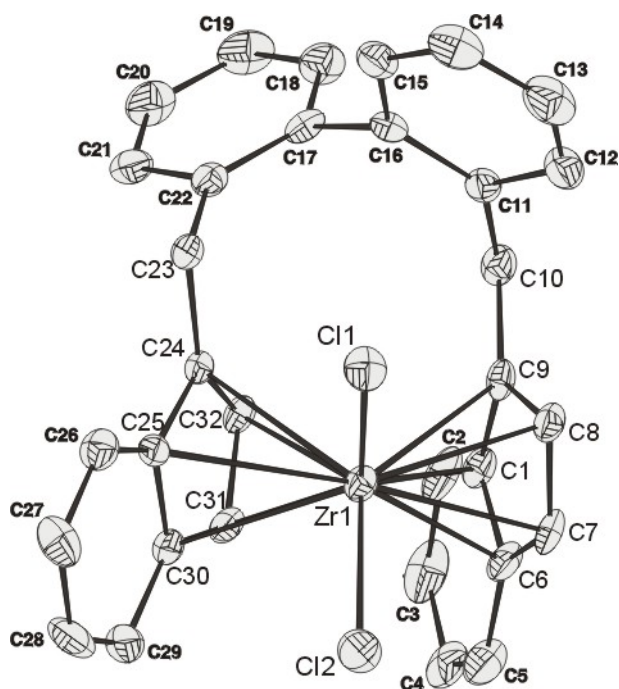
<sup>b)</sup>  $\delta$  (ppm) rel. CDCl<sub>3</sub> (7.24 ppm, <sup>1</sup>H NMR and 77.0 ppm, <sup>13</sup>C NMR) at 298 K.

<sup>c)</sup> Two isomers, data given for the most intensive signals.

### 2.3.6 Crystal structure of complex 41

The solid state molecular structure of the zirconocene complex **41** was determined by single crystal X-rays diffraction analysis. Crystals suitable for X-ray measurements were grown from a concentrated solution of a pentane/toluene mixture. The ORTEP view of the molecular structure of complex **41** is displayed in Scheme 48. The crystallographic

data and structural refinement are presented in Table 16 while the selected bond lengths and angles are collected in Table 17. The arrangement of the two five-membered ring centroids and the two chlorine atoms around the zirconium can be described as a pseudo tetrahedral geometry. The two indenyl ligands are aligned in a staggered conformation leading to an asymmetric rac orientation. In consistence with this, the values of the angles Cl1-Zr-Cl2 and Cen-Zr-Cen are  $97.23^\circ$  and  $128.73^\circ$ . These values correspond to those of previously characterized bridged metallocene complexes.<sup>[87]</sup> The bond lengths of the zirconium atom with the carbon atoms vary between 2.46-2.61 and 2.43-2.65 Å. for the two five-membered rings. The two phenyl rings of the biphenyl bridge are aligned in different planes with a dihedral angle of  $79.8^\circ$ . The value of the dihedral angle between the two planes of the five rings centroids is  $53.72^\circ$  which is smaller compared to the value known for  $\text{Me}_2\text{Si}(\text{Ind})_2\text{ZrCl}_2$  ( $61.9^\circ$ ).<sup>[93]</sup>



**Scheme 48:** The ORTEP diagram of the complex **41**, ellipsoids are drawn in a 30% probability level. Hydrogen atoms are omitted for clarity.

**Table 16:** Crystal data for complex **41**.

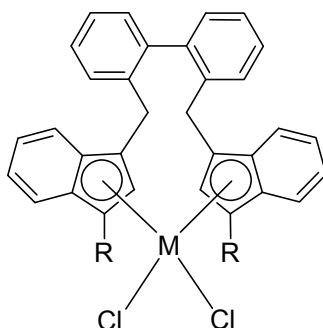
Formula	C <sub>32</sub> H <sub>24</sub> C <sub>12</sub> Zr <sub>1</sub>
Space group	I 4 <sub>1</sub> /a, Tetragonal
Z	16
a (Å)	26.045(2)
b (Å)	26.045(2)
c (Å)	14.9997(10)
α(°)	90
β(°)	90
γ(°)	90
Volume (Å <sup>3</sup> )	10175.1(13)
<i>F</i> (000)	4640.0
Temperature (K)	293
Wave length (Å)	0.71069
Crystal dimensions (mm <sup>3</sup> )	0.30 × 0.28 × 0.20
<i>R</i> <sub>int</sub>	0.125
[ <i>Sin</i> (θ)/λ] <sub>max</sub> (Å <sup>-1</sup> )	0.600
Density (g cm <sup>-3</sup> )	1.4896
Absorption coefficient (mm <sup>-1</sup> )	0.662
Observed Criteria	I > 3σ(I)
No. of observed/all reflections	2054/4589
<i>wR</i> <sub>F</sub> (obs/all)	0.0435/0.0544
<i>R</i> <sub>F</sub> (obs/all)	0.0522/0.1801
Δρ <sub>max</sub> / Δρ <sub>min</sub> (eÅ <sup>-3</sup> )	1.22/-1.46
<i>GoF</i> (obs/all)	1.59/2.00

**Table 17:** Selected bond lengths and angles

<u>Selected bond lengths[Å]</u>		C(23)-C(24)	1.5075(1)
Zr-Cl(1)	2.4245(1)	Zr-Cen1	2.2230(5)
Zr-Cl(2)	2.4279(1)	Zr-Cen2	2.2486(5)
Zr-C(1)	2.6147(2)	Cen1-Cen2	4.0317(2)
Zr-C(6)	2.5122(1)	<u>Selected bonds angles[°]</u>	
Zr-C(7)	2.4627(1)	Cl(1)-Zr-Cl(2)	97.233(2)
Zr-C(8)	2.4989(1)	C(1)-C(9)-C(10)	124.566(4)
Zr-C(9)	2.5434(1)	C(9)-C(10)-C(11)	115.183(4)
Zr-C(24)	2.5775(2)	C(23)-C(24)-C(25)	123.387(4)
Zr-C(25)	2.6504(1)	C(22)-C(23)-C(24)	113.375(4)
Zr-C(30)	2.6049(2)	Cen1-Zr-Cen2	128.734(3)
Zr-C(31)	2.4291(1)	Cen (1) ^ Cen(2)	53.723(4)
Zr-C(32)	2.4723(1)	Ph(1) ^ Ph(2)	79.829(5)
C(9)-C(10)	1.5092(1)		

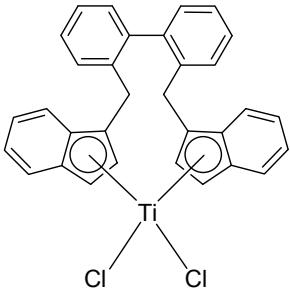
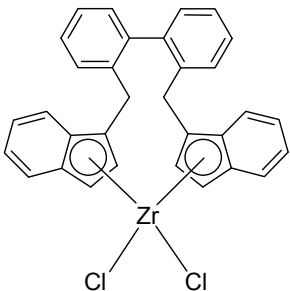
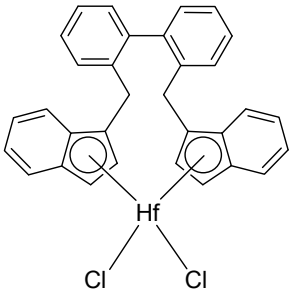
### 2.3.7 Ethylene polymerization studies of complexes 40-44

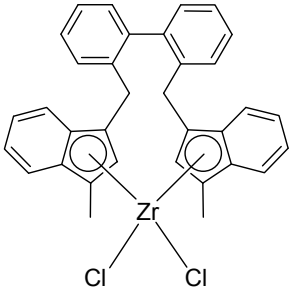
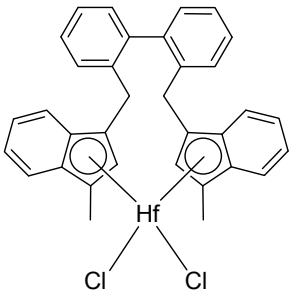
Complexes **40-44** are ansa-metallocene dichloride complexes of group IV metals (Ti, Zr, and Hf). The two indenyl ligands are tethered through the 3-positions via a 2,2'-bis(methylene)-1,1'-biphenylidene bridge. The general structure formula of the complexes is illustrated in Scheme 49.

**Scheme 49:** Structural formula of complexes **40-44**.

The catalytic activities of complexes **40-44** in the homogeneous polymerization of ethylene were investigated after activation with methylaluminumoxane (M:Al = 1:2000). The experiments were conducted at a polymerization temperature of 60°C, 10 bar ethylene pressure, and in 250 ml of pentane for one hour. The produced polyethylene samples were analyzed by DSC and viscosimetry. The results are illustrated in Table 18.

**Table 18:** Activities and polymer analysis results of catalysts **40-44**

Complex	No.	Activity [kg PE/mol cat. h]	DSC $\Delta H_m$ [J/g] $T_m$ [°C] [ $\alpha$ ]	$M_n$ [g/mol]
	<b>40</b>	Inactive	-	-
	<b>41</b>	12460	148.1 135.0 0.51	355000
	<b>42</b>	3810	144.9 135.2 0.5	310000

	<b>43</b>	3010	145.1 135.4 0.5	485000
	<b>44</b>	1020	n.d.	n.d.

In the series of complexes **40-44**, the zirconium catalyst **41**/MAO was the most active catalyst [12460 kg PE/mol cat. h] whereas the hafnium catalyst **42**/MAO bearing the same ligand showed lower activity [3810 kg PE/mol cat. h]. The titanium complex **40** was inactive in ethylene polymerization under the prescribed conditions. This inactivity can be attributed to the instability of Ti(IV) complexes and their tendency to reduction to give inactive Ti(III) species at conventional polymerization temperatures.<sup>[105]</sup> On going from **41**/MAO to the 3-methyl substituted zirconium catalyst **43**/MAO, a marked decrease in activity is observed (from 12460 to 3010 kg PE/mol cat. h). A similar decrease in activity has been observed when using the 3-alkyl substituted Me<sub>2</sub>Si-bridged catalysts [Me<sub>2</sub>Si(3-R-Ind)<sub>2</sub>]ZrCl<sub>2</sub><sup>[85]</sup>. In this regard, the drop in activity can be attributed to the increase of steric congestion around the metal center caused by the two methyl groups at the indenyl ligands.

Across the series, changing the metal and introduction of methyl groups proved to have no influence on the thermal properties and the crystallinities of the produced polymers. By comparing the catalytic performance of **41**/MAO with the previously reported relevant ansa-catalysts, there is a good correlation between the catalytic activity of the ansa-catalysts and their dihedral angles. The dihedral angle of complex **41** is 53.7° (Table 17) which is smaller than that of the CH<sub>2</sub>-bridged (72.4°) and the Me<sub>2</sub>C-bridged metallocene

complexes (70.9°). However, catalyst **41**/MAO exhibited higher catalytic activity (12460 kg PE/mol cat. h) than the CH<sub>2</sub>-bridged catalyst (6900 kg PE/mol cat. h)<sup>[97]</sup> and the Me<sub>2</sub>C-bridged catalyst (10000 kg PE/mol cat. h)<sup>[97]</sup>. This could be originated to the thermal instability of the single carbon atom bridged metallocene complex. Moreover, catalyst **41**/MAO produces a polyethylene with higher molecular weight compared with the above mentioned single carbon atom bridged metallocene complexes. Additionally, catalyst **41**/MAO showed a better catalytic performance in terms of both activity and molecular weight of the produced polymers compared with the *o*-xylylene<sup>[88]</sup> and the 1,2-bis(dimethylsilyl)ethylene-bridged<sup>[102]</sup> metallocene catalysts.

The catalytic activity performed by **41**/MAO is significantly lower than the activity reported for the unbridged catalyst (29300 kg PE/mol cat. h)<sup>[77]</sup>, the Me<sub>2</sub>Si-bridged catalyst (19870 kg PE/mol cat. h)<sup>[85]</sup>, and the ethylidene-bridged catalyst<sup>[101]</sup> (16500 kg PE/mol cat. h) due to the remarkable difference in the dihedral angle values and thus the accessibility of the metal center.

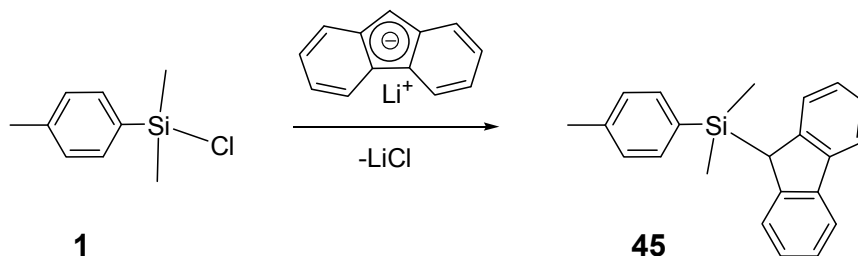
## 2.4 9-Substituted silylfluorenyl complexes of zirconium and hafnium

### 2.4.1 General remarks

Bridged fluorenyl complexes are known to be highly active catalyst precursors in olefin polymerization<sup>[33]</sup> However, the unbridged mixed fluorenyl and cyclopentadienyl complexes are far less active towards olefin polymerization due to the ring slippage phenomenon.<sup>[106]</sup> To date, symmetrical unbridged 9-silyl-substituted fluorenyl dichloride metallocene complexes still have not been reported. Herein, the synthesis of the zirconium and hafnium complexes of 9-(4-tolyldimethylsilyl)fluorenyl and their behavior in ethylene polymerization are reported.

### 2.4.2 Synthesis of the potential ligand **45**

The 9-substituted silylfluorenyl compound **45** was obtained by the reaction of fluorenyllithium, prepared separately by the deprotonation of fluorene with n-BuLi, and an equivalent amount of p-tolylchlorodimethylsilane **1** in diethyl ether (Scheme 50).

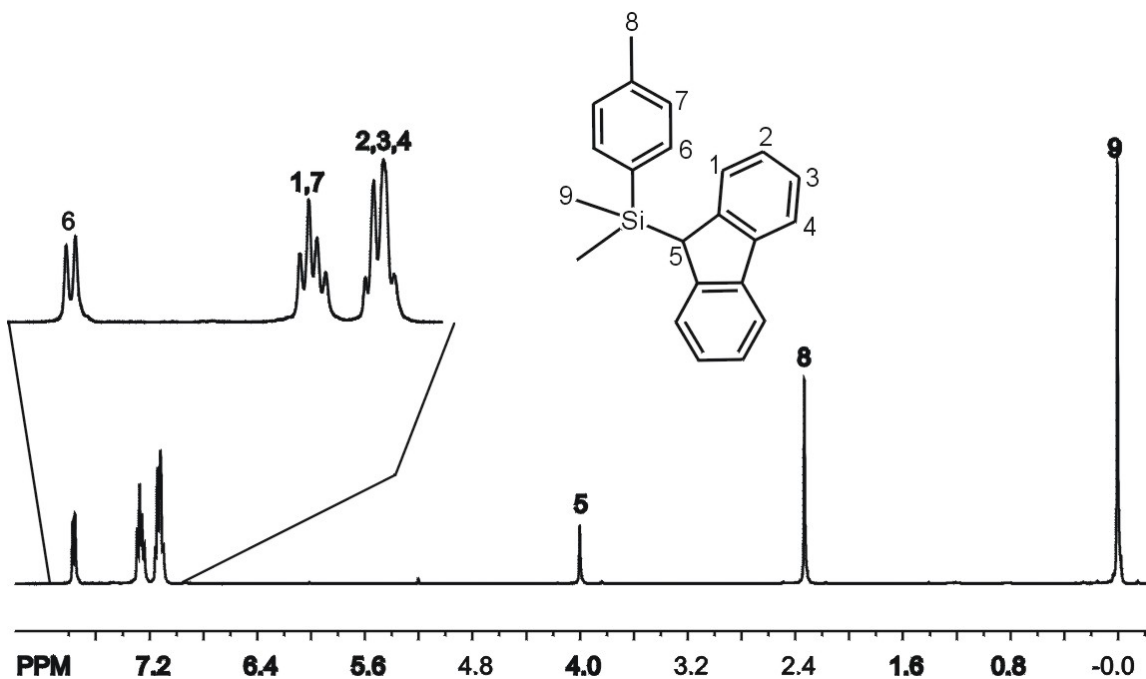


**Scheme 50:** Preparation of compound **45**.

### 2.4.3 Characterization of compound **45**

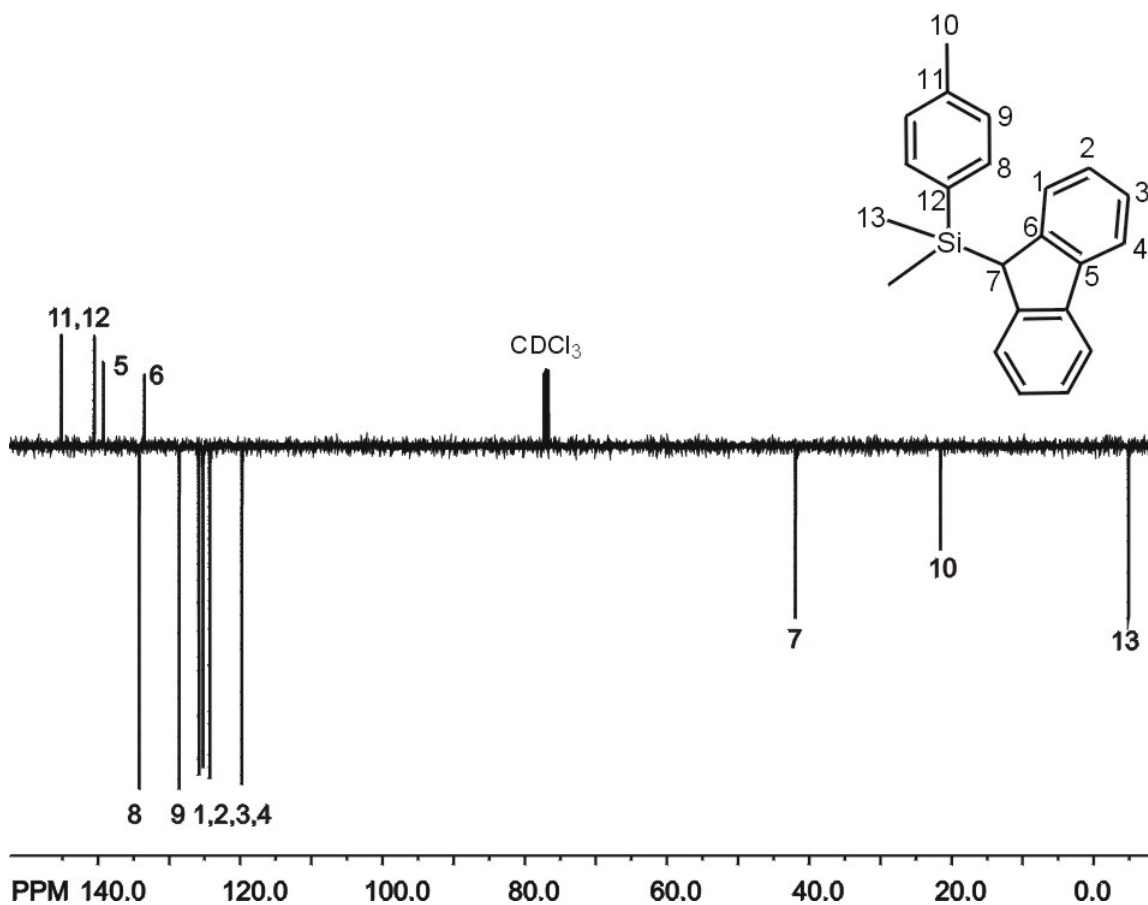
The <sup>1</sup>H NMR spectrum of compound **45** (Scheme 51) shows a doublet at  $\delta = 7.76$  ppm (d, <sup>3</sup>J = 7.4 Hz, 2H) which can be assigned to the aromatic protons H6 belonging to the silyl phenyl ring while the protons H7 and H1 produce the overlapping multiplet at  $\delta = 7.29$ -7.24 ppm (4H). The other aromatic protons belonging to the fluorenyl moiety (H2, H3, and H4) give rise to the multiplet which appears at  $\delta = 7.17$ -7.09 ppm (m, 6H). The singlet at  $\delta = 4.00$  ppm (1H) is assigned to the proton (H5) while the singlet at  $\delta = 2.33$

ppm (s, 3H) is characteristic for the tolyl methyl protons (H8). The singlet appearing further upfield at  $\delta = 0.01$  ppm (s, 6H) corresponds to the equivalent methyl group protons (H9) attached to the silicon atom.



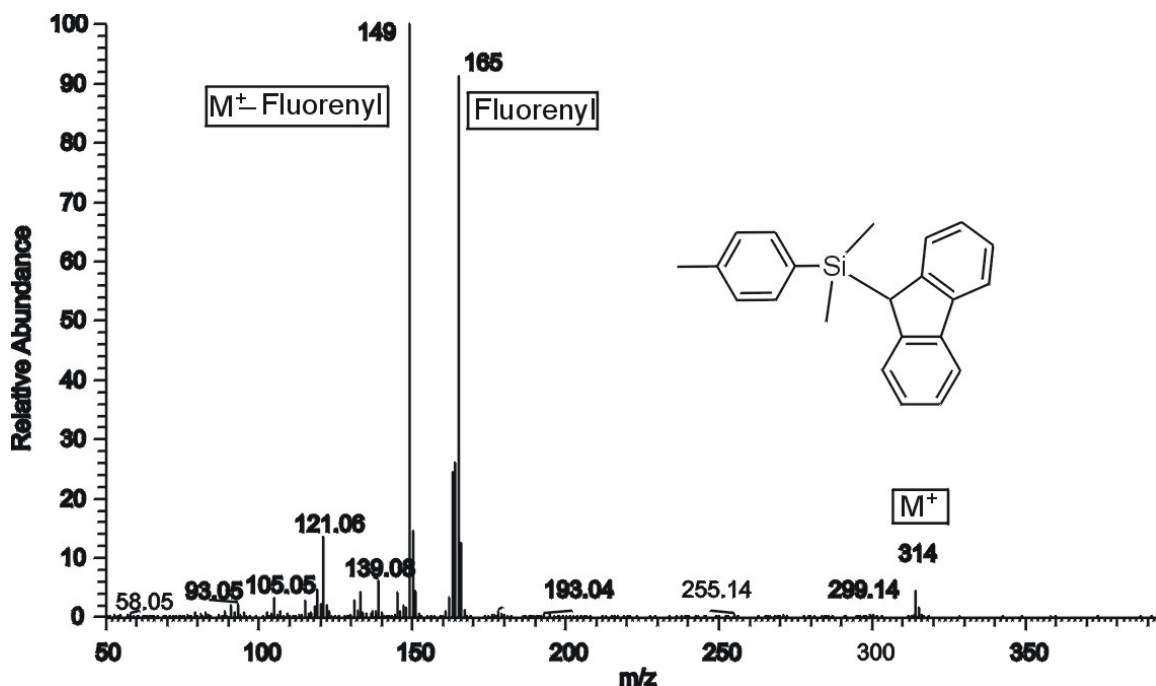
**Scheme 51:** <sup>1</sup>H NMR spectrum of compound 45.

The <sup>13</sup>C NMR spectrum of compound 45 (Scheme 52) reveals thirteen signals which can be explained as follows: four signals at  $\delta = 145.1$ , 140.5, 139.2, and 133.5 ppm belong to the quaternary carbon atoms C11, C12, C5, and C6. Six equally intensive signals appear at  $\delta = 134.2$ , 128.6, 125.8, 125.2, 124.3, and 119.8 ppm and represent the CH-type carbon atoms C8, C9, C1, C2, C3, and C4. The signal at  $\delta = 41.9$  ppm is generated by C7 at the 9-position of the fluorenyl moiety whereas the signals at  $\delta = 21.5$  and  $-4.9$  ppm can be assigned to the methyl group carbon atoms C10 and C13.



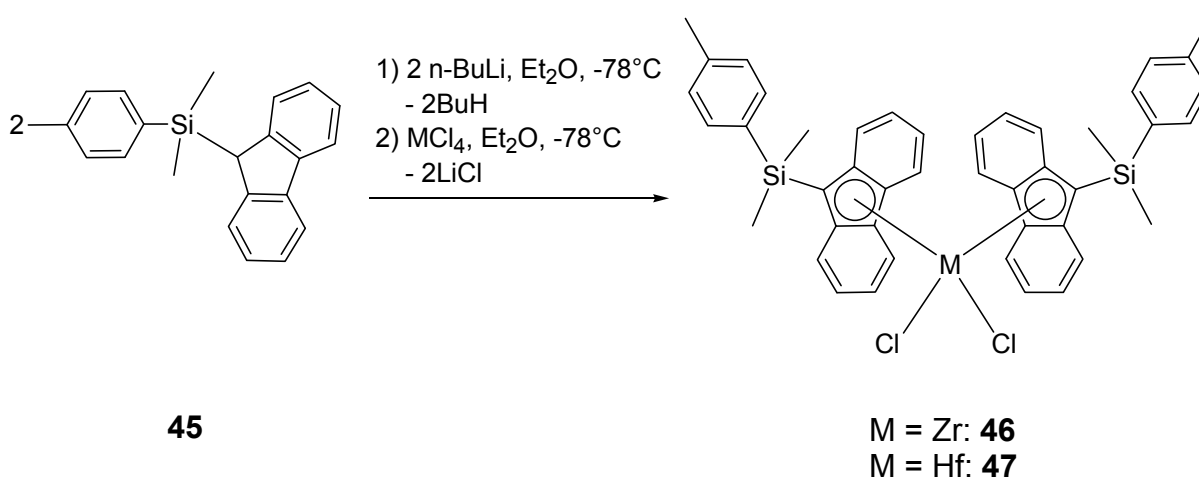
**Scheme 52:** <sup>13</sup>C NMR spectrum of compound **45**.

The mass spectrum of compound **45** (Scheme 53) shows the molecular ion peak at  $m/z = 314$  with 6% intensity relative to the base peak. The fragmentation of the compound through the silicon fluorene bond results in two smaller fragments: the fluorene fragment produces the peak at  $m/z = 165$  with 94% intensity, and the tolyldimethylsilyl fragment generates the base peak at  $m/z = 149$ .

Scheme 53: Mass spectrum of compound **45**.

#### 2.4.4 Synthesis of complexes **46** and **47**

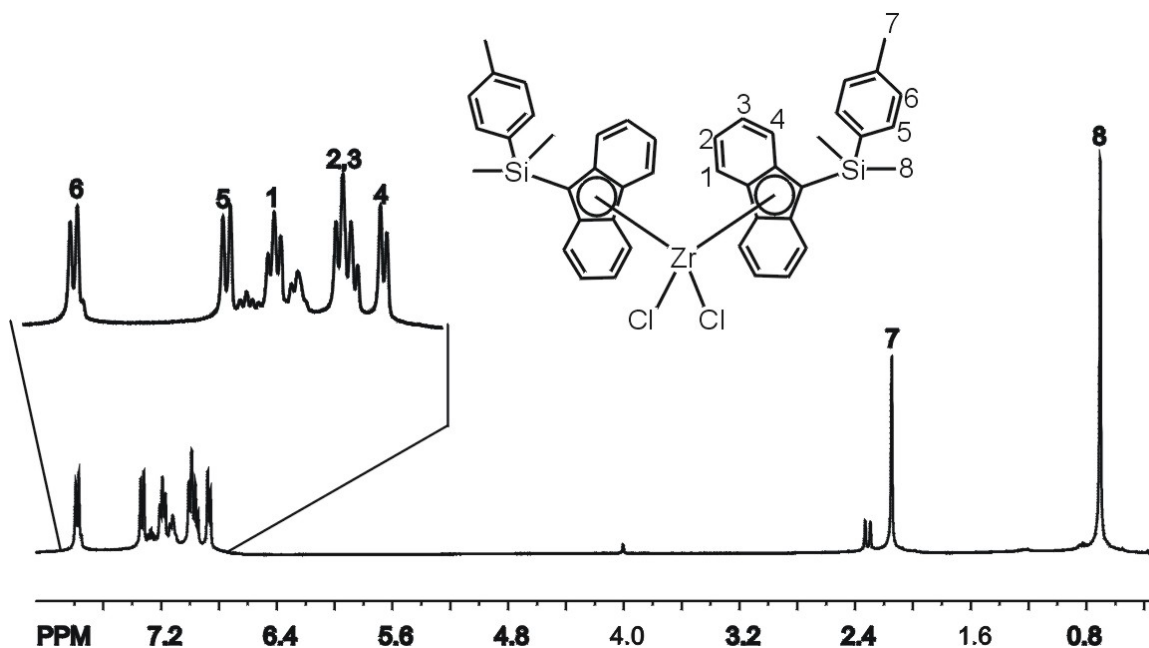
The conversion of the ligand precursor **45** to the corresponding lithium salt was accomplished via deprotonation by a stoichiometric amount of *n*-butyllithium in diethyl ether. A subsequent metallation of the lithiated ligand with 0.5 equivalents of zirconium tetrachloride or hafnium tetrachloride in diethyl ether afforded the desired complexes **46** and **47** in 60-70% yield (Scheme 54).

Scheme 54: Synthesis of complexes **46** and **47**.

### 2.4.5 Characterization of complexes **46** and **47**

Complexes **46** and **47** were characterized by elemental analysis (see the experimental part) and NMR spectroscopy (Table 19).

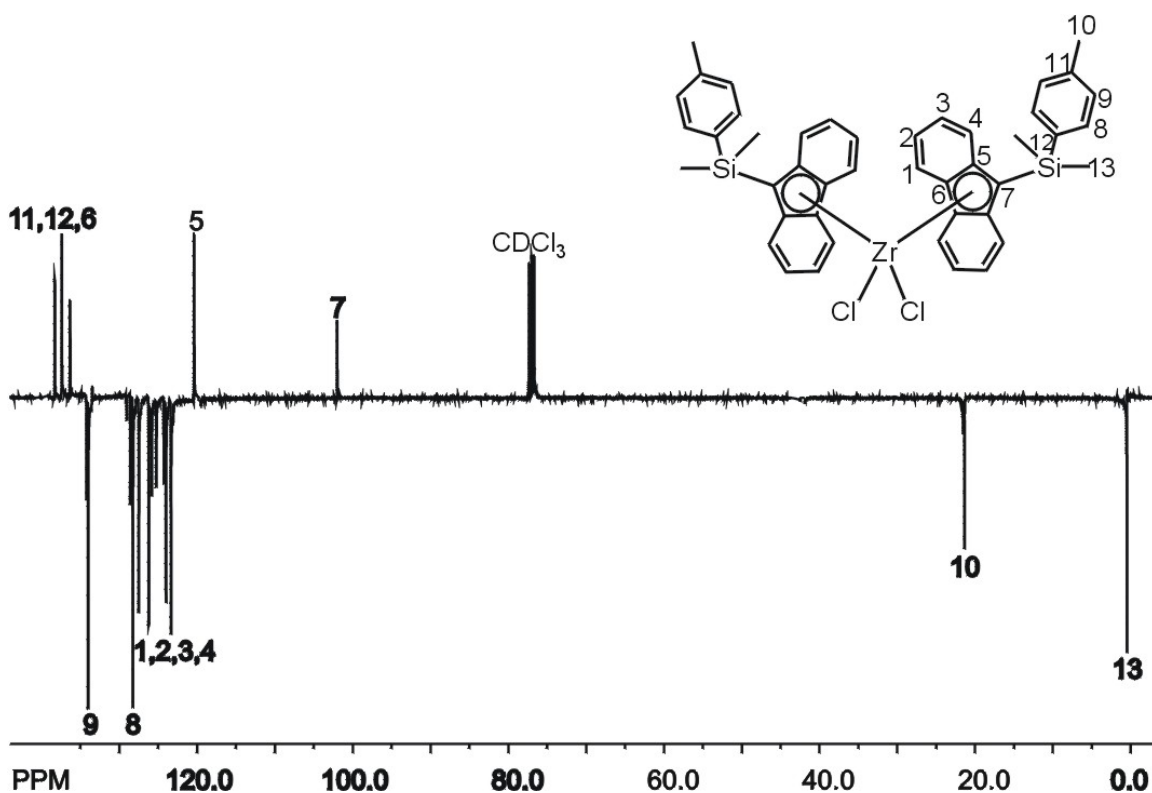
The  $^1\text{H}$  and  $^{13}\text{C}$  NMR spectra of complex **46** are discussed as examples. The  $^1\text{H}$  NMR spectrum of complex **46** (Scheme 55) exhibits seven resonance signals that can be interpreted as follows: the two doublets at  $\delta = 7.78$  ppm ( $^3J = 8.2$  Hz, 4H) and 7.33 ppm ( $^3J = 8.2$  Hz, 4H) are assigned to the aromatic protons (H6 and H5) belonging to silyl phenyl rings. The protons at the fluorenyl moieties (H1, H2, H3, and H4) produce the three signals at  $\delta = 7.20$ -7.17 (t, 4H), 7.00-6.94 (m, 8H), and 6.87 (d,  $^3J = 7.3$  Hz, 4H) ppm. The signal for the tolyl methyl protons (H7) appears at  $\delta = 2.15$  ppm as a singlet with (6H) intensity, while the signal associated to the silyl methyl groups (H8) appears as a singlet at  $\delta = 0.70$  ppm.



**Scheme 55:**  $^1\text{H}$  NMR spectrum of complex **46**.

The  $^{13}\text{C}$  NMR spectrum of complex **46** (Scheme 56) shows three signals at  $\delta = 138.3$ , 137.4 and 136.3 ppm representing the quaternary carbon atoms C11, C12, and C6. The

CH-type carbon atoms of the silyl phenyl rings (C9 and C8) appear at  $\delta = 134.0$  and  $128.3$  ppm while the CH-type carbon atoms at the fluorenyl moieties (C1, C2, C3, and C4) give rise to the signals at  $\delta = 127.5$ ,  $126.2$ ,  $124.0$  and  $123.3$  ppm. The signal at  $\delta = 120.4$  ppm is assigned to the quaternary carbon atom C5 while the signal at  $\delta = 102.0$  ppm can be interpreted for the quaternary carbon atom C7. The methyl groups (C10 and C13) furnish the upfield shifted signals at  $\delta = 21.3$  and  $0.5$  ppm.



**Scheme 56:**  $^{13}\text{C}$  NMR spectrum of complex 46.

**Table 19:**  $^1\text{H}$  and  $^{13}\text{C}$  NMR<sup>a</sup> spectra of complexes **46** and **47**.

No.	$^1\text{H}$ NMR	$^{13}\text{C}$ NMR
<b>46</b>	7.78 d ( $^3J = 8.2$ Hz, 4H, Ar-H) 7.33 d ( $^3J = 8.2$ Hz, 4H, Ar-H) 7.20-7.17 t (4H) 7.00-6.94 m (8H) 6.87 d ( $^3J = 7.3$ Hz, 4H) 2.15 s (6H, Ar-CH <sub>3</sub> ) 0.70 s (12H, Si(CH <sub>3</sub> ) <sub>2</sub> )	138.3, 137.4, 136.3 (C <sub>q</sub> ) 134.0, 128.3, 127.5, 126.2, 124.0, 123.3 (CH) 120.4, 102.0 (C <sub>q</sub> ) 21.3, (CH <sub>3</sub> ) 0.5 (Si(CH <sub>3</sub> ) <sub>2</sub> )
<b>47</b>	7.81 d ( $^3J = 9.1$ Hz, 4H, Ar-H) 7.39 d ( $^3J = 9.1$ Hz, 4H, Ar-H) 7.21-7.12 t (4H) 7.05-6.89 m (8H) 6.85 d ( $^3J = 7.3$ Hz, 4H) 2.15 s (6H, Ar-CH <sub>3</sub> ) 0.70 s (12H, Si(CH <sub>3</sub> ) <sub>2</sub> )	139.7, 137.9, 136.1 (C <sub>q</sub> ) 134.6, 128.4, 127.7, 126.5, 124.2, 123.1 (CH) 120.9, 103.1 (C <sub>q</sub> ) 21.4, 0.5 (CH <sub>3</sub> ) 0.5 (Si(CH <sub>3</sub> ) <sub>2</sub> )

<sup>a</sup>  $\delta$  (ppm) rel. CDCl<sub>3</sub> (7.24 ppm,  $^1\text{H}$  NMR and 77.0 ppm,  $^{13}\text{C}$  NMR) at 298 K.

#### 2.4.6 Ethylene polymerization experiments with complexes **45** and **46**

Complexes **46** and **47** were tested for ethylene polymerization after activation with methylaluminoxane (MAO) with a M:Al ratio of 1:2000. The experiments were conducted at 60°C and 10 bar ethylene pressure in 250 ml of pentane. These complexes were found to be inactive in polymerization reactions. The same result was reported by Alt et al.<sup>[107]</sup> using unbridged 9-substituted phenyl fluorenyl complexes for the polymerization of ethylene and propene. The inertness of the fluorenyl complexes **46** and **47** could be attributed to the thermal instability resulting from ring-slippage reactions changing the hapticity of the fluorenyl rings from  $\eta^5 \rightarrow \eta^3 \rightarrow \eta^1$ <sup>[106]</sup>. The bulkiness of the substituents may also be a reason for the inactivity of **46** and **47**.

### 3. Experimental Part

#### 3.1 General

All reactions were carried out under an inert gas atmosphere of pure oxygen-free argon using standard Schlenk techniques. n-Pentane, n-hexane, diethyl ether, toluene, and tetrahydrofuran were purified by distillation over Na/K alloy. Diethyl ether was additionally distilled over lithium aluminum hydride. Toluene was additionally distilled over phosphorus pentoxide. Methylene chloride and carbon tetrachloride were dried over phosphorus pentoxide. Deuterated organic solvents ( $\text{CDCl}_3$ ,  $\text{CD}_2\text{Cl}_2$ , and  $\text{C}_6\text{D}_6$ ) for NMR spectroscopy were purchased from Euriso-Top and stored over molecular sieves (3 Å). Argon (5.0) and ethylene (3.5) were purchased from Rießner Company. Methylaluminoxane (10% in toluene) was purchased from Chemtura Europe Limited (Bergkamen). All other starting materials were commercially available and used without further purification.

#### 3.2 NMR spectroscopy

NMR spectra were recorded with Bruker ARX (250 MHz), Varian Inova (300 MHz) or Varian Inova (400 MHz) spectrometers. All spectra were recorded at 298 K. In the  $^1\text{H}$ -NMR spectra, the chemical shift of the residual proton signal of the solvent was used as a reference ( $\delta = 7.24$  ppm for chloroform,  $\delta = 5.32$  ppm for methylene chloride,  $\delta = 7.16$  ppm for benzene). In the  $^{13}\text{C}$ -NMR spectra, the chemical shift of the solvent was used as a reference ( $\delta = 77.0$  ppm for chloroform- $\text{d}_1$ ,  $\delta = 54.0$  ppm for methylene chloride- $\text{d}_2$ ,  $\delta = 128.0$  ppm for benzene- $\text{d}_6$ ).

#### 3.3 GC/MS

GC/MS spectra were recorded with a Thermo FOCUS gas chromatograph combined with a DSQ mass detector. A 30 m HP-5 fused silica column (internal diameter 0.32 mm, film 0.25  $\mu\text{m}$  and flow 1 ml/min) was used and helium (4.6) was applied as carrier gas. The measurements were recorded using the following temperature program:

Starting temperature: 50 °C, duration: 2 minutes;

Heating rate: 20 °K/minute, duration: 12 minutes;

Final temperature: 290 °C, duration: 27 minutes.

### 3.4 Mass spectrometry

Mass spectra were recorded with a VARIAN MAT CH-7 instrument (direct inlet, EI, E = 70 eV) and a VARIAN MAT 8500 spectrometer at the Zentrale Analytik of the University of Bayreuth. Matrix Assisted Laser Desorption Ionization Time-of-Flight Mass Spectrometry (MALDI-TOF-MS) measurements were performed on a Bruker Daltonic Reflex TOF using graphite as the matrix. The laser intensity was set to 60-65 %. The sample solutions were prepared in toluene or methylene chloride at a concentration of 1 mg/ml.

### 3.5 Elemental analysis

Elemental analyses were performed with a Vario EL III CHN instrument. Therefore, 4-6 mg of the complex were weighed into a standard tin pan. The tin pan was carefully closed and introduced into the auto sampler of the instrument. The values of C, H and N were calibrated using acetamide as a standard.

### 3.6 DSC analysis

DSC analyses were performed on a Mettler Toledo DSC/SDTA 821e instrument. The polymer samples were prepared by enclosing 4-6 mg of the polymers in standard aluminum pans. The samples were introduced into the auto sampler of the instrument and the measurements were recorded using the following temperature program:

First heating phase: from 50 °C to 160 °C (10 °C/minute);

Cooling phase: 160 °C to 50 °C (10 °C/minute);

Second heating phase: from 50 °C to 160 °C (10 °C/minute).

Liquid nitrogen was used as a cooling medium. Melting enthalpies and melting points were taken from the second heating phase. The values were calibrated using indium as a standard (m.p. 429.78 K,  $H_m = 28.45$  J/g).

### 3.7 Viscosimetry analysis

Viscosimetry analyses for the determination of the viscosity average molecular weights  $[M_\eta]$  of the polyethylene samples were performed on an Ubbelohde precision capillary viscometer in cis/trans-decalin at  $135 \pm 0.1$  °C. For the preparation of the sample solutions, an amount of 50 mg of the polymer was dissolved in decalin (45 ml) by heating for 3 hours at 135 °C.  $M_\eta$  values were determined by comparing the obtained values with calibration curves available for different polymer concentrations.

### 3.8 Single crystal X-rays diffraction

The crystal structure analysis of complex **34** was performed with a STOE-IPDS II diffractometer equipped with an Oxford Cryostream low-temperature unit. The crystal structure analysis of complexes **35** and **41** was performed with a MarIP MAR345DTB device (Mo-K $\alpha$  radiation,  $\lambda = 0.71073$  Å).

#### Crystal data:

**Complex 34:** Yellow cubic crystals, crystal system is triclinic; space group is P-1;  $a = 9.1925(18)$  Å,  $b = 10.110(2)$  Å,  $c = 15.726(3)$  Å;  $\alpha = 91.36(3)^\circ$ ,  $\beta = 100.26(3)^\circ$ ,  $\gamma = 111.24(3)^\circ$ ; volume is  $1333.6(5)$  Å<sup>3</sup>;  $d_{(\text{calc})} = 1.451$  g/cm<sup>3</sup>; wavelength =  $0.71073$  Å; absorption coefficient =  $0.718$  mm<sup>-1</sup>;  $F(000) = 596$ ; reflections collected 6271; independent reflections 4372 [ $R(\text{int}) = 0.0396$ ]; Goodness-of-fit = 0.938; R indices ( $R1 = 0.0547$ ,  $wR2 = 0.1022$ ).

**Complex 35:** Yellow cubic crystals, crystal system is triclinic; space group is P-1;  $a = 10.0503(18)$  Å,  $b = 9.1624(16)$  Å,  $c = 15.643(3)$  Å;  $\alpha = 91.567(19)^\circ$ ,  $\beta = 100.285(18)^\circ$ ,  $\gamma = 111.167(8)^\circ$ ; volume is  $1315.0(4)$  Å<sup>3</sup>;  $d = 1.6918$  g/cm<sup>3</sup>; wavelength =  $0.71069$  Å; absorption coefficient =  $4.276$  mm<sup>-1</sup>;  $F(000) = 660$ ; no. of all reflections 11018; no. of observed reflections 8001 [ $R(\text{int}) = 0.056$ ]; GOF (obs/all) = 1.01/-0.87;  $R(F) = 0.0422$  ( $wR(F) = 0.0395$ ).

**Complex 41:** Yellow cubic crystals, crystal system is tetragonal; space group is  $I 4_1/a$ ;  $Z = 16$ ;  $a = b = 26.045(2) \text{ \AA}$ ,  $c = 14.9997(10) \text{ \AA}$ ;  $\alpha = \beta = \gamma = 90^\circ$ ; volume is  $10175(13) \text{ \AA}^3$ ;  $d = 1.4896 \text{ g/cm}^3$ ; wavelength =  $0.71069 \text{ \AA}$ ; absorption coefficient =  $0.662 \text{ mm}^{-1}$ ;  $F(000) = 4640$ ; no. of all reflections 4589; no. of observed reflections 2054 [ $R(\text{int}) = 0.125$ ]; GOF (obs/all) =  $1.59/2.00$ ;  $R(F) = 0.0522$  ( $wR(F) = 0.0435$ ).

### 3.9 Polymerization of ethylene

Few milligrams of the complexes were dissolved or suspended in toluene (5-10 ml) and mixed with the appropriate amount of methylaluminoxane (MAO). The activated complexes were suspended in pentane (250 ml) in a 1l Schlenk flask and then transferred under argon to a 1l Büchi autoclave. The temperature of the thermostat was adjusted to the desired value and an ethylene pressure of 10 bar was applied for one hour. After releasing the pressure, the obtained polymer was filtered over a frit, washed with dilute hydrochloric acid, water, and finally with acetone and dried under vacuum.

### 3.10 Synthesis procedures

#### 3.10.1 General synthesis of the arylchlorodimethylsilane compounds 1-4

A solution of a 4-substituted 1-bromobenzene (15.0 mmol) in THF (40 ml) was added dropwise at room temperature to a mixture of magnesium powder (20.0 mmol) and dichlorodimethylsilane (52.0 mmol) in THF (100 ml). After the addition was complete, the flask content was heated at reflux for approximately 4 hours and subsequently stirred at room temperature overnight. The solvent and the excess dichlorodimethylsilane were removed in vacuo (25 mbar). The residue was extracted three times with n-pentane (300 ml) and the excess magnesium and magnesium salts were filtered off. The combined pentane solutions were concentrated under vacuum and the residue was distilled under reduced pressure. The compounds **1-4** were obtained as colorless liquids in 60-75% yields.

### 3.10.2 General synthesis of the 1-(aryldimethylsilyl)indenyl compounds 5-8

An amount of 10 mmol of n-butyllithium (1.6 M in hexanes) was added to 10 mmol of indene dissolved in 100 ml of diethyl ether at 0°C. The solution was stirred for 2 hours at room temperature. The solution was again cooled to 0 °C and then an equivalent amount of the appropriate arylchlorodimethylsilane (**1-4**) in diethyl ether was added slowly. The resulting solution was stirred overnight at room temperature. The solvent was removed in vacuo and the residue was extracted twice with pentane. The suspension was filtered and passed through silica gel. After removing the solvent, compounds **5-8** were obtained as yellow oily liquids in 70-80% yields.

### 3.10.3 Synthesis of 2-bromoindene

To a mixture of indene (200 mmol), distilled water (15 ml) and dimethyl sulfoxide (70 ml) was added portion wise an amount of 210 mmol of N-bromosuccinimide. The resulting orange solution was stirred for 10 hours at room temperature, hydrolyzed with chilled water (100 ml), and extracted with diethyl ether (3 x 100 ml). The combined extracts were dried with magnesium sulphate and concentrated to give crystals of 2-bromoindan-1-ol upon standing overnight at -24 °C. The obtained 2-bromoindan-1-ol (120 mmol) was suspended in 100 ml of toluene and mixed with a catalytic amount of para-toluenesulfonic acid monohydrate. The mixture was heated at reflux for 12 hours, and water was removed by a Dean-Stark apparatus. The resulting dark brown suspension was filtered and the volatiles were removed under vacuum. The residue was passed through silica gel using pentane as eluent, then the solvent was evaporated, and the crude product was distilled in vacuo. 2-Bromoindene was finally obtained as yellow crystals in 55% yield.

### 3.10.4 General synthesis of the 2-(aryldimethylsilyl)indenyl compounds 9-12

Magnesium powder (18.0 mmol) and 15 ml of THF were placed in a 250 ml flask. A solution of 2-bromoindene (15.0 mmol) in 40 ml of THF was added over a period of 40 minutes using a pressure equalizing-addition funnel. After the addition was completed, the reaction mixture was heated at reflux for 4 hours. The unreacted magnesium was filtered off and the violet-red coloured Grignard solution was added dropwise to a stirred

solution of the appropriate arylchlorodimethylsilane **1-4** (15.0 mmol) and 50 ml of THF at room temperature. The resulting mixture was stirred for another 12 hours. The solvent was removed under vacuum and the residue was extracted twice with n-pentane. The suspension was filtered and passed through silica gel. After removing the solvent, compounds **9-12** were obtained as red or yellow oily liquids in 65-80% yields.

### 3.10.5 General synthesis of the transition metal complexes **13-24**

An amount of 2 mmol of the appropriate 1- or 2-substituted indenyl compound was dissolved in 50 ml of diethyl ether. To this solution, n-butyllithium (2 mmol 1.6 M in hexanes) was added at -78 °C. This solution was allowed to warm to room temperature and stirred for further 3 hours. Subsequently, this mixture was transferred to a suspension of zirconium tetrachloride (1 mmol) or hafnium tetrachloride (1 mmol) in 20 ml of diethyl ether at -78 °C. The mixture was slowly allowed to come to room temperature and stirred for further 24 hours. Diethyl ether was removed and toluene (100 ml) was added. The toluene suspension was filtered, the volume of the filtrate was reduced, and the complexes were precipitated by addition of n-pentane. After filtration, the precipitate was washed several times with n-pentane and dried in vacuo to obtain the desired complexes as coloured powders in 60-70% yields.

**Table 20:** Elemental analysis data of complexes **13-24**.

No.	C <sub>exp</sub> %	C <sub>theor</sub> %	H <sub>exp</sub> %	H <sub>theor</sub> %
<b>13</b>	62.21	62.76	5.41	5.56
<b>14</b>	54.93	55.70	4.52	4.93
<b>15</b>	59.10	59.97	4.88	5.31
<b>16</b>	52.75	53.50	4.35	4.74
<b>17</b>	58.15	58.60	4.82	4.63
<b>18</b>	51.20	52.08	4.25	4.11
<b>19</b>	62.05	62.76	5.22	5.56
<b>20</b>	54.01	55.70	5.30	4.93
<b>21</b>	58.99	59.97	5.04	5.31
<b>22</b>	52.66	53.50	4.37	4.74
<b>23</b>	58.03	58.60	4.99	4.63
<b>24</b>	51.66	52.08	4.55	4.11

### 3.10.6 Preparation of 1,2-bis(chlorodimethylsilyl)benzene (**26**)

A solution of 1,2-dibromobenzene (16.5 g, 70 mmol) in 70 ml of THF was added slowly to a stirred mixture of magnesium powder (3.7 g, 147 mmol) and chlorodimethylsilane (14.0 g, 147 mmol) in 15 ml of THF. The mixture was refluxed for 3 hours. After cooling, the solution was decanted from solid magnesium salts and the solvent was removed under vacuum. The residual oil was extracted and washed with a large amount of n-hexane. After removal of the solvent, the residue was purified by distillation under reduced pressure to afford 1,2-bis(dimethylsilyl)benzene (**25**) in 60% yield. Compound **25** (20 mmol) was mixed with 40 ml of dry carbon tetrachloride and 0.2 g of palladium dichloride in a 100 ml two necked flask equipped with a reflux condenser. The mixture was refluxed for 3 hours and excess carbon tetrachloride and chloroform were removed by evacuation. The residual oil was distilled at 85 °C (1 mbar) to obtain compound **26** in 90% yield.

### 3.10.7 Preparation of 2-methylindene (**28**)

A quantity of 48 mmol of methyl magnesium bromide (3M in ether) was added dropwise to a solution of 2-indanone (6.0 g, 48 mmol) in 100 ml of diethyl ether. Afterwards, the resulting mixture was stirred for 2 hours at room temperature and then hydrolyzed with 150 ml of diluted hydrochloric acid (1.0 M). The ether containing layer was separated and the aqueous layer was extracted four times with ether (each 100 ml). The organic extracts were combined, dried over sodium sulphate, and the solvent was removed with a rotary evaporator. The residue was mixed with 100 ml of toluene and a catalytic amount of para-toluenesulfonic acid monohydrate (PTSA). The suspension was refluxed for 3 hours in a Dean-Stark apparatus. The resulting dark brown suspension was filtered and the volatiles were removed under vacuum. The residue was passed through silica gel using pentane as eluent. The solvent was removed by distillation at atmospheric pressure to afford 2-methylindene as a light yellow oil in 40% yield.

### 3.10.8 General synthesis of the ligand precursors **27**, **29**, and **30**

An amount of 16 mmol of indene, 2-methylindene, or fluorene was dissolved in 70 ml of diethyl ether and cooled to -5 °C. Subsequently, n-butyllithium (16 mmol) was added

dropwise over 30 minutes followed by stirring at room temperature for 2 hours. To this mixture, another solution of 1,2-bis(chlorodimethylsilyl)benzene (8 mmol) in 50 ml of diethyl ether was added dropwise from a dropping funnel equipped with a pressure equalizer. After the addition was completed, the solution was stirred for one hour and filtered from the solid lithium chloride. The solution was evaporated and methylene chloride (200ml) was added. After filtration, the solvent was removed under high vacuum. Compounds **27** and **29** were obtained as heavy brownish waxy materials in 80-90% yields, while compound **30** was obtained as a solid which was further purified by crystallization from methylene chloride at -24 °C.

### 3.10.9 Preparation of 1,3-bis(chlorodimethylsilyl)benzene (**32**)

A mixture of 1,3-dibromobenzene (19.0 g, 80 mmol) and diethoxydimethylsilane (166 mmol) in THF (40 ml) was added over a period of 1 hour to magnesium powder (170 mmol) suspended in 20 ml of THF. After the mixture was heated to reflux for 3 hours and then cooled, the resulting magnesium salts were filtered off. The solvent was evaporated and the residue was distilled under reduced pressure to give pure 1,3-bis(ethoxydimethylsilyl)benzene (**31**) in 70% yield. An amount of 50 mmol of compound **31** was placed in a 100 ml two-necked flask and mixed with 0.2 ml of pyridine and 30 ml of acetyl chloride. After the mixture was heated to reflux for 72 hours, excess acetyl chloride and the resulting ethyl acetate were evaporated, and the residue was distilled under reduced pressure to give the desired compound as a colourless liquid in 95% yield.

### 3.10.10 Preparation of 1,3-bis(inden-1-yl)dimethylsilyl)benzene (**33**)

To a solution of indene (23 mmol) in diethyl ether (100 ml) at 0 °C, n-butyllithium (23 mmol) was added dropwise. The resulting solution was stirred for 2 hours at room temperature till gas evolution had ceased. A solution of 1,3-bis(chlorodimethylsilyl)benzene (**32**) (11.5 mmol) in diethyl ether (40 ml) was added over 1 hour at room temperature. After the addition was completed, the mixture was stirred for further 4 hours and distilled water (100 ml) was added. The organic layer was separated and the aqueous layer was extracted with ether (2×100 ml). The organic

portion was dried over sodium sulphate, and the volatiles were removed under high vacuum to obtain the desired compound as a brown coloured oil in 70% yield.

### 3.10.11 General synthesis of the transition metal complexes **34** and **35**

A quantity of 2 mmol of 1,2-bis(1-indenyldimethylsilyl)benzene (**27**) was dissolved in 50 ml of THF and cooled to -78 °C. To this solution, n-butyllithium (4 mmol, 1.6 M in hexanes) was slowly syringed. This solution was allowed to warm to room temperature and stirred for further 3 hours till no more gas evolution was observed. The resulting solution was transferred via cannula to a solution of zirconium tetrachloride (2 mmol) or hafnium tetrachloride (2 mmol) in 20 ml of THF at -78 °C. After warming to room temperature, the mixture was subsequently stirred for 48 hours at 60-65 °C. The solvent was removed in vacuo and toluene (100) ml was added. The toluene suspension was filtered, the clear solution was concentrated to approximately 5 ml and the complexes were precipitated by the addition of n-pentane. After filtration, the precipitate was washed several times with n-pentane and dried in vacuo to obtain the desired complexes as yellow powders in 70-75% yields. Both complexes were crystallized from concentrated pentane/toluene mixtures to obtain yellow cubic crystals suitable for X-ray crystallography analysis.

**Table 21:** Elemental analysis data of complexes **34** and **35**.

No.	C <sub>exp</sub> %	C <sub>theor</sub> %	H <sub>exp</sub> %	H <sub>theor</sub> %
<b>34</b>	57.65	57.70	4.79	4.84
<b>35</b>	49.75	50.19	4.25	4.21

### 3.10.12 Preparation of 2,2'-bis(bromomethyl) biphenyl (**37**)

A solution of diphenic acid (7.74 g, 32 mmol) in 40 ml of THF was added over 40 minutes to a suspension of lithium aluminum hydride (2.508 g, 66.0 mmol) and 50 ml THF at 0 C°. After the addition, the flask contents were heated under reflux over night. Then, the reaction was carefully hydrolyzed with water (75 ml) and a 15% sodium hydroxide solution (75 ml). Diethyl ether (100 ml) was added and the organic phase was separated, dried over sodium sulphate, and evaporated to dryness. The residue was

purified by crystallization from methanol at  $-20^{\circ}\text{C}$  to afford 2,2'-bis(hydroxymethyl) biphenyl **36** as yellow crystals in 60% yield. A solution of compound **36** (10 mmol) in methylene chloride (70 ml) was cooled to  $0^{\circ}\text{C}$  and phosphorus tribromide (30 mmol) was added dropwise via a syringe. The reaction mixture was stirred at room temperature for 12 hours and washed with distilled water ( $3 \times 100$  ml). After drying of the methylene chloride phase over sodium sulphate, the solvent was removed by evacuation to afford 2,2'-bis(bromomethyl) biphenyl as a yellow powder in 80% yield.

### 3.10.13 Preparation of 2,2'-bis(inden-1-ylmethyl) biphenyl (**38**)

An amount of 24 mmol of n-butyllithium (1.6M in hexanes) was added dropwise to a solution of indene (24 mmol) in 100 ml of THF at  $0^{\circ}\text{C}$ . The resulting mixture was stirred at room temperature for 3 hours and cooled to  $-40^{\circ}\text{C}$ . To this mixture was added a solution of 2,2'-bis(bromomethyl)biphenyl (**37**) (12 mmol) in 40 ml of THF and the mixture was stirred over night at room temperature. After removal of the solvent under vacuum, distilled water was added and an extractive workup was performed by adding methylene chloride ( $3 \times 100$  ml). Drying of the organic phase over sodium sulphate and removal of the solvent under vacuum gave the crude product as yellow powder. The pure product was obtained as shining yellow crystals upon crystallization from a methylene chloride/pentane mixture in 75% yield.

### 3.10.14 General synthesis of the transition metal complexes 40-42

An amount of 2 mmol of 2,2'-bis(inden-1-ylmethyl) biphenyl **38** was dissolved in 50 ml of diethyl ether. To this solution, n-butyllithium (4 mmol, 1.6 M in hexanes) was added dropwise at  $-78^{\circ}\text{C}$ . The solution was allowed to come to room temperature and stirred for 3 hours. This solution was then added to titanium tetrachloride (2 mmol), zirconium tetrachloride (2 mmol), or hafnium tetrachloride (2 mmol), respectively, suspended in 50 ml of diethyl ether at  $-78^{\circ}\text{C}$ . The corresponding mixture was slowly allowed to come to room temperature and stirred for 24 hours. The solvent was evaporated to dryness and an amount of 100 ml of toluene was added. The toluene suspension was filtered, the volume of the filtrate was reduced and the complexes were precipitated by the addition of n-pentane. After filtration, the precipitate was washed several times with n-pentane

and dried by evacuation to obtain the desired complexes **40-42** as yellow powders in 60-65% yields. Complex **41** afforded shining cubic crystals suitable for X-rays diffraction analysis upon crystallization from a toluene/pentane mixture.

### 3.10.15 General synthesis of the transition metal complexes **43** and **44**

An amount of 4 mmol of n-butyllithium (1.6 M in hexanes) was added to 2 mmol of 2,2'-bis(inden-1-ylmethyl) biphenyl (**38**) dissolved in 50 ml of diethyl ether at -78 °C. After stirring for further 3 hours at room temperature, the solution was cooled to -78 °C and an amount of 4 mmol of methyl iodide was carefully added. The solution was allowed to come to room temperature and stirred for one hour. Then it was cooled again to -78 °C and an amount of 4 mmol of n-butyllithium was added. After stirring at room temperature overnight, the solution was transferred to a suspension of zirconium tetrachloride (2 mmol) or hafnium tetrachloride (2 mmol) in 50 ml of diethyl ether at -78 °C. The mixture was allowed to come to room temperature slowly and it was stirred for further 24 hours. Diethyl ether was evaporated and toluene (100 ml) was added. The toluene suspension was filtered, the volume of the filtrate was reduced and the complexes were precipitated by addition of n-pentane. After filtration, the precipitate was washed several times with n-pentane and dried by evacuation to obtain the desired complexes **43** and **44** as yellow powders in 40-55% yields.

**Table 22:** Elemental analysis data of complexes **40-44**.

No.	C <sub>exp</sub> %	C <sub>theor</sub> %	H <sub>exp</sub> %	H <sub>theor</sub> %
<b>40</b>	72.02	72.89	4.73	4.59
<b>41</b>	67.14	67.35	4.35	4.24
<b>42</b>	57.50	58.42	3.91	3.68
<b>43</b>	67.23	68.21	4.44	4.71
<b>44</b>	58.66	59.53	3.86	4.11

### 3.10.16 Preparation of 9-tolyldimethylsilylfluorene (**45**)

n-Butyllithium (12 mmol, 1.6 M in hexanes) was added to 12 mmol of fluorene dissolved in 100 ml of diethyl ether at -78 °C. The solution was stirred for 12 hours at room temperature and then cooled to 0 °C. Tolychlorodimethylsilane **1** (12 mmol) in 50 ml of

diethyl ether was added slowly. The resulting solution was stirred overnight at room temperature and then hydrolyzed by the addition of 100 ml of distilled water. The organic phase was separated and dried by passing through a sodium sulphate column. The solution was reduced in volume and kept at -24 °C for 72 hours to give **45** as yellow crystals in 85 % yield.

### 3.10.17 General synthesis of the transition metal complexes **46** and **47**

n-Butyllithium (4 mmol, 1.6 M in hexanes) was added to 4 mmol of compound **45** dissolved in 50 ml of diethyl ether at -78 °C. This solution was allowed to warm up to room temperature and it was stirred overnight. The mixture was transferred to a suspension of either zirconium tetrachloride (2 mmol) or hafnium tetrachloride (2 mmol) in 50 ml of diethyl ether at -78 °C. The mixture was slowly allowed to come to room temperature and stirred for further 24 hours. Diethyl ether was removed in vacuo and toluene (100 ml) was added. The toluene suspension was filtered, the volume of the filtrate was reduced and the complexes were precipitated by the addition of n-pentane. After filtration, the precipitate was washed several times with n-pentane and dried in vacuo to obtain the desired complexes **46** and **47** as yellow powders in 70-75% yields.

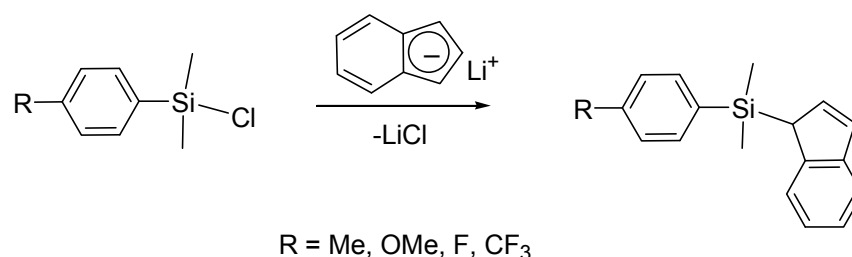
**Table 23:** Elemental analysis data of complexes **46** and **47**.

No.	C <sub>exp</sub> %	C <sub>theor</sub> %	H <sub>exp</sub> %	H <sub>theor</sub> %
<b>46</b>	64.33	66.97	4.19	5.36
<b>47</b>	57.52	60.30	3.35	4.83

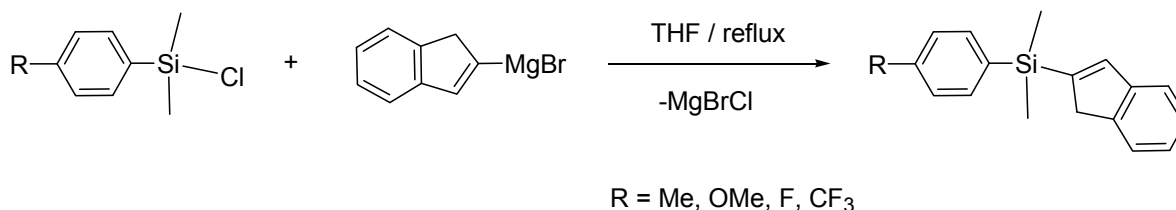
## 4. Summary

The aim of this project was the synthesis and characterization of novel bridged and unbridged bis(indenyl) complexes of group IV metals including a study of their catalytic performance in the homogeneous polymerization of ethylene. To accomplish this goal, various ligand precursors were prepared which include 1- and 2-substituted silylindenyl compounds, 1,2-bis(inden-1-yl)dimethylsilylbenzene, 2,2'-bis(inden-1-yl)methyl-1,1'-biphenyl and 9-substituted silylfluorenes. The corresponding dichloride complexes of group IV metals were synthesized and used as catalyst precursors in ethylene polymerization reactions.

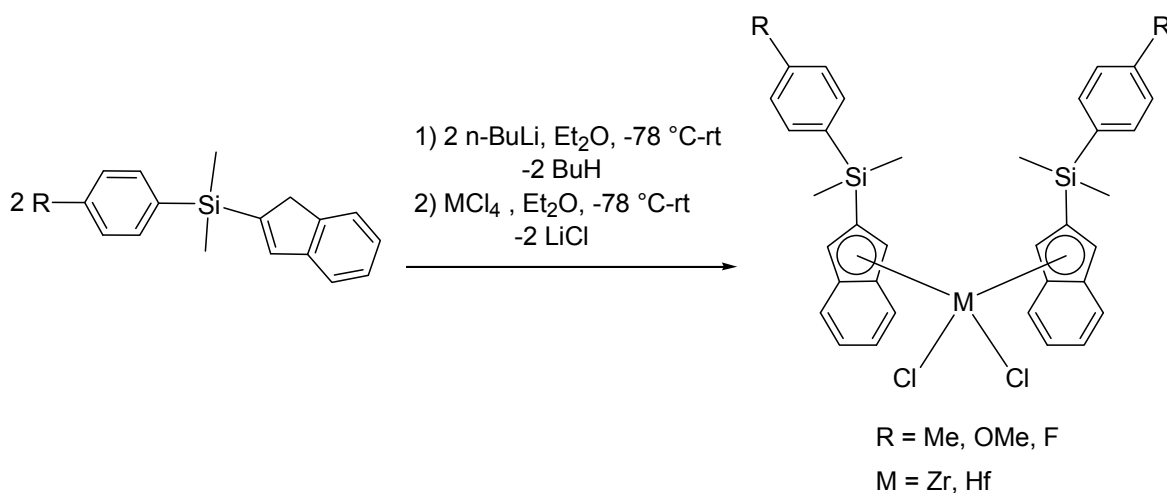
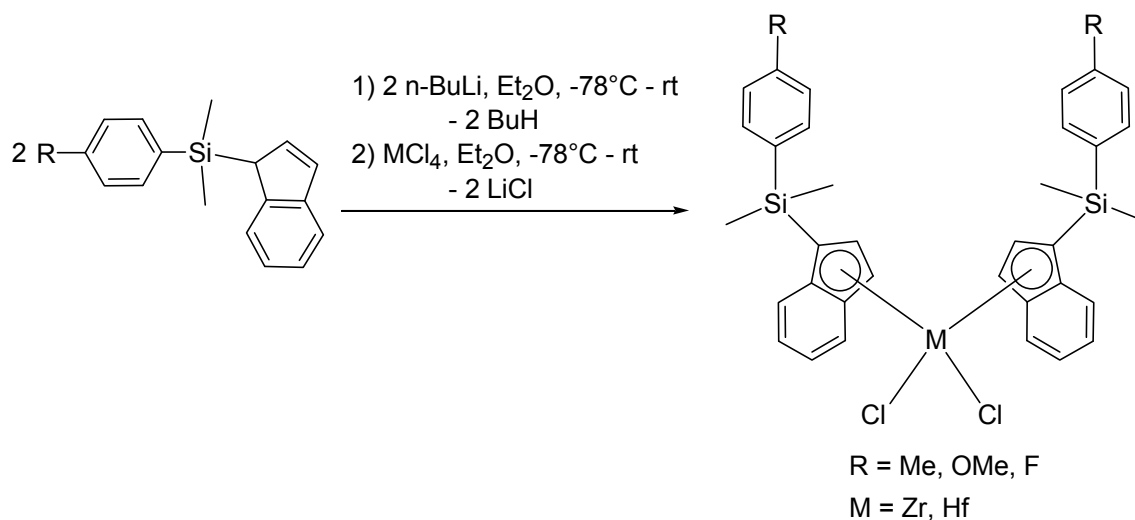
The first part of this work deals with the synthesis of symmetrical unbridged complexes of zirconium and hafnium derived from 1- and 2-substituted silylindenes and the investigation of their potential in ethylene polymerization reactions. The 1-substituted silylindenyl compounds were obtained by the reactions of chlorosilanes and indenyllithium.



The 2-substituted silylindenyl ligand precursors were obtained by a Grignard coupling reaction of aryl dimethylchlorosilanes and 2-bromoindene.



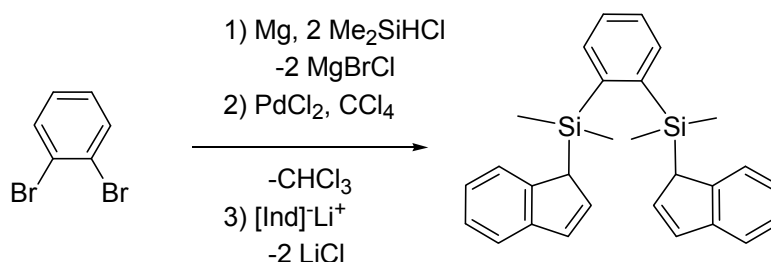
The corresponding dichloride complexes were synthesized by deprotonation of the substituted indenyl compounds with *n*-butyllithium and subsequent reactions with zirconium or hafnium tetrachloride in diethyl ether.



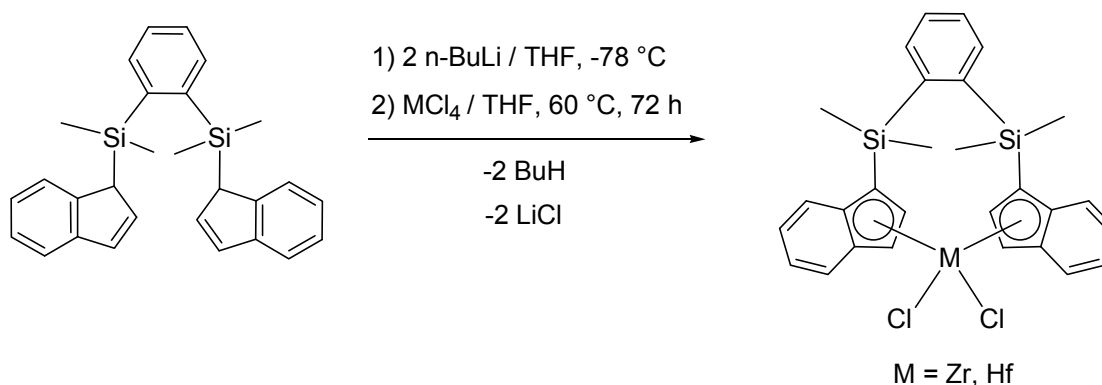
Applying MAO as a co-catalyst, the synthesized complexes were used in the polymerization of ethylene and the dependence of the activity on the substitution pattern was studied. Among the 1-substituted metallocene catalysts **13-18**, catalyst **17** bearing a fluoro atom at the para position of the silyl phenyl group showed the highest activity (4470 kg PE/mol cat. h) while catalyst **16** bearing a methoxy group at the same position was the least active (50 kg PE/mol cat. h). A similar trend was observed for the 2-substituted catalysts (**19-24**). In general, the 1-substituted catalysts were much more active than the 2-substituted counterparts. The obtained polymers were analyzed by differential scanning calorimetry (DSC) and viscosimetry.

The second part describes the synthesis and characterization of a new class of ansa bis(indenyl) complexes of zirconium and hafnium in which the two indenyl moieties are linked at the 1-,1'-positions via a 1,2-bis(dimethylsilyl)-benzene unit. The ligand

precursor was prepared via three reaction steps including Grignard coupling of chlorodimethylsilane and 1,2-dibromobenzene, PdCl<sub>2</sub>-catalyzed chlorination, and the reaction with indenyllithium.



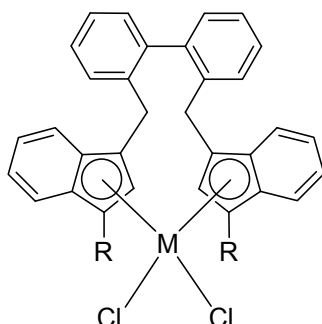
The corresponding zirconium and hafnium complexes were obtained by deprotonation of the corresponding bis-(indenyl) compound with n-BuLi followed by metalation reactions of MCl<sub>4</sub> (M = Zr, Hf) in THF.



The solid state molecular structures of both complexes were established by single crystal X-ray diffraction analyses. In ethylene polymerization reactions, both complexes exhibited high activities. The zirconocene catalyst **34** showed a higher activity (7610 kg PE/mol cat. h) compared to the hafnium catalyst **35** (3590 kg PE/mol cat. h).

A second type of ansa-metallocene complexes was synthesized and tested in the homogeneous polymerization of ethylene. The ligand system comprises two indenyl moieties tethered at 3,3'-positions via a 2,2'-dimethyl biphenyl bridge. The ligand precursor was obtained by the reduction of diphenic acid using lithium aluminum hydride (LiAlH<sub>4</sub>), the reaction with phosphorus tribromide, and, finally, the reaction with indenyllithium. The corresponding group (IV) metal complexes were synthesized by

deprotonation of the ligand precursors using n-BuLi followed by reactions of the corresponding metal tetrachloride.



The series of the unsubstituted ansa-complexes (R = H) showed higher activities compared to the methyl substituted counterparts. The zirconium complex **42** showed the highest activity (12460 kg PE/mol cat. h) followed by the hafnium complex **43** (3820 kg PE/mol cat. h) while the titanium complex **40** was inactive which could be attributed to thermal instability and a tendency to decomposition. The introduction of methyl groups at the 1-position of the indenyl moieties leads to a remarkable decrease in the activity probably due to steric hindrance resulting from the two methyl groups. The obtained polyethylenes were analyzed by differential scanning calorimetry (DSC) and viscosimetry.

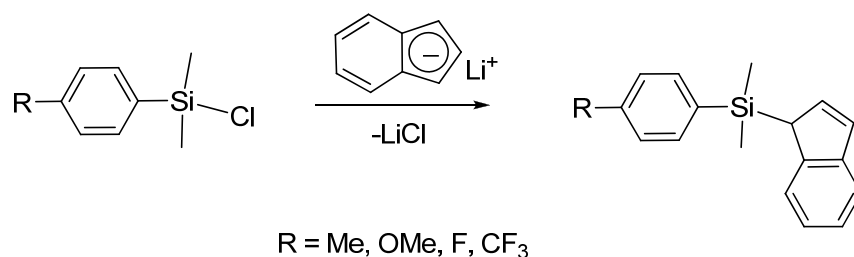
A series of symmetric unbridged 9-substituted dimethyl(tolyl)silyl-fluorenyl complexes of zirconium and hafnium was synthesized, characterized and tested in catalytic ethylene polymerization reactions. These complexes were inactive in the MAO assisted polymerization of ethylene. This could be referred to their instability towards ring-slippage reactions changing the hapticity ( $\eta^5 \rightarrow \eta^3 \rightarrow \eta^1$ ) of the fluorenyl rings.

## 5. Zusammenfassung

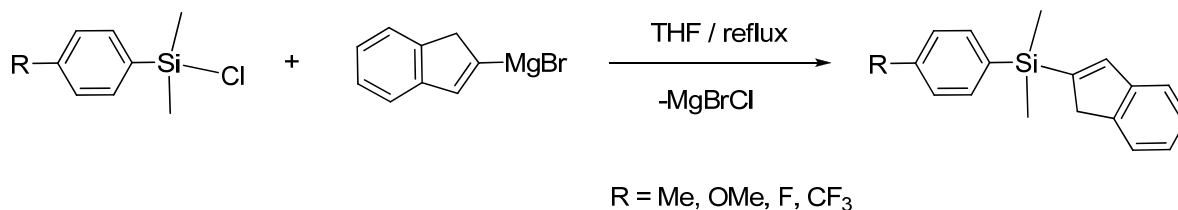
Die Ziel der vorliegenden Arbeit waren die Synthese und Charakterisierung neuartiger verbrückter und unverbrückter Bis(indenyl)-Komplexe von Metallen der IV. Nebengruppe und die Untersuchung ihrer katalytischen Eigenschaften bei der homogenen Ethenpolymerisation. Zu diesem Zweck wurden verschiedene Ligandenvorstufen synthetisiert, wie z.B. Silylindenyl-Verbindungen mit Substituenten in 1- und 2-Position, 1,2-Bis(inden-1-yl)dimethylsilyl)benzol, 2,2'-Bis(inden-1-ylmethyl)-1,1'-biphenyl und Fluorenylderivate mit Silylsubstituenten in 9-Position. Die entsprechenden Dichlorid-Komplexe der Gruppe-IV-Metalle wurden synthetisiert und als Katalysatorvorstufen für die Ethenpolymerisation eingesetzt.

Der erste Teil dieser Arbeit beschreibt die Synthese symmetrischer, unverbrückter Zirkonium- und Hafniumkomplexe mit Silylindenyl-Liganden, die Substituenten in 1- und 2-Position tragen, und die Untersuchung ihres Potentials für die Ethenpolymerisation.

Silylindenyl-Verbindungen mit Substituenten in Position 1 resultierten aus der Reaktion der entsprechenden Monochlorsilane mit Indenyllithium.

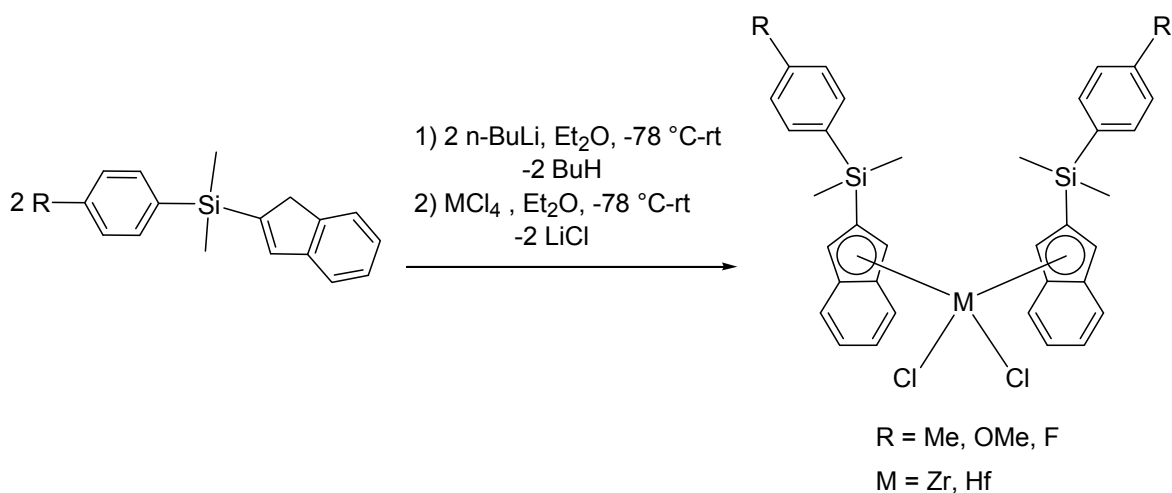
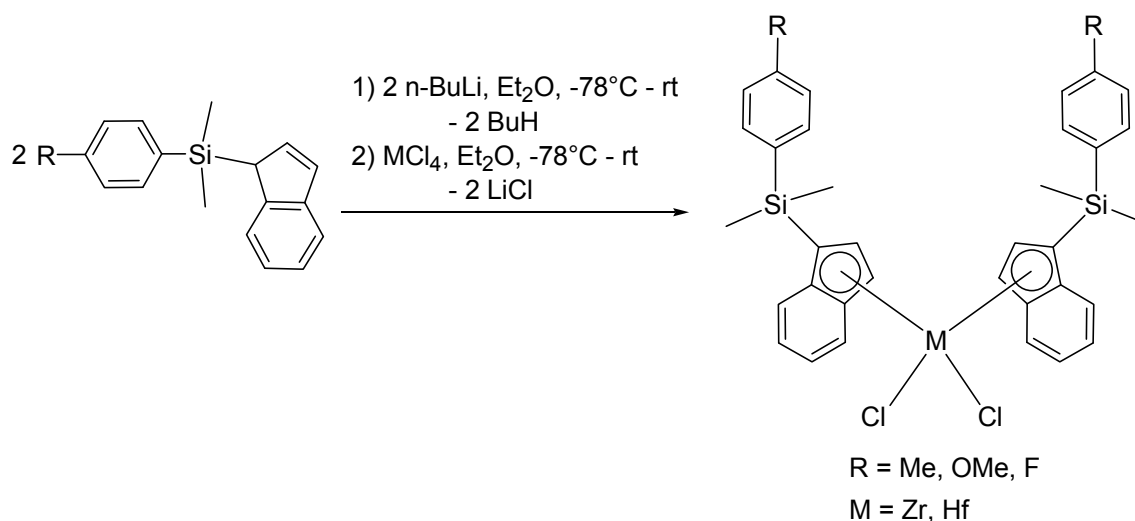


Silylindenyl-Ligandvorstufen mit Substituenten in Position 2 wurden durch die Grignard-Reaktion von Aryldimethylchlorosilanen mit 2-Brominden erhalten.



## Zusammenfassung

Um die entsprechenden Dichlorid-Komplexe zu erhalten wurden zunächst die substituierten Indenylverbindungen mit n-Butyllithium deprotoniert und anschließend mit Zirkonium- oder Hafniumtetrachlorid in Diethylether umgesetzt.



Die so hergestellten Komplexe wurden mit MAO als Cokatalysator für die Ethenpolymerisation eingesetzt, um den Einfluss des Substitutionsmusters auf die Aktivität zu untersuchen.

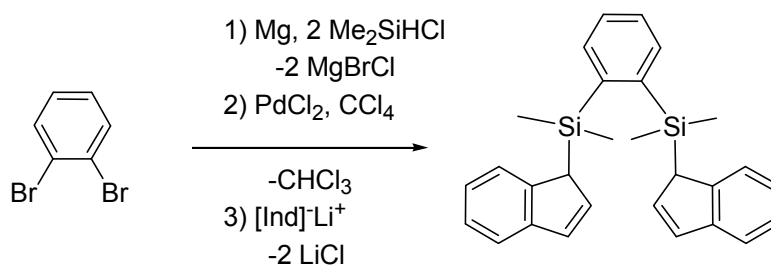
Komplex **17** mit einem Fluoratom in para-Position der Silylphenyl-Gruppe zeigte dabei die höchste Aktivität (7740 kg PE/mol Kat. h) unter den Metallocenkomplexen **13-18** mit Substituenten in Position 1.

Im Gegensatz dazu wies Komplex **16** mit einer Methoxygruppe an derselben Position die geringste Aktivität (50 kg PE/mol Kat. h) auf. Ein ähnliches Verhalten war bei den Komplexen mit Substituenten in Position 2 (**19-24**) zu beobachten. Grundsätzlich waren jedoch die Komplexe mit Substituenten in Position 1 sehr viel aktiver als deren Analoga mit Substituenten in Position 2.

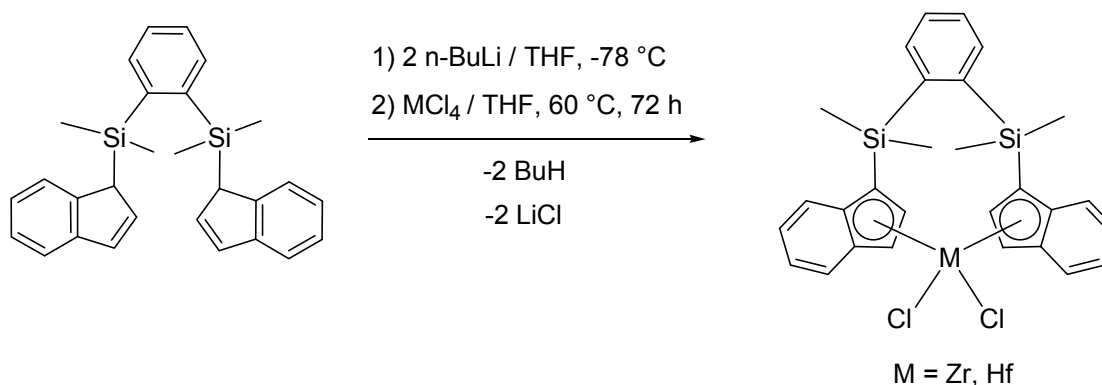
Die erhaltenen Polymere wurden mit Hilfe von „differential scanning calorimetry“ (DSC) und Viskosimetrie-Messungen charakterisiert.

Der zweite Teil der Arbeit beschäftigt sich mit der Synthese und Charakterisierung einer neuen Klasse von Zirkonium- und Hafniumkomplexen mit ansa-Bis(indenyl)-Liganden, in welchen die beiden Indenylreste durch eine 1,2-Bis(dimethylsilyl)benzol-Brücke in den Positionen 1 und 1' verbunden sind.

Die Ligandenvorstufen wurde in drei Schritten hergestellt. Nach der Grignard-Reaktion von Chlordimethylsilan mit 1,2-Dibrombenzol und der PdCl<sub>2</sub>-katalysierten Chlorierung wurde die Ligandenvorstufe durch die Umsetzung mit Indenyllithium erhalten.



Die entsprechenden Zirkonium- und Hafniumkomplexe resultierten aus der Deprotonierung der Bis(indenyl)-Verbindung mit n-BuLi gefolgt von einer Umsetzung mit dem entsprechenden Metalltetrachlorid in THF.

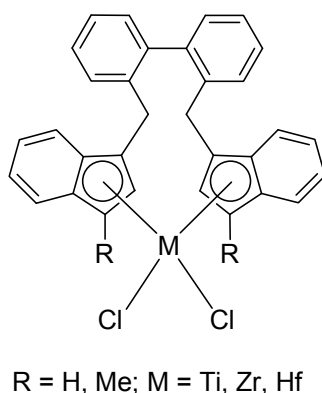


Die Festkörperstrukturen beider Komplexe wurden mit Hilfe von Kristall-Strukturanalysen aufgeklärt. Beide Komplexe erwiesen sich als sehr aktiv bei der Ethenpolymerisation. Der Zirkonium-Komplex **34** war dabei noch aktiver (7610 kg PE/mol Kat. h) als sein Hafnium-Analogon **35** (3590 kg PE/mol Kat. h).

Weiterhin wurde ein zweiter Strukturtyp von ansa-Metallocenen synthetisiert und dessen Eigenschaften bei der homogenen Ethenpolymerisation untersucht. Das Ligandsystem besteht aus zwei Indenylgruppen, die über eine 2,2'-Dimethylbiphenyl-Brücke an den Positionen 3 und 3' verbunden sind.

Die Reduktion von Diphensäure mit Lithiumaluminiumhydrid (LiAlH<sub>4</sub>) gefolgt von den Reaktionen mit Phosphortribromid und Indenyllithium lieferte die Ligandvorstufe.

Um die entsprechenden Komplexe der Gruppe-IV-Metalle zu erhalten, wurden zunächst die substituierten Indenylverbindungen mit n-Butyllithium deprotoniert und anschließend mit den entsprechenden Metalltetrachloriden umgesetzt.



Im Vergleich zu den methylsubstituierten Derivaten ( $R = \text{Me}$ ) zeigten die unsubstituierten ansa-Komplexe ( $R = \text{H}$ ) höhere Aktivitäten. Die höchste Aktivität wurde dabei vom Zirkoniumkomplex **42** erzielt (12460 kg PE/mol Kat. h) gefolgt vom Hafniumkomplex **43** (3816 kg PE/mol Kat. h). Der Titan-Komplex **40** hingegen war inaktiv, was durch dessen thermische Instabilität und Tendenz zur Zersetzung begründet werden könnte.

Die Einführung von Methylsubstituenten in Position 1 der Indenylgruppen führt zu einem beachtlichen Rückgang der Aktivität. Der Grund dafür liegt wahrscheinlich in der sterischen Hinderung durch die beiden Methylgruppen.

Die erhaltenen Polyethylene wurden mit Hilfe von „differential scanning calorimetry“ (DSC) und Viskosimetrie-Messungen charakterisiert.

Weiterhin wurden eine Reihe symmetrisch unverbrückter (Tolyl)fluorenyl-Zirkonium- und Hafniumkomplexe synthetisiert, charakterisiert und für die Ethenpolymerisation untersucht. Diese Komplexe erwiesen sich dabei als inaktiv in Kombination mit MAO. Der Grund für deren Inaktivität ist sehr wahrscheinlich in „ring-slippage“-Reaktionen zu suchen, die mit wechselnden Haptizitäten ( $\eta^5 \rightarrow \eta^3 \rightarrow \eta^1$ ) der Fluorenylliganden einhergehen. Diese Reaktionen sind allgemein bekannt für unverbrückte Fluorenylkomplexe.

## 6. References

- [1] S. S. Ivanchev, *Russ. Chem. Rev.*, **2007**, 76 (7), 617.
- [2] S. Neufeldt, *Chronik der Chemie 1800-1980*, VCH, Weinheim, **1987**.
- [3] I. Strube, *Geschichte der Chemie, Verl. der Wissenschaften*, Berlin, **1987**.
- [4] R. B. Seymour, T. Cheng, *History of Polyolefins*, **1986**, Riedel Pub. Co., New York.
- [5] J. P. Hogan, R. L. Banks, *Belg. Pat. 530617*, **1955**; *U. S. 2825721*, **1958**.
- [6] K. Ziegler, H. Gellert, H. Kühlnhorn, H. Martin, K. Meyer, K. Nagel, H. Sauer, K. Zosel, *Angew. Chem.* **1952**, 64, 323.
- [7] K. Ziegler, H. Kühlnhorn, H. Breil, H. Martin, *Angew. Chem.* **1955**, 67, 541.
- [8] G. Natta, *Angew. Chem.* **1956**.
- [9] K. Ziegler, *Angew. Chem.* **1964**, 76, 545.
- [10] G. Natta, *Angew. Chem.* **1964**, 76, 553.
- [11] V. Warzelhan, D. Scherzer, *Int. Symp. On Engineering Plastics*, **2007**, Aug. 19–24, Urumqi, Chinese Academy of Sciences, Beijing, China.
- [12] W. Kaminsky, *Rap. Rev. Rep.* **1999**, 10, 115.
- [13] D. S. Breslow, N. R. Newburg, *J. Am. Chem. Soc.* **1957**, 79, 5072.
- [14] G. Natta, P. Pino, G. Mazzanti, V. Giannini, *J. Am. Chem. Soc.* **1957**, 79, 2975.
- [15] H. Sinn, W. Kaminsky, H. J. Vollmer, *Angew. Chem.* **1980**, 92, 396.
- [16] H. Sinn, W. Kaminsky, *Adv. Organomet. Chem.* **1980**, 99, 18.
- [17] Y. Koide, S.G. Bott, A. R. Barron, *Organometallics* **1996**, 15, 2213.
- [18] W. Kaminsky, *Macromol Chem. Phys.* **1996**, 197, 3907.
- [19] H. Sinn, *Makromol. Chem., Makromol. Symp.* **1995**, 97, 27.
- [20] M. R. Mason, J. M. Smith, S. G. Bott, A. R. Barron, *J. Am. Chem. Soc.* **1993**, 115, 4971.
- [21] P. Cossee, *J. Catal.* **1964**, 3, 80.
- [22] E. J. Arlman, *J. Catal.* **1964**, 3, 89.
- [23] E. J. Arlman, P. Cossee, *J. Catal.* **1964**, 3, 99.
- [24] J. Zhang et al., *Coord. Chem. Rev.* **2006**, 250, 95.
- [25] H. G. Alt, A. Köppl, *Chem. Rev.* **2000**, 100, 1205.

## References

---

- [26] F. R. W. P. Wild, L. Zsolnai, G. Huttner, H. H. Brintzinger, *J. Organomet. Chem.* **1982**, 232, 233.
- [27] J. A. Ewen, *J. Am. Chem. Soc.* **1984**, 106, 6355.
- [28] J. A. Ewen, R. L. Jones, A. Razavi, J. D. Ferrara, *J. Am. Chem. Soc.* **1988**, 110, 6255.
- [29] W. A. Herrmann, J. Rohrmann, *Angew. Chem., Int. Ed. Engl.* **1989**, 28, 1511.
- [30] C. J. Schaverien, R. Ernst, P. Schut, T. Dall'Occo, *Organometallics* **2001**, 20, 3436.
- [31] C. J. Schaverien, R. Ernst, J. D. van Loon, T. Dall'Occo, *Eur. Pat. Appl.* **1999**, 941997.
- [32] R. L. Halterman, T. M. Ramsey, *Organometallics* **1993**, 12, 2879.
- [33] H. G. Alt, W. Milius, S. J. Palackal, *J. Organomet. Chem.* **1994**, 472, 113.
- [34] W. Kaminsky, *Catalysis Today* **2000**, 62, 23.
- [35] G. W. Coates, R. M. Waymouth, *Science* **1995**, 267, 217.
- [36] E. Hauptman, R. M. Waymouth, *J. Am. Chem. Soc.* **1995**, 117, 11586.
- [37] R. Kravchenko, A. Masood, R. M. Waymouth, *Organometallics* **1997**, 16, 3635.
- [38] J. L. M. Petoff, M. D. Bruce, R. M. Waymouth, A. Masood, T. K. Lal, R. W. Quan, S. J. Behrend, *Organometallics* **1997**, 16, 5909.
- [39] M. D. Bruce, G. W. Coates, E. Hauptman, R. M. Waymouth, J. W. Ziller, *J. Am. Chem. Soc.* **1997**, 119, 11174.
- [40] R. Schmidt, M. Deppner, H. G. Alt, *Journal of Molecular Catalysis A: Chemical* **2001**, 172, 43.
- [41] R. Leino, P. Lehmus, A. Lehtonen, *Eur. J. Inorg. Chem.* **2004**, 3201.
- [42] C. Schmidt, H. G. Alt, M. Bruce, *Eur. Pat. Appl.* **1997**, EP 798306. A1 19971001
- [43] N E. Grimmer, N. J. Coville, C. B. de Koning, *J. Organomet. Chem.* **2002**, 642, 195.
- [44] A. Hannisdal, A. C. Möller, E. Rytter, R. Bolm, *Macromol. Symp.* **2004**, 213, 79.
- [45] S. E. Reybuck, R. M. Waymouth, *Macromolecules* **2004**, 37, 2342.
- [46] S. E. Reybuck, R. Meyer, R. M. Waymouth, *Macromolecules* **2002**, 35, 637.
- [47] J. S. Yoon, D. H. Lee, E. S. Park, D. K. S. O Jung, *J. Appl. Polym. Sci.* **2000**, 75, 928.

## References

---

- [48] J. A. Van Beek, J. G. de Vries, H. J. Arts, R. Persad, G. H. J. van Doremaele, *U.S. Patent* 5646322, **1997**.
- [49] N. Piccolrovazzi, P. Pino, G. Consiglio, A. Sironi, M. Moret, *Organometallics* **1990**, *9*, 3098.
- [50] H. H. Brintzinger, D. Fischer, R. Mühlhaupt, B. Rieger, R. Waymouth, *Angew. Chem.* **1995**, *107*, 1255.
- [51] M. Bochmann, *J. Chem. Soc., Dalton Trans.* **1996**, 255.
- [52] P. C. Möhring, N. J. Coville, *J. Organomet. Chem.* **1994**, *479*, 1.
- [53] A. C. Möller, R. Blom, R. H. Heyn, O. Swang, J. Kopfc, T. Seraidaris, *Dalton Trans.* **2006**, 2098.
- [54] S. Lin, E. Hauptman, T. K. Lal, R. M. Waymouth, R. W. Quan, A. B. Ernst, *J. Mol. Catal. A: Chem.* **1998**, *136*, 23.
- [55] G. Jany, M. Gustafsson, T. Repo, E. Aitola, J. A. Dobado, M. Klinga, M. Leskelä, *J. Organomet. Chem.* **1998**, *553*, 173.
- [56] R. Leino, H. Luttikhedde, P. Lehmus, C. Wilen, R. Sjöholm, A. Lehtonen, J. V. Seppälä, J. H. Näsman, *Macromolecules* **1997**, *30*, 3477.
- [57] H. H. Brintzinger, D. Fischer, R. Mühlhaupt, B. Rieger, R. M. Waymouth, *Angew. Chem., Int. Ed. Engl.* **1995**, *34*, 1143.
- [58] R. Leino, H. Luttikhedde, C. Wilén, R. Sillanpää, J. H. Näsman, *Organometallics* **1996**, *15*, 2450.
- [59] S. Knüppel, J.-L. Fauré, G. Erker, G. Kehr, M. Nissinen, R. Fröhlich, *Organometallics* **2000**, *19*, 1262.
- [60] H. Luttikhedde, R. Leino, M. J. Ahlgrén, T. A. Pakkanen, J. H. Näsman, *J. Organomet. Chem.* **1998**, *557*, 227.
- [61] H. Luttikhedde, R. Leino, C. Wilén, J. H. Näsman, M. J. Ahlgrén, T. A. Pakkanen, *Organometallics* **1996**, *15*, 3092.
- [62] T. Dreier, G. Erker, R. Fröhlich, B. Wibbeling, *Organometallics* **2000**, *19*, 4095.
- [63] T. Dreier, G. Unger, G. Erker, B. Wibbeling, R. Fröhlich, *J. Organomet. Chem.* **2001**, *622*, 143.
- [64] T. Dreier, K. Bergander, E. Wegelius, R. Fröhlich, G. Erker, *Organometallics* **2001**, *20*, 5067.

## References

---

- [65] H. Schumann, D. F. Karasiak, S. H. Mühle, W. Kaminsky, U. Weingarten, *J. Organomet. Chem.* **2001**, 636, 31.
- [66] R. Schmidt, H. G. Alt, *J. Organomet. Chem.* **2001**, 621, 304.
- [67] G. Y. Lee, M. Xue, M. S. Kang, O. C. Kwon, J.-S. Yoon, Y.-S. Lee, H. S. Kim, H. Lee, I.-M. Lee, *J. Organomet. Chem.* **1998**, 558, 11.
- [68] S. C. Collins, Y. Hong, R. Ramachandran, N. J. Taylor, *Organometallics* **1991**, 10, 2349.
- [69] T. Cuenca, P. Royo, *Coord. Chem. Rev.* **1999**, 193–195, 447.
- [70] O. W. Lofthus, C. Slebodnick, P. A. Deck, *Organometallics* **1999**, 18, 3702.
- [71] N. E. Grimmer, N. J. Coville, C. B. de Koning, J. M. Smith, L. M. Cook, *J. Organomet. Chem.* **2000**, 616, 112.
- [72] N. E. Grimmer, N. J. Coville, C. B. de Koning, *J. Organomet. Chem.* **2002**, 642, 195.
- [73] A. C. Möller, R. H. Heyn, R. Blom, O. Swang, C. H. Görbitz, J. Kopf, *Dalton Trans.* **2004**, 1578.
- [74] C. Eaborn, K. L. Jones, P. D. Lickiss, *J. Organomet. Chem.* **1994**, 466, 35.
- [75] C. Beyer, U. Böhme, C. Pietzsch, G. Röwer, *J. Organomet. Chem.* **2002**, 654, 187.
- [76] W. A. Lindley, D. W. H. MacDowell, *J. Org. Chem.* **1982**, 47, 705.
- [77] C. Schmid, Ph.D. Thesis, University of Bayreuth **1996**.
- [78] E. Aitola, M. Surakka, T. Repo, M. Linnolahti, K. Lappalainen, Kaisa Kervinen, M. Klinga, T. Pakkanen, M. Leskelä, *J. Organomet. Chem.* **2005**, 690, 773.
- [79] J. A. Simoes, J. L. Beauchamp, *Chem. Rev.* **1990**, 90, 629.
- [80] I.M. Lee, W. Gauthier, J. M. Ball, B. Iyengar, S. Collins, *Organometallics* **1992**, 11, 2115.
- [81] G. Luft, M. Dorn, *Angew. Makromol. Chem.* **1991**, 188, 177.
- [82] F. Wild, M. Wasiucionek, G. Huttner, H. H. Brintzinger, *J. Organomet. Chem.* **1985**, 288, 63.
- [83] S. Miyake, Y. Okumura, S. Inazawa, *Macromolecules* **1995**, 28, 3074.
- [84] L. Resconi, F. Piemontesi, I. Camurati, O. Sudmeijer, I. E. Ninfant'ev, P. V. Ivchenko, L. G. Kuz'mina, *J. Am. Chem. Soc.* **1998**, 120, 2308.

## References

---

- [85] C. Alonso-Moreno, J. Sancho, F. Carrillo-Hermosilla, A. Otero, A. Antiñolo, I. López-Solera, *Inorg. Chem. commun.* **2009**, *12*, 184.
- [86] A. Puranen, *Organometallics* **2010**, *29*, 4018.
- [87] B. Wang, *Coord. Chem. Rev.* **2006**, *250*, 242.
- [88] T. K. Han, B. y. W. Woo, J. T. Park, Y. DO, Y. S. Ko, S. I. WOO, *Macromolecules* **1995**, *28*, 4801.
- [89] H. G. Alt, R. W. Baker, M. Dakkak, M. A. Foulkes, M. O. Schilling, P. Turner, *J. Organomet. Chem.* **2004**, *689*, 1965.
- [90] M. Ishikawa, *J. Polym. Sci.: Part A: Polym. Chem.* **1993**, *31*, 3281.
- [91] T. Gibson, *Organometallics* **1987**, *6*, 918.
- [92] T. Repo, M. Klinga, I. Mutikainen, Y. Su, M. Leskelä, M. Polamo, *Acta Chem. Scand.* **1996**, *50*, 1116.
- [93] W. Spaleck, M. Antberg, J. Rohrmann, A. Winter, B. Bachmann, P. Kiprof, J. Behm, W. A. Herrmann, *Angew. Chem.* **1992**, *104 (10)*, 1373.
- [94] J. A. Ewen, K. Robinson, *Macromol. Chem., Macromol. Symp.* **1991**, *48-49*, 253.
- [95] D. T. Mallin, M. D. Rausch, J. D. W. Chien, *Polym. Bull.* **1988**, *20*, 421.
- [96] A. Laine, M. Linnolahti, T. A. Pakkanen, J. R. Severn, E. Kokko, A. Pakkanen, *Organometallics* **2010**, *29*, 1541.
- [97] V. A. Dang, L.-C. Yu, D. Balboni, T. Dall'Occo, L. Resconi, P. Mercandelli, M. Moret, A. Sironi, *Organometallics* **1999**, *18*, 3781.
- [98] A. Y. Agarkov, V. V. Izmer, A. N. Riabov, L. G. Kuz'mina, J. A. K. Howard, I. P. Beletskaya, A. Z. Voskoboynikov, *J. Organomet. Chem.* **2001**, *619*, 280.
- [99] A. Z. Voskoboynikov, A. Y. Agarkov, E. A. Chernyshev, I. P. Beletskaya, A. V. Churakov, L. G. Kuz'mina, *J. Organomet. Chem.* **1997**, *530*, 75.
- [100] F. Piemontesi, I. Camurati, L. Resconi, D. Balboni, A. Sironi, M. Moret, R. Zeigler, N. Piccolrovazzi, *Organometallics* **1995**, *14*, 1256.
- [101] L. W. M. Lee, W. E. Piers, M. Parvez, S. J. Rettig, V. G. Young, *Organometallics* **1999**, *18*, 3904.
- [102] W. A. Herrmann, J. Rohrmann, E. Herdtweck, W. Spaleck, A. Winter, *Angew. Chem.* **1989**, *101*, 1536.
- [103] L. M. Tolbert, M. Z. Ali, *J. Org. Chem.* **1982**, *47*, 4793.

## References

---

- [104] T. Ooi, Y. Uematsu, M. Kameda, K. Maruoka, *Tetrahedron* **2006**, 62, 11425.
- [105] J. C. W. Chien, *J. Am. Chem. Soc.* **1959**, 81, 86.
- [106] H. G. Alt, *Chem. Soc. Rev.* **1998**, 27, 322.
- [107] K. Patsidis, H. G. Alt, *J. Organomet. Chem.* **1995**, 501, 31.

## Erklärung

Hiermit erkläre ich, dass ich die Arbeit selbständig verfasst und keine anderen als die angegebenen Quellen und Hilfsmittel benutzt habe.

Ferner erkläre ich, dass ich nicht andersweitig mit oder ohne Erfolg versucht habe, eine Dissertation zu diesem oder gleichartigem Thema einzureichen oder mich der Doktorprüfung zu unterziehen.

Bayreuth, den 11. Oktober 2011



---

Mohamed Elnaiem Mohamed Abdelbagi